

Properties of Air Bubbles in Air Entrained Concrete

by

Le Tuan Pham

A dissertation submitted in partial fulfillment of

the requirements for the degree of

Doctor of Philosophy

(Civil and Environmental Engineering)

at the

UNIVERSITY OF WISCONSIN-MADISON

2019

Date of final oral examination: 11/19/2018

The dissertation is approved by the following members of the Final Oral Committee:

Steven M. Cramer, Professor, Civil and Environmental Engineering (Advisor)

Walter J. Drugan, Professor Emeritus, Engineering Physics

Gustavo J. Parra-Montesinos, Professor, Civil and Environmental Engineering

Jose A. Pincheira, Associate Professor, Civil and Environmental Engineering

Dedicated to my parents

ACKNOWLEDGEMENTS

I would like to sincerely thank:

- My advisor Professor Steven Cramer for his mentorship, kindness, and unparalleled consideration for my professional development and family.
- My advisory committee members Professor Walt Drugan, Professor Gustavo Parra-Montesinos, and Professor Jose Pincheira for their support, guidance, and teaching.
- Mr. Kevin McMullen of the Wisconsin Concrete Pavement Association for his support and insightful advice.
- Mr. James Schmitt and Mr. Gregory Schmitt for their training and permission to use their laboratory equipment.
- Mr. Brian Hess and Mr. Bil Schneider at the UW-Madison Department of Geoscience, Ms. Julie Last and Mr. Richard Noll at the UW-Madison Materials Science Center for their help and training.
- Staff and students at the Wisconsin Structures and Materials Testing Laboratory.
- The Wisconsin Department of Transportation through the Wisconsin Highway Research Program for providing funding for this research.
- The University of Wisconsin-Madison College of Engineering Shared Research Facilities and the National Science Foundation through the Materials Science Research and Engineering Center (DMR-1720415) for the instrumentation provided at the UW-Madison Materials Science Center.

Last but not least, I am grateful for the continuous encouragement from my family.

ABSTRACT

It is widely accepted that air entrainment, a purposeful introduction of small air bubbles in concrete, is critical to the long-term durability of concrete in freeze-thaw environments. Air entraining admixtures (AEA) are added to the mixture to stabilize air bubbles created during mixing, ensuring a proper air void system in the hardened concrete. Despite the complexity of creating a suitable air void system in concrete, previous study and experience established the reliability and robustness of such systems under a variety of conditions through use of neutralized vinsol resin (NVR) AEA products. In recent years, synthetic AEAs have been used more frequently due to limited supply of NVR to the concrete industry. With the use of synthetic AEAs, there are more reports of new problems including difficulties in accurately measuring the air content.

This study was conducted to find the root cause of the increasing difficulties in controlling the air contents in portland cement concrete associated with synthetic AEAs. Main challenges included the lack of existing techniques to evaluate AEAs and air bubbles in concrete, and lack of data to help identify causes. Given these challenges, a multi-scale experimental study that included testing of field and laboratory concrete, and testing of foam and individual air bubbles was undertaken. The results indicate that the disparity between QC test results and the actual air contents in concrete pavements associated with the use of synthetic AEAs could be attributed to less robust air bubbles stabilized with synthetic AEAs compared to those entrained with NVR and the resulting increased loss of these air bubbles during concrete sampling. The cause of this decreased robustness and resulting air loss was traced directly to the properties of the bubble shells. The shells of air bubbles in concrete entrained with synthetic AEAs were thinner and less stiff than those associated with an NVR AEA. Through this research new test protocols were developed to measure stiffness and thickness of the shell of air bubbles extracted from cement paste and to quantify stability of foams of AEAs in a cementitious environment. These tests could be used by researchers and practitioners who are interested in developing new admixtures and/or identifying admixtures with undesirable performance.

Table of Contents

ABSTRACT	iii
Table of Contents	iv
List of Tables	vii
List of Figures	ix
CHAPTER 1 INTRODUCTION	1
1.1 Problem Statement.....	1
1.2 Research Goals and Methods.....	2
1.3 Structure.....	3
CHAPTER 2 EXPERIMENTAL STUDY ON THE AIR VOID SYSTEM IN WISCONSIN CONCRETE PAVEMENTS.....	5
2.1 Introduction.....	5
2.2 Literature Review Summary.....	6
2.3 Experimental Procedures	7
2.4 Project Data.....	11
2.4.1 Mix Design.....	11
2.4.2 Construction Parameters	11
2.5 Results.....	13
2.5.1 Air Void Analysis of WisDOT Cores (Projects of 2013)	13
2.5.2 Fresh Concrete Properties of Projects Visited in 2014	14
2.5.3 Air Contents of Fresh and Hardened Concretes.....	15
2.5.4 Characteristics of Hardened Air Voids in Cylinders and Cores	28
2.6 Discussion.....	39
2.6.1 Concrete Air content in Fresh and Hardened states	39

2.6.2 Air contents of Drilled Cores and Cylinders.....	40
2.7 Conclusions.....	41
CHAPTER 3 ROBUSTNESS OF CONCRETE AIR ENTRAINING ADMIXTURES AND FOAM DRAINAGE TEST	45
3.1 Introduction.....	45
3.2 Samples and Materials	48
3.2.1 Preliminary Concrete Tests	48
3.2.2 Primary Concrete Tests	50
3.2.3 Modified Foam Drainage Test	51
3.3 Results and Discussion	53
3.3.1 Preliminary Concrete Tests	53
3.3.2 Primary Concrete Tests	55
3.3.3 Modified FDT	57
3.4 Conclusions.....	62
CHAPTER 4 MECHANICAL PROPERTIES AND MICROSTRUCTURE OF AIR BUBBLE SHELLS IN CEMENT PASTE.....	65
4.1 Introduction.....	65
4.2 Experimental Methods.....	67
4.2.1 Materials and Bubble Extraction.....	67
4.2.2 AFM Tests of Air Bubbles in Liquid	68
4.2.3 Nanoindentation Test of Dried Bubble Shells	70
4.2.4 Microstructure of Bubble Shells using SEM	71
4.2.5 Shell Thickness Measurements using SEM	71
4.2.6 Surface Tension of AEA Solutions	73
4.3 Results and Discussion	74
4.3.1 AFM Test Results	74

4.3.2 Nanoindentation	79
4.3.3 SEM-EDS.....	81
4.3.4 Surface Tension Test Results	89
4.3.5 Mechanism for Formation and Stability of the Air Bubble Shell	91
4.4 Conclusions.....	93
CHAPTER 5 CONCLUSIONS AND RECOMMENDATIONS	98
5.1 Conclusions.....	98
5.1.1 Findings from Experimental Study on the Air Void System in Wisconsin Concrete Pavements (Chapter 2):.....	98
5.1.2 Findings from Robustness of AEAs and the Foam Drainage Test (Chapter 3)	99
5.1.3 Findings from Micro-properties of the Shells of Air Bubbles (Chapter 4)	99
5.1.4 Overall Conclusions	100
5.2 Recommendations for Future Research.....	101
APPENDIX - LITERATURE SURVEY FOR CHAPTER 2	102

List of Tables

Table 1. Testing Matrix.....	10
Table 2. Mix characteristics of WisDOT cores in 2013 (Quantities per cubic yard of concrete)	12
Table 3. Mix characteristics of projects visited in 2014 (Quantities per cubic yard of concrete)	12
Table 4. Construction parameters of projects visited in 2014	13
Table 5. Comparison of C457 results of WisDOT cores and QC air contents	14
Table 6. Properties of fresh concrete sampled in front of the paver	15
Table 7. Air contents by different methods (%)	16
Table 8. Comparison of fresh air content by pressure method and hardened air content by ASTM C457 of concrete in front of paver	18
Table 9. Comparison of fresh air content by pressure method and hardened air content by ASTM C457 of concrete behind paver	19
Table 10. Comparison of pressure air content (ASTM C231) before paver and core air content (ASTM C457)	21
Table 11. Comparison of fresh air content by volumetric method (ASTM C173) and hardened air content by ASTM C457 of concrete in front of paver	23
Table 12. Comparison of fresh air content by volumetric method (ASTM C173) and hardened air content by ASTM C457 of concrete behind paver	24
Table 13. Comparison of fresh air content by the gravimetric method (ASTM C138) vs hardened air content in cylinders by ASTM C457 for concrete in front of paver.....	26
Table 14. Comparison of fresh air content by the gravimetric method (ASTM C138) vs hardened air content in cylinders by ASTM C457 for concrete behind paver	27
Table 15. Paired t-tests for air contents of fresh concrete and hardened cylinders at significance level of 5%	28
Table 16. Comparison of hardened air contents (ASTM C457) of cylinders and drilled cores ..	35
Table 17. Comparison of void frequencies of cylinders and drilled cores	36
Table 18. Effect of AEA on the air content difference between cores and cylinders (percentage points)	37
Table 19. Effect of coarse aggregates on the difference in air contents between cores vs cylinders (percentage points)	38

Table 20. Effect of paver type on the difference in air contents between cores vs cylinders	39
Table 21. Effect of batch sequence on the difference in air contents between cores vs cylinders	39
Table 22. Concrete mixture proportions in preliminary tests (lb)	49
Table 23. Properties of aggregates.....	49
Table 24. Concrete mixture proportions (lb)	51
Table 25. Characteristics of hardened air voids in preliminary tests.....	55
Table 26. Properties of fresh concrete mixtures	56
Table 27. Reduction of air content due to hand-rodding for different AEAs	57
Table 28. Reduction of void frequency due to hand-rodding for different AEAs.....	57
Table 29. Drainage after 20 minutes, D_{20} , for different mixtures.....	62
Table 30. Previous research on bubble shells in cementitious systems.....	67
Table 31. Coalescence resistance of air bubbles extracted from cement paste	77
Table 32. Nanoindentation test results.....	79
Table 33. Ca/Si ratios of the bubble shells (standard deviations in parentheses)	87
Table 34. Observed and actual thicknesses and diameters of bubble shells (standard deviations in parentheses)	89

List of Figures

Figure 1.	Approximate locations of projects visited in 2014	9
Figure 2.	Sampling locations at each site.....	10
Figure 3.	Fresh air contents by pressure method vs hardened air content in cylinders by ASTM C457 for concrete in front of paver.....	17
Figure 4.	Fresh air contents by pressure method vs hardened air content in cylinders by ASTM C457 for concrete behind paver.....	17
Figure 5.	Comparison of pressure air content (ASTM C231) before paver and core air content (ASTM C457).....	20
Figure 6.	Fresh air contents by volumetric method vs hardened air content in cylinders by ASTM C457 for concrete in front of paver.....	22
Figure 7.	Fresh air contents by volumetric method vs hardened air content in cylinders by ASTM C457 for concrete behind paver.....	22
Figure 8.	Fresh air contents by gravimetric method vs hardened air content in cylinders by ASTM C457 for concrete in front of paver.....	25
Figure 9.	Fresh air contents by gravimetric method vs hardened air content in cylinders by ASTM C457 for concrete behind paver.....	25
Figure 10.	ASTM C457 air contents: cylinders vs drilled cores.....	30
Figure 11.	Difference between air contents of cores and cylinders; positive values indicate higher air content in the cores.....	31
Figure 12.	Difference between air contents of cylinders before and after paver; positive values indicate a decrease in air content after the paver.....	32
Figure 13.	Void frequency: cylinders vs drilled cores	33
Figure 14.	Spacing factor: cylinders vs drilled cores.....	34
Figure 15.	Average air contents for different AEAs.....	37
Figure 16.	Variation in the growth rate of air bubble by rectified diffusion with surface tension for a bubble of radius 50 μm , a gas saturated liquid, and an acoustic pressure amplitude of 0.22 bar, frequency of 22.1 KHz [5].....	48
Figure 17.	Vibrated specimen: (a) plan view; (b) C457 sliced sample.....	50
Figure 18.	Particles attached to air bubbles can reduce flow of the liquid film between the bubbles [13]	51

Figure 19.	An example of foam drainage in a graduated cylinder; the arrow indicates the drained liquid volume	53
Figure 20.	Comparison of hardened air contents in preliminary tests	54
Figure 21.	Reductions of air content and void frequency due to hand rodding for different AEA's (each data point is an average of three sets of samples).....	56
Figure 22.	Drainage curves for different AEA's in DI water	60
Figure 23.	Drainage curves for different AEA's in lime water	60
Figure 24.	Drainage curves for different AEA's in DI water with 5g cement	61
Figure 25.	Effect of cement on drainage for different AEA's.....	61
Figure 26.	A diagram showing key components of an AFM [15]	68
Figure 27.	AFM Testing of air bubbles in liquid: (a) Individual bubble; (b) Pair of bubbles ..	70
Figure 28.	Nanoindentation testing of a dried bubble shell	71
Figure 29.	An epoxy-embedded bubble shell for thickness measurements (not to scale)	73
Figure 30.	An example of force – displacement curve of bubble shell; red arrow indicates the linear part where the shell stiffness was determined; green arrows indicate damages in the shell	75
Figure 31.	Diagram of bubble-cantilever system; K_b and K_c are stiffness values of the bubble and cantilever respectively.....	75
Figure 32.	Comparison of average shell stiffnesses for different AEA's (10 samples per AEA)	76
Figure 33.	Shell stiffness and diameter of individual bubble shells.....	76
Figure 34.	Example of coalescence occurring during loading	77
Figure 35.	Example of coalescence occurring during holding using loading scheme b).....	78
Figure 36.	Example of coalescence occurring during unloading using loading scheme b).....	78
Figure 37.	Strengths of dried bubble shells measured using nanoindenter.....	80
Figure 38.	Punch-through failure of dried bubble shell; left: before testing; right: after failure, arrow indicates the hole punched by the nanoindenter	80
Figure 39.	Fracture failure of dried bubble shell; left: before testing; right: after failure, arrows indicate shell fragments after failure.....	81
Figure 40.	The outer surface of NVR bubble shells hydrated for 4 h and 24 h at different magnifications; blue ellipse indicates a C-S-H area; red cross indicates ettringite	82

Figure 41.	The outer surface of SYN_1 bubble shells hydrated for 4 h and 24 h at different magnifications; blue ellipse indicates a C-S-H area; red cross indicates ettringite	83
Figure 42.	The outer surface of SYN_2 bubble shells hydrated for 4 h and 24 h at different magnifications; blue ellipse indicates a C-S-H area; red cross indicates ettringite	84
Figure 43.	Inner surfaces of 4-h bubble shells for NVR (top row), SYN_1 (second row) and SYN_2 (third row); blue ellipse indicates a C-S-H area; red cross indicates ettringite; yellow rectangle indicates a membrane of unknown nature.....	85
Figure 44.	Cross section of a 4-h NVR bubble shell; blue ellipse indicates a C-S-H area	86
Figure 45.	SEM images of an epoxy-embedded bubble shell; red arrows indicate the observed thickness.....	88
Figure 46.	Observed thicknesses vs diameters of bubble shells	88
Figure 47.	Surface tensions of NVR solutions in DI and lime waters	90
Figure 48.	Surface tensions of SYN_1 solutions in DI and lime waters.....	90
Figure 49.	Surface tensions of SYN_2 solutions in DI and lime water	91
Figure 50.	Surface tensions of solutions of different AEAs in lime water; the dotted frame indicates manufacturer's recommended dosages for $w/c = 0.4$	91
Figure 51.	Formation of a cement shell on an air bubble.....	92

CHAPTER 1

INTRODUCTION

1.1 Problem Statement

Concrete infrastructure in cold climates suffers from freeze-thaw deterioration. It is widely accepted that air entrainment, a purposeful introduction of small air bubbles in concrete, is critical to the long-term durability of concrete in freeze-thaw environments. Air entraining admixtures (AEA) are added to the mixture to stabilize air bubbles created during mixing, ensuring a proper entrained air void system in the hardened concrete. The role of entrained air voids is to provide reservoirs for water displaced due to the volume increase as water turns into ice. Ice forming in the air voids can also create suction that draws water from the surrounding mesopores, reducing the pressure in these pores and providing protection to the concrete body [1]. Although the structure of the air void system is critical to concrete freeze-thaw resistance, it is hard to measure in fresh concrete. In practice, measuring the total air content of fresh concrete at the point of placement using the pressure method ASTM C231 is the most common quality control (QC) practice in the United States. Typical air contents required for concrete in wet freeze-thaw environment are 5% – 7% by volume of concrete. Despite the complexity of creating a suitable air void system in concrete, previous study and experience established the reliability and robustness of such systems under a variety of conditions through use of neutralized vinsol resin AEA products.

Vinsol resin is extracted as a byproduct of a process for recovering various solvents and rosins from pine wood and has a complex chemical composition. According to Whiting and Nagi [2], the resin is made up of approximately 60% phenolic compounds, 15% waxes and terpenes, and resin acids and is insoluble in water. To work as an AEA in concrete, it is converted into a soluble form through a neutralization process with sodium hydroxide. The product is then termed neutralized vinsol resin (NVR). In recent years, synthetic AEAs have been used more frequently due to limited supply of NVR to the concrete industry. Common synthetic AEAs are derived from sulfonic acids that are produced as byproducts in the production of lubricating oil and kerosene [2]. Examples of commercial synthetic AEAs used in concrete are sodium benzene sulfonate and sodium olefin sulfonate.

With the use of synthetic AEAs, there are more reports of new problems including difficulty in measuring the air content and sporadic clustering of air voids near aggregates [3] [4] [5]. A study sponsored through the Wisconsin Highway Research Program (WHRP) [3] showed that the air contents in hardened pavement (measured using the ASTM C457) were as much as 5 percentage points¹ higher than that in fresh concrete (measured using the ASTM C231), introducing unacceptable uncertainty to quality control (QC) of air content and properties of the air void system. On one hand, this uncertainty could lead to pavement with too much air and thus lower strength. For each percentage point of air added to the concrete, a reduction of 5% in compressive strength can be expected [2]. For plain concrete pavement, this strength loss could increase cracking and reduce its service life. On the other hand, if the air content measured in fresh concrete is low, the contractor may face significant penalties unless the actual air void system in the pavement is found by other means to be within standards.

1.2 Research Goals and Methods

The goal of this study was to find the root cause of the disparity between the air content measured with the prevailing QC test and the actual air content in concrete pavements. The biggest challenge in achieving this goal was the lack of existing techniques to evaluate performance of AEAs and air bubbles in concrete. Another challenge was that the problem was not previously identified in any repeatable and statistically valid manner. In the WHRP study mentioned above [3], issues with consolidation of concrete samples confounded the results and provided little information that identified causes. To overcome those challenges and achieve the research goal, a multi-scale study on concrete air voids was required and ultimately undertaken with the following tasks:

- a) Identify the problem(s) associated with synthetic AEAs with a reasonable level of certainty through a field study on concrete pavements in Wisconsin
- b) Establish new test protocols for micro-properties of air bubbles in a cementitious environment

¹ A percentage point is the unit for the arithmetic difference of two percentages. E.g., if the air content rises from 6% to 11%, it increases by 5 percentage points.

- c) Link the micro-properties of air bubbles with bulk properties of the air void system measured in concrete tests
- d) Evaluate robustness of AEAs used in concrete using the new test protocols

1.3 Structure

This dissertation is structured as follows:

- Chapter 1 – Introduction
- Chapter 2 – Experimental Study on the Air Void System in Wisconsin Concrete Pavements. This chapter presented a study on Wisconsin pavements to identify the problem and possible causes.
- Chapter 3 –Robustness of Concrete AEAs and Foam Drainage Test. This chapter presents experimental tests on laboratory concrete to examine the causes of the problem found in Chapter 2. The Foam Drainage Test (FDT) was evaluated for use as a tool to identify AEAs that have undesirable performance.
- Chapter 4 – Mechanical Properties and Microstructure of Bubble Shells. This chapter investigated different techniques including Atomic Force Microscopy (AFM), nanoindentation, and Scanning Electron Microscopy (SEM) to evaluate the shell of air bubble. The goal is to link micro-properties of the bubble shell with concrete test results in Chapters 2 and 3, and thus verify the cause of the problem with synthetic AEAs
- Chapter 5 – Conclusions

REFERENCES FOR CHAPTER 1

- [1] Z. Sun and G. W. Scherer, “Effect of air voids on salt scaling and internal freezing,” *CEMCON Cem. Concr. Res.*, vol. 40, no. 2, pp. 260–270, 2010.
- [2] D. Whiting and M. Nagi, *Manual on control of air content in concrete*. Skokie, Ill.: Portland Cement Association, 1998.
- [3] P. Ram, T. Van Dam, L. Sutter, G. Anzalone, and K. Smith, “Field Study of Air Content Stability in the Slipform Paving Process,” *Transp. Res. Rec. J. Transp. Res. Board*, vol. 2408, pp. 55–65, Aug. 2014.
- [4] Eickschen, “Working mechanisms of air-entraining admixtures and their subsequent activation potential,” *Am Concr Inst ACI Spec Publ Am. Concr. Inst. ACI Spec. Publ.*, vol. 288, no. 288 SP, pp. 305–315, 2012.
- [5] R. L. Kozikowski, *Factors affecting the origin of air-void clustering*. Skokie, Ill.: Portland Cement Association, 2005.

CHAPTER 2

EXPERIMENTAL STUDY ON THE AIR VOID SYSTEM IN WISCONSIN CONCRETE PAVEMENTS

2.1 Introduction

As mentioned in Chapter 1, Wisconsin Department of Transportation (WisDOT) and others have noted significant disparities between air content as measured in QC tests (using the ASTM C231) and the actual air content in hardened concrete pavement cores (using the ASTM C457) when synthetic AEAs were used in place of the NVR AEA. The objective of research reported in this chapter was to verify this problem with a reasonable level of certainty and identify causes.

There are two potential sources of the measured air content disparity. The first one is from the methods of measuring air content. ASTM C457 test of air void system in hardened concrete is generally considered the most reliable method to determine concrete air content whereas the accuracy of the ASTM C231 pressure method of measuring fresh air content is an indirect measure thought to be affected by the sizes of the air bubbles. There is concern that synthetic AEAs may reduce surface tension of air bubbles in concrete so much that many air bubbles are very small and less compressible rendering that portion of the air content more difficult to detect in the pressure method [1], [2], [3]. In response to this concern, several new methods have been developed to measure fresh concrete air content, including the Air Void Analyzer (AVA) and the Super Air Meter (SAM). An advantage of these methods over the pressure meter is the potential to provide a measurement of the air bubble size distribution; but they do not necessarily offer a more reliable measurement of the air content. There have been studies showing that in the normal range of air contents (4% - 8%) in concrete pavement where both NVR and non-NVR air entraining admixtures have been used, the pressure meter and the C457 test were in reasonable agreement [4], [5], [6], [7]. Studies by Nagi et al. (2007) [8] and Nagi and Whiting (1994) [9] showed that the difference between the two methods was generally within ± 2 percentage points.

The second potential source of the disparity between the air contents of fresh concrete and drilled cores is from the difference in the concrete samples used in the two tests. The typical quality

control air test using the ASTM C231B pressure method is almost always conducted with concrete sampled in front of the paver. This concrete is later spread, vibrated, and leveled by the slip-form paver. The operations of the paver and the setting of concrete may change the air bubble system, leading to the higher or lower air content observed in the cores extracted from the hardened concrete pavement. On the other hand, sampling may remove so many air bubbles from the concrete leading to a lower air content in QC tests. A WHRP study [10] reported abnormal differences between the pressure meter measurements and the C457 test of concrete cores. However, this study was inconclusive due to issues with consolidation of the concrete cylinders. Studies by Eickschen in Germany [11] showed that compared to wood-resin AEA, certain synthetic active agents have higher potential of reactivation and could lead to more air bubbles created and stabilized during extended mixing. On the contrary, most studies on paving and vibration showed that these activities tend to remove air bubbles from concrete instead of producing new ones [12], [13], [14], [15]. Some authors suggested that air content can significantly increase during setting of concrete [16] while others doubted this can occur in at-rest concrete [17].

To date, it is believed a problem exists, but previous studies have not identified the problem in any repeatable and statistically valid manner. The focus of the study reported in this chapter was to conduct a larger number of these tests to gain a more thorough and valid definition of the air void systems of Wisconsin field concrete associated with the use of synthetic air entraining agents. In creating this data set, the impacts on the air void system created with non-Vinsol resin AEA's before and after the paver were investigated.

2.2 Literature Review Summary

Literature is referenced in each chapter of this document to provide a context for each portion of the research. For the portion of research in this chapter, a survey of literature was conducted on the following topics and is provided in Appendix A:

- a) Accuracy of the pressure method ASTM C231
- b) Changes of air voids in fresh concrete at rest and in movement
- c) Effects of type of AEA on concrete air voids

d) Instability of air bubbles in concrete

Main findings from the survey are summarized below:

- Most studies on the discrepancy between the ASTM C231 pressure method and ASTM C457 utilized NVR or other wood-derived products rather than synthetic AEAs. The results were inconsistent. Several studies using both NVR and synthetic AEAs showed that the total fresh air content (ASTM C231) was in reasonably good agreement with the hardened air content [6], [7].
- Diffusion of air bubbles in fresh concrete at rest has been suggested as a potential source of the discrepancy between fresh and hardened air contents. Test results concerning this hypothesis, mostly with NVR, were inconsistent.
- It is known in the field of bubble dynamics that gas bubbles can grow in a fluid under an oscillating pressure field such as an acoustic field, a phenomenon called “rectified diffusion” [18]. Consolidation of concrete by vibration imposes an oscillating pressure on the air bubbles and theoretically, can make the bubbles grow. There has been no study on possible impacts of this phenomenon on concrete air void systems.
- To the authors’ knowledge, all of the previous work on effects of compaction on the concrete air void system used NVR or other wood-derived products in contrast to synthetic AEAs. Most studies found that compaction either by hand-rodding or vibration tends to reduce the air content in concrete.
- Certain synthetic AEAs have higher reactivation potential than NVR and thus could result in a significant increase of air content during extended mixing. Based on this, overdose of synthetic AEAs and short mixing time have been suggested as a potential cause of the reported high air content in pavement cores [11]. This hypothesis has been evaluated in laboratory studies but not confirmed by experiments in the field. Effects of vibration on this hypothesis have not been investigated.

2.3 Experimental Procedures

The focus of the research presented in this chapter was to gather sufficient data to examine, with a reasonable level of certainty, the relationship between air entrainment measured at the time of

construction, the air entraining agent used, and the actual void structure in the hardened pavement. This involved comparison of fresh and hardened air content measurements in concretes prepared from cementitious materials, chemical admixtures, and aggregate mineralogy relevant to concrete paving projects in the state of Wisconsin. The research team worked with WisDOT, the Wisconsin Concrete Pavement Association (WCPA) and its participating contractors to identify and gain access to project sites. Approximate locations of the projects visited are shown in Figure 1. The testing matrix is provided in Table 1.

The primary variables were measurement of the air content and air void system including:

- AASHTO T152/ASTM C231, Pressure method,
- AASHTO T121/ASTM C138, Gravimetric method
- AASHTO T196/ASTM C 173, Volumetric method, and
- ASTM C457, Hardened Concrete Air Void, Method A, Linear traverse

Secondary variables were recorded, including:

- Mix variables including coarse aggregate type, AEA type, cementitious materials
- Paving temperature and general weather conditions at time of sampling,
- Batch plant sequence of AEA introduction,
- Typical haul time from batch plant to sampling location,
- Paver type and vibration characteristics.

At each site, the following tests and samples were taken:

- AASHTO T119/ASTM C143, Slump of concrete
- AASHTO T309/ASTM C1064, Temperature of concrete
- AASHTO T152/ASTM C231, Pressure method

- AASHTO T121/ASTM C138, Gravimetric method
- AASHTO T196/ASTM C 173, Volumetric method
- One cylinder before paver, one cylinder after paver, and one drilled core. The cylinders were compacted by hand-rodding.

Tests of fresh air contents were conducted for concrete before and after the paver. Tests of concrete slump and temperature were taken before the paver only. A diagram of sampling locations at each site is provided in Figure 2.

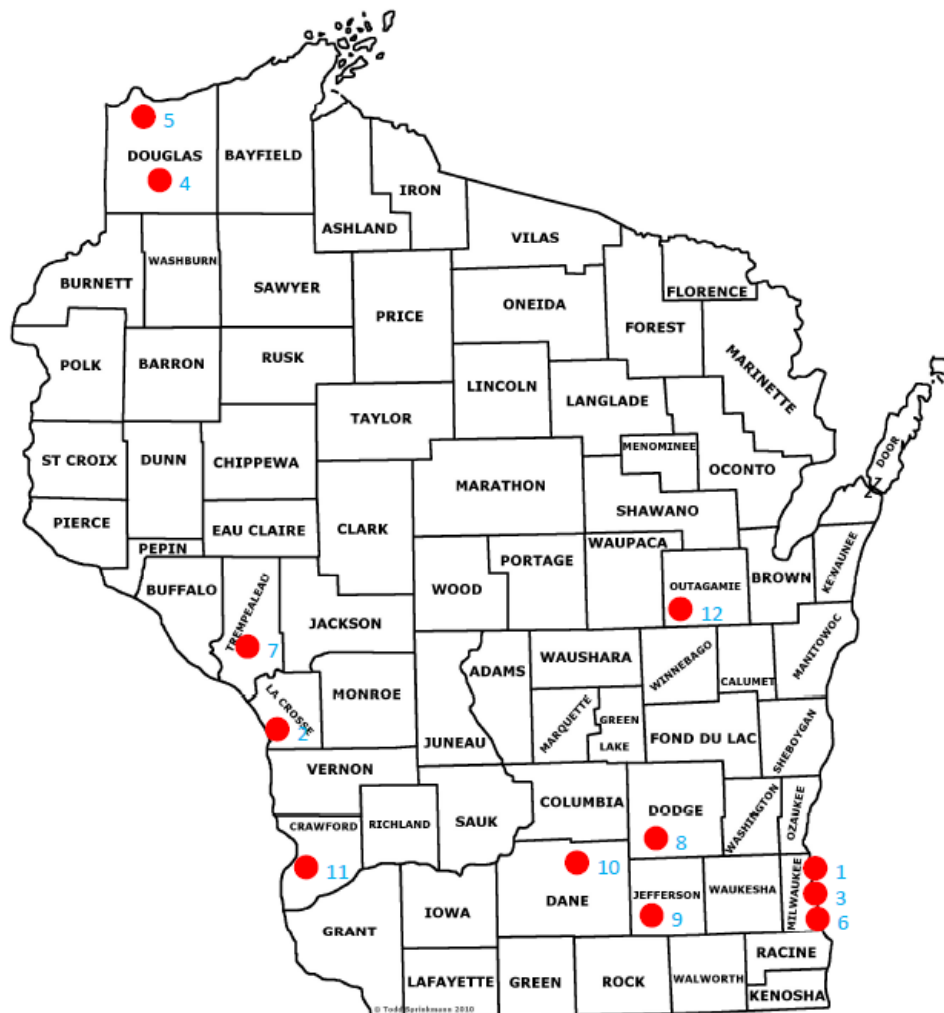


Figure 1. Approximate locations of projects visited in 2014

Table 1. Testing Matrix

Coarse aggregate types	Crushed limestone	Gravel
From previous projects (2013)		
WisDOT cores	4	1
Total ASTM C457 Tests	4	1
Field testing by research team (2014)		
Projects visited	8	4
Sample sites per project	2	2-4
Unique samples taken per site (2 cylinders & 1 core)	3	3
Total ASTM C457 tests from cylinders and cores	48	30
AASHTO T121/ASTM C138 (Gravimetric)	32	20
AASHTO T152/ASTM C231 (Pressure)	32	20
AASHTO T196/ASTM C173 (Volumetric)	32	20

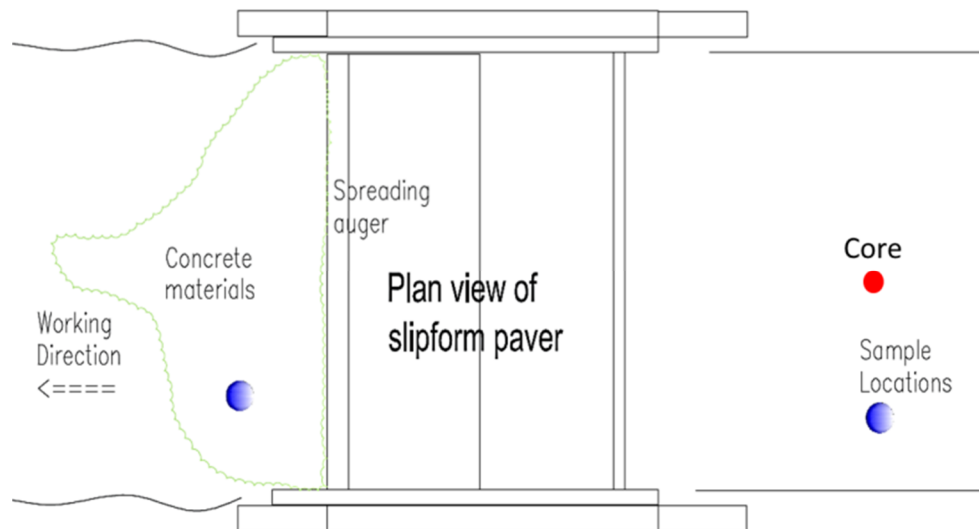


Figure 2. Sampling locations at each site

2.4 Project Data

2.4.1 MIX DESIGN

Mix characteristics associated with WisDOT cores from 2013-projects are presented in Table 2 and projects visited in 2014 are presented in Table 3. In most projects, mixes of Portland cement and 15-30% Class C fly ash were used. Among the projects visited in 2014, ten projects used synthetic AEA products and two projects used NVR or chemically similar products. In Table 2 and Table 3, SYN_1 and SYN_1A are synthetic AEAs based on sodium (C14-16) olefin sulfonate from two different manufacturers, NVR_1 is an aqueous solution of NVR, and NVR_2 is described by the manufacturer as a saponified rosin that is chemically similar to NVR.

2.4.2 CONSTRUCTION PARAMETERS

Construction parameters of the projects visited in 2014 are presented in Table 4. In most projects, concrete was mixed at a mobile or central plant for 60 seconds and delivered to the site in dump trucks. Haul time from the plant to the site ranged from 5 to 30 minutes. There were two main types of slip-form pavers. Type-I pavers have a spreader plow which spreads concrete without a rotating action. Type-II pavers have spreader augers which rotate to move concrete from the middle to the sides of the paving lane. The vibration frequency of each paver was generally between 6000 and 8500 vibrations per minute (vpm). Admixtures (water reducer and air entraining agent) were generally not mixed together before being dispersed into the mixing drum (sequences A and B) except for two projects (No. 3 and No. 11) where it was reported that both admixtures had been added to the water tank before mixing started.

Table 2. Mix characteristics of WisDOT cores in 2013 (Quantities per cubic yard of concrete)

Project No.	Region	Mix Type ⁽¹⁾	Coarse Aggregate Type	Type I Cement (lb)	Class C Fly Ash (lb)	w/cm	AEA Type	Water reducer C494 Type
I	SE	AFA 30%	Crushed stone	395	170	0.37	SYN_1	A
II	NE	AFA 30%	Crushed stone	396	170	0.37	unknown	unknown
III	SW	AFA 30%	Crushed stone	395	170	0.43	SYN_1	A
IV	NE	AFA 30%	Crushed stone	395	170	0.37	SYN_1	A
V	SW	AFA 30%	Gravel	395	170	0.37	SYN_1	A

⁽¹⁾ AFA 30% indicates a mixture using 30% fly ash by weight of cementitious materials

Table 3. Mix characteristics of projects visited in 2014 (Quantities per cubic yard of concrete)

Project No.	Region	Mix Type ⁽¹⁾	Coarse Aggregate Type	Type I Cement (lb)	Class C Fly Ash (lb)	Grade 100 Slag (lb)	w/cm	AEA Type	Water reducer C494 Type ⁽²⁾	Other admixtures C494 Type ⁽²⁾
1	SE	AFA 30%	Crushed stone	395	170	none	0.37	SYN_1	A	
2	SW	AFA 30%	Crushed stone	395	170	none	0.40	SYN_1	A	
3	SE	AFA 30%	Crushed stone	395	170	none	0.36	SYN_1A	A,F	B,D
4	NW	AFA 15%	Crushed stone	480	85	none	0.40	SYN_1	A	
5	NW	AFA 15%	Gravel	480	85	none	0.37	SYN_1	A	
6	SE	AFA 30%	Gravel	395	170	none	0.42	SYN_1A	A,B,D	
7	NW	AFA 30%	Crushed stone	395	170	none	0.42	SYN_1	A	
8	SW	AFA 30%	Crushed stone	395	170	none	0.40	SYN_1A	A,B,D	
9	SW	AFA 30%	Gravel	395	170	none	0.38	SYN_1	A	
10	SW	AFA 30%	Gravel	395	170	none	0.37	SYN_1	A	
11	SW	ASA	Crushed stone	452	none	113	0.35	NVR_2	A,D	
12	NE	AFA 20%	Crushed stone	455	110	none	0.41	NVR_1	A,D	

⁽¹⁾ AFA 30% indicates a mixture using 30% fly ash by weight of cementitious materials; ASA indicates a mixture using slag cement

⁽²⁾ ASTM C494 admixture type: A-Water reducing admixtures, B-Retarding admixtures, D-Water reducing and retarding admixtures, E-Water reducing and accelerating admixtures

Table 4. Construction parameters of projects visited in 2014

Project No.	Mixing plant type	Mix time (sec)	Haul time from plant to site (min)	Haul truck type	Paver Type ⁽¹⁾	Vibration frequency (vpm)	Batch plant sequence of AEA ⁽²⁾
1	Mobile	90	15-30	Dump	I-A	unknown	unknown
2	unknown	unknown	15-30	Dump	II-A	7000-8000	A
3	Central	unknown	5-10	Agitator	II-A	unknown	C
4	Central	60	15-30	Dump	II-A	7000-8000	A
5	Mobile	60	10-20	Dump	II-A	unknown	A
6	Mobile	60	10-15	Dump	II-A	7500-8000	B
7	Mobile	60	5-10	Dump	II-A	7000-8000	A
8	Central	60	5-10	Dump	I-B	unknown	A
9	Central	60	5-10	Dump	I-B	unknown	B
10	Central	60	20-30	Dump	II-B	8500	B
11	Truck	6 min.	15-30	Mixing	II-A	6000	D
12	Mobile	100	15-20	Agitator	II-A	unknown	A

⁽¹⁾ I-A: Spreader plow; I-B: Spreader plow with bar inserter; II-A: Spreader auger; II-B: Spreader auger with bar inserter.

⁽²⁾ A: Dry materials (aggregates, cementitious materials), then AEA, WR, and water are charged into the water line at the same time; B: same as A, but AEA is sprayed directly into mixing drum; C: All admixtures are poured into the water tank, then 80% of mix water into the mixing drum, aggregates, cementitious materials, and 20% of mix water; D: same as C, but truck mixing

2.5 Results

2.5.1 AIR VOID ANALYSIS OF WISDOT CORES (PROJECTS OF 2013)

Results of C457 testing of five cores from 2013-projects are compared with those of the QC air tests conducted at locations nearest to the cores in Table 5. The difference between air contents in the cores and QC air tests varied from -0.1 to 1.7 percentage points. On average, cores had higher air contents than in QC tests by 0.7 percentage points. Spacing factors of all the cores were lower than 0.008 in, the value commonly recommended for adequate freeze-thaw durability (ACI 201.2R).

Table 5. Comparison of C457 results of WisDOT cores and QC air contents

Project	QC Air content (Pressure)	Core air content (ASTM C457)	Core - Pressure	1 - Pressure/Core	Core spacing factor
No.	%	%	%	%	in.
I	6.5	7.4	0.9	12.2	0.005
II	6.0	7.7	1.7	22.1	0.005
III	7.8	7.7	-0.1	-1.3	0.004
IV	8.4	8.7	0.3	3.4	0.004
V	7.0	7.8	0.8	10.3	0.005
Max	8.4	8.7	1.7	22.1	0.005
Min	6.0	7.4	-0.1	-1.3	0.004
Average	7.1	7.9	0.7	9.3	0.004

2.5.2 FRESH CONCRETE PROPERTIES OF PROJECTS VISITED IN 2014

Slump, concrete and ambient temperatures, and fresh air contents by the pressure meter (ASTM C231) are presented in Table 6. The samples for these tests were taken from concrete on the ground in front of the paver. In the site ID, the first number represents the project, and the second number is the testing site.

Table 6. Properties of fresh concrete sampled in front of the paver

Site ID	Slump	Air Temp.	Concrete Temp.	Pressure Air Content (ASTM C231)
	in	°F	°F	%
1-1	1.25	70	70	5.0
1-2	0.25	76	80	4.7
2-1	1.75	80	74	7.4
2-2	2.75	85	75	8.5
3-1	2.00	80	80	7.8
3-2	1.25	80	80	6.9
4-2	1.25	75	65	5.9
4-3	1.00	75	75	6.0
5-1	1.25	70	70	6.6
5-2	1.50	71	70	5.3
5-3	2.50	72	72	6.1
6-1	0.25	76	76	4.8
6-2	1.25	82	82	8.6
7-1	0.75	75	75	5.4
7-2	0.75	75	75	6.2
8-1	1.00	73	73	5.4
8-2	0.75	80	79	6.1
9-1	1.25	70	70	7.1
9-2	1.00	75	75	6.9
10-1	1.00	77	77	8.8
10-3	1.50	78	78	7.8
10-4	0.50	83	83	6.7
11-1	1.50	75	73	7.7
11-2	2.00	80	76	8.3
12-1	1.50	80	76	6.5
12-2	-	-	-	6.0

2.5.3 AIR CONTENTS OF FRESH AND HARDENED CONCRETES

2.5.3.1 Air contents by different methods

Air contents of concrete before and after the paver by different methods are presented in Table 7. Fresh concrete samples taken in front of the paver tend to be slightly higher in air content than those taken behind the paver.

Table 7. Air contents by different methods (%)

Site ID	In front of the paver				Behind the paver				
	Gravimetric ASTM C138	Pressure ASTM C231	Volumetric ASTM C173	Cylinder ASTM C457	Gravimetric ASTM C138	Pressure ASTM C231	Volumetric ASTM C173	Cylinder ASTM C457	Core ASTM C457
1-1	5.9	5.0	5.5	5.6	6.3	5.2	5.3	5.9	6.7
1-2	5.5	4.7	5.3	5.1	6.5	5.5	5.8	6.1	6.6
2-1	5.9	7.4	7.8	6.7	5.5	6.6	6.5	5.7	9.9
2-2	7.9	8.5	9.3	8.6	5.5	6.7	7.3	7.6	8.4
3-1	10.2	7.8	7.3	6.4	7.0	5.5	5.8	5.9	8.0
3-2	7.6	6.9	7.0	7.5	6.8	5.7	5.5	6.3	7.6
4-2	6.2	5.9	6.8	5.4	6.0	5.5	6.0	6.4	5.9
4-3	5.4	6.0	7.0	7.5	5.1	5.7	6.8	5.6	8.3
5-1	4.9	6.6	7.3	5.5	6.8	7.9	8.0	7.5	10.1
5-2	3.4	5.3	6.3	4.3	4.7	6.4	7.0	6.5	9.2
5-3	5.2	6.1	7.3	5.5	5.9	7.3	8.3	7.2	9.3
6-1	4.3	4.8	6.0	4.6	4.8	5.4	5.8	6.1	7.7
6-2	8.4	8.6	8.8	6.6	6.1	6.7	6.5	5.1	7.6
7-1	5.3	5.4	6.0	5.8	4.2	4.6	5.0	5.1	6.0
7-2	5.8	6.2	7.0	6.0	4.1	4.9	5.3	4.8	7.0
8-1	4.0	5.4	5.8	5.3	2.6	4.1	5.0	4.5	6.3
8-2	3.9	6.1	6.0	5.0	2.3	4.8	4.8	4.0	6.0
9-1	5.2	7.1	7.8	5.8	5.2	6.4	6.5	6.0	9.4
9-2	5.7	6.9	8.5	5.6	4.8	6.3	7.3	5.4	9.8
10-1	8.4	8.8	8.3	7.6	6.6	7.6	7.5	8.1	8.7
10-3	7.6	7.8	7.8	6.5	5.7	6.5	6.5	5.6	7.9
10-4	6.1	6.7	7.0	6.0	4.8	5.7	6.0	5.3	8.2
11-1	8.2	7.7	8.0	6.9	7.8	6.7	6.8	5.8	7.2
11-2	8.9	8.3	9.0	7.1	5.7	5.7	6.0	5.1	5.0
12-1	5.0	6.5		5.0	2.9	4.9		5.0	4.3
12-2	4.7	6.0		5.1	3.2	5.0		4.0	5.6

2.5.3.2 Comparison of air contents by the pressure method (ASTM C231) and ASTM C457

The differences between fresh air content measured by the pressure meter and hardened air content in cylinders for both concretes in front of and behind paver were within $\pm 2\%$ as shown in Figure 3 and Figure 4 as deviations from the line of equality. On average, air contents of the hardened cylinders (by C457) were lower than the fresh air contents by 0.6 percentage points for concrete

in front of the paver, and by 0.1 percentage points for concrete behind the paver (Table 8 and Table 9). These differences are in the normal range that has been reported in the literature [8], [14].

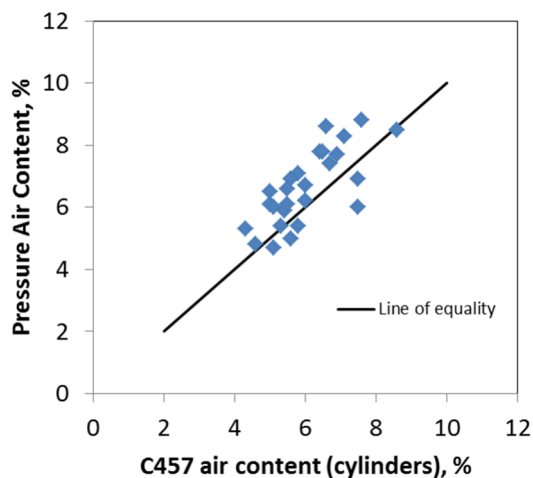


Figure 3. Fresh air contents by pressure method vs hardened air content in cylinders by ASTM C457 for concrete in front of paver

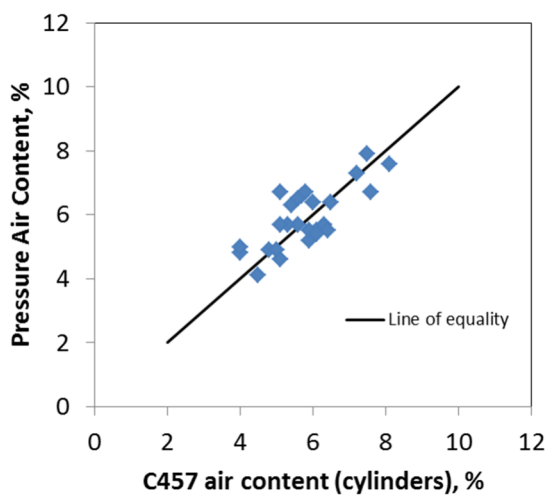


Figure 4. Fresh air contents by pressure method vs hardened air content in cylinders by ASTM C457 for concrete behind paver

Table 8. Comparison of fresh air content by pressure method and hardened air content by ASTM C457 of concrete in front of paver

Site ID	Fresh air content (Pressure)	Hardened air content (C457)	Hardened - Fresh	(1-Fresh/Hardened)x100
	%	%	%	%
1-1	5.0	5.6	0.6	11
1-2	4.7	5.1	0.4	8
2-1	7.4	6.7	-0.7	-10
2-2	8.5	8.6	0.1	1
3-1	7.8	6.4	-1.4	-22
3-2	6.9	7.5	0.6	8
4-2	5.9	5.4	-0.5	-9
4-3	6.0	7.5	1.5	20
5-1	6.6	5.5	-1.1	-20
5-2	5.3	4.3	-1.0	-23
5-3	6.1	5.5	-0.6	-11
6-1	4.8	4.6	-0.2	-4
6-2	8.6	6.6	-2.0	-30
7-1	5.4	5.8	0.4	7
7-2	6.2	6.0	-0.2	-3
8-1	5.4	5.3	-0.1	-2
8-2	6.1	5.0	-1.1	-22
9-1	7.1	5.8	-1.3	-22
9-2	6.9	5.6	-1.3	-23
10-1	8.8	7.6	-1.2	-16
10-3	7.8	6.5	-1.3	-20
10-4	6.7	6.0	-0.7	-12
11-1	7.7	6.9	-0.8	-12
11-2	8.3	7.1	-1.2	-17
12-1	6.5	5.0	-1.5	-30
12-2	6.0	5.1	-0.9	-18
Max	8.8	8.6	1.5	20
Min	4.7	4.3	-2.0	-30
Average	6.6	6.0	-0.6	-10
Stand. Dev.	1.2	1.0	0.8	13

Table 9. Comparison of fresh air content by pressure method and hardened air content by ASTM C457 of concrete behind paver

Site ID	Fresh air content (Pressure)	Hardened air content (C457)	Hardened - Fresh	(1-Fresh/Hardened)x100
	%	%	%	%
1-1	5.2	5.9	0.7	12
1-2	5.5	6.1	0.6	10
2-1	6.6	5.7	-0.9	-16
2-2	6.7	7.6	0.9	12
3-1	5.5	5.9	0.4	7
3-2	5.7	6.3	0.6	10
4-2	5.5	6.4	0.9	14
4-3	5.7	5.6	-0.1	-2
5-1	7.9	7.5	-0.4	-5
5-2	6.4	6.5	0.1	2
5-3	7.3	7.2	-0.1	-1
6-1	5.4	6.1	0.7	11
6-2	6.7	5.1	-1.6	-31
7-1	4.6	5.1	0.5	10
7-2	4.9	4.8	-0.1	-2
8-1	4.1	4.5	0.4	9
8-2	4.8	4.0	-0.8	-20
9-1	6.4	6.0	-0.4	-7
9-2	6.3	5.4	-0.9	-17
10-1	7.6	8.1	0.5	6
10-3	6.5	5.6	-0.9	-16
10-4	5.7	5.3	-0.4	-8
11-1	6.7	5.8	-0.9	-16
11-2	5.7	5.1	-0.6	-12
12-1	4.9	5.0	0.1	2
12-2	5.0	4.0	-1.0	-25
Max	7.9	8.1	0.9	14
Min	4.1	4.0	-1.6	-31
Average	5.9	5.8	-0.1	-3
Stand. Dev.	0.9	1.0	0.7	13

2.5.3.3 Comparison of pressure air content (ASTM C231) before paver and core air content (ASTM C457)

The pressure meter air content measured from samples in front of the paver represents what typically constitutes the quality control measure. The core air content best reflects the true air

content of the pavement. The difference between these two values has implications especially for contractors who are held to specification requirements. The values of air content measured by the pressure meter before the paver and hardened air content in cores are shown with their differences in Table 10. On average the core air content was 0.9 percentage points or almost a full percent higher than the pressure meter reading, however, differences exceeding ± 3 percentage points occurred. As shown in Figure 5 considerable variability existed in these measurements but with 70% of comparison points falling below the line of equality, the cores tended to have consistently higher air contents than would be indicated by the pressure meter test.

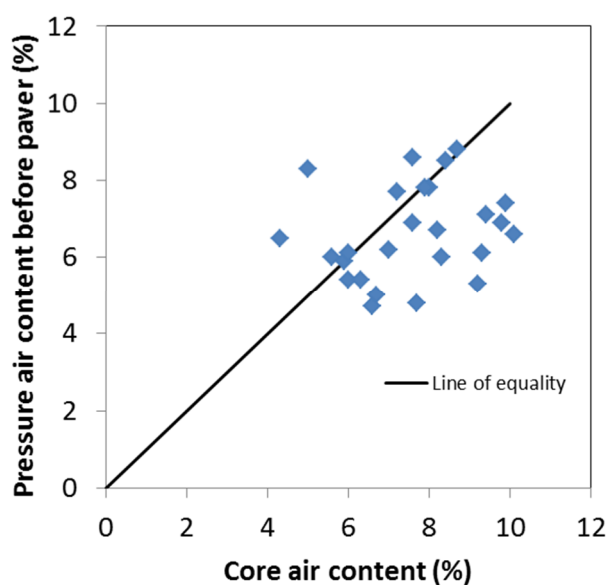


Figure 5. Comparison of pressure air content (ASTM C231) before paver and core air content (ASTM C457)

Table 10. Comparison of pressure air content (ASTM C231) before paver and core air content (ASTM C457)

Site ID	Pressure (C231)	Core (C457)	Core - Pressure
	%	%	%
1-1	5.0	6.7	1.7
1-2	4.7	6.6	1.9
2-1	7.4	9.9	2.5
2-2	8.5	8.4	-0.1
3-1	7.8	8.0	0.2
3-2	6.9	7.6	0.7
4-2	5.9	5.9	0.0
4-3	6.0	8.3	2.3
5-1	6.6	10.1	3.5
5-2	5.3	9.2	3.9
5-3	6.1	9.3	3.2
6-1	4.8	7.7	2.9
6-2	8.6	7.6	-1.0
7-1	5.4	6.0	0.6
7-2	6.2	7.0	0.8
8-1	5.4	6.3	0.9
8-2	6.1	6.0	-0.1
9-1	7.1	9.4	2.3
9-2	6.9	9.8	2.9
10-1	8.8	8.7	-0.1
10-3	7.8	7.9	0.1
10-4	6.7	8.2	1.5
11-1	7.7	7.2	-0.5
11-2	8.3	5.0	-3.3
12-1	6.5	4.3	-2.2
12-2	6.0	5.6	-0.4
Max	8.8	10.1	3.9
Min	4.7	4.3	-3.3
Average	6.6	7.6	0.9
Stand. Dev.	1.2	1.5	1.7

2.5.3.4 Comparison of air contents by the volumetric method (ASTM C173) and ASTM C457

The differences between fresh air content measured by the volumetric method and hardened air content in cylinders for concretes in front of and behind paver were mostly within ± 2 percentage points as shown in Figure 6 and Figure 7 as deviations from the line of equality. On average, air

contents of the hardened cylinders were lower than the fresh air contents by 1.1 percentage points for concrete in front of paver, and by 0.4 percentage points for concrete behind paver (Table 11 and Table 12). Fresh air content by the volumetric method was generally higher than measurements by the other methods and also higher than hardened air content of cylinder by ASTM C457.

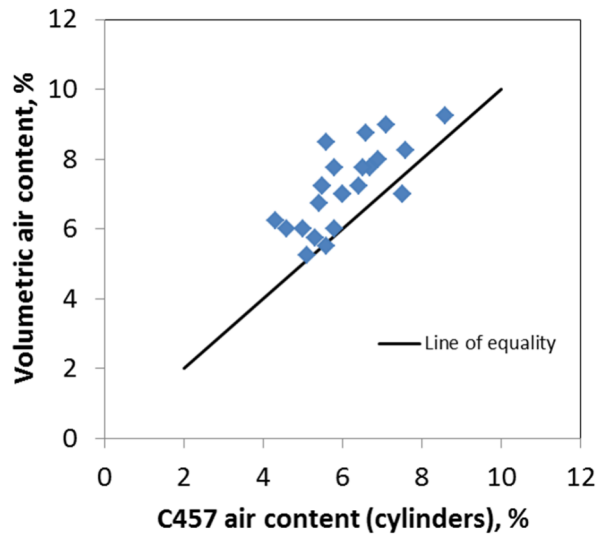


Figure 6. Fresh air contents by volumetric method vs hardened air content in cylinders by ASTM C457 for concrete in front of paver

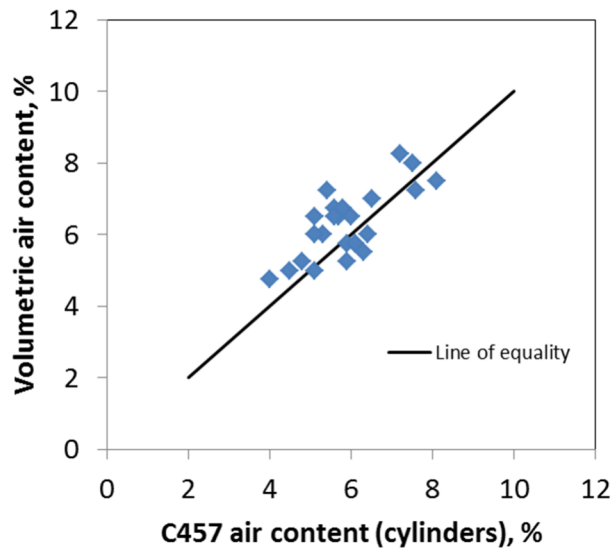


Figure 7. Fresh air contents by volumetric method vs hardened air content in cylinders by ASTM C457 for concrete behind paver

Table 11. Comparison of fresh air content by volumetric method (ASTM C173) and hardened air content by ASTM C457 of concrete in front of paver

Site ID	Fresh air content (Volumetric)	Hardened air content (C457)	Hardened - Fresh	(1-Fresh/Hardened)x100
	%	%	%	%
1-1	5.5	5.6	0.1	2
1-2	5.3	5.1	-0.2	-3
2-1	7.8	6.7	-1.1	-16
2-2	9.3	8.6	-0.7	-8
3-1	7.3	6.4	-0.9	-13
3-2	7.0	7.5	0.5	7
4-2	6.8	5.4	-1.4	-25
4-3	7.0	7.5	0.5	7
5-1	7.3	5.5	-1.8	-32
5-2	6.3	4.3	-2.0	-45
5-3	7.3	5.5	-1.8	-32
6-1	6.0	4.6	-1.4	-30
6-2	8.8	6.6	-2.2	-33
7-1	6.0	5.8	-0.2	-3
7-2	7.0	6.0	-1.0	-17
8-1	5.8	5.3	-0.5	-8
8-2	6.0	5.0	-1.0	-20
9-1	7.8	5.8	-2.0	-34
9-2	8.5	5.6	-2.9	-52
10-1	8.3	7.6	-0.7	-9
10-3	7.8	6.5	-1.3	-19
10-4	7.0	6.0	-1.0	-17
11-1	8.0	6.9	-1.1	-16
11-2	9.0	7.1	-1.9	-27
Max	9.3	8.6	0.5	7
Min	5.3	4.3	-2.9	-52
Average	7.2	6.1	-1.1	-18
Stand. Dev.	1.1	1.0	0.8	15

Table 12. Comparison of fresh air content by volumetric method (ASTM C173) and hardened air content by ASTM C457 of concrete behind paver

Site ID	Fresh air content (Volumetric)	Hardened air content (C457)	Hardened - Fresh	(1-Fresh/Hardened)x100
	%	%	%	%
1-1	5.2	5.9	0.7	11
1-2	5.7	6.1	0.4	6
2-1	6.5	5.7	-0.8	-14
2-2	7.2	7.6	0.4	5
3-1	5.7	5.9	0.2	3
3-2	5.5	6.3	0.8	13
4-2	6.0	6.4	0.4	6
4-3	6.8	5.6	-1.2	-21
5-1	8.0	7.5	-0.5	-7
5-2	7.0	6.5	-0.5	-8
5-3	8.3	7.2	-1.1	-15
6-1	5.7	6.1	0.4	6
6-2	6.5	5.1	-1.4	-27
7-1	5.0	5.1	0.1	2
7-2	5.3	4.8	-0.5	-9
8-1	5.0	4.5	-0.5	-11
8-2	4.8	4.0	-0.8	-19
9-1	6.5	6.0	-0.5	-8
9-2	7.3	5.4	-1.9	-34
10-1	7.5	8.1	0.6	7
10-3	6.5	5.6	-0.9	-16
10-4	6.0	5.3	-0.7	-13
11-1	6.8	5.8	-1.0	-16
11-2	6.0	5.1	-0.9	-18
Max	8.3	8.1	0.8	13
Min	4.8	4.0	-1.9	-34
Average	6.3	5.9	-0.4	-7
Stand. Dev.	0.9	1.0	0.7	12

2.5.3.5 Comparison of air contents by the gravimetric method (ASTM C138) and ASTM C457

The differences between fresh air content measured by gravimetric method and hardened air content in cylinders for concretes in front of and behind the paver were mostly within $\pm 2\%$ of air content as shown in Figure 8 and Figure 9 as deviations from the line of equality. On average, air contents of the hardened cylinders were lower than the fresh air contents by 0.1 percentage points

for concrete in front of paver, and higher by 0.5 percentage points for concrete behind paver (Table 13 and Table 14).

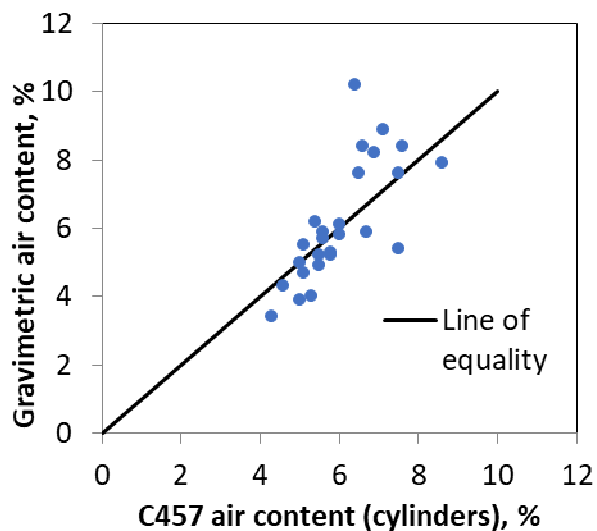


Figure 8. Fresh air contents by gravimetric method vs hardened air content in cylinders by ASTM C457 for concrete in front of paver

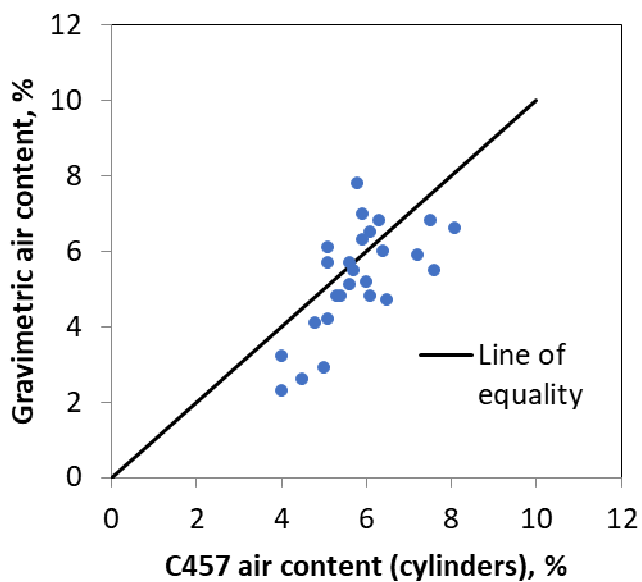


Figure 9. Fresh air contents by gravimetric method vs hardened air content in cylinders by ASTM C457 for concrete behind paver

Table 13. Comparison of fresh air content by the gravimetric method (ASTM C138) vs hardened air content in cylinders by ASTM C457 for concrete in front of paver

Site ID	Fresh air content (Gravimetric)	Hardened air content (C457)	Hardened - Fresh	(1-Fresh/Hardened)x100
	%	%	%	%
1-1	5.9	5.6	-0.3	-5
1-2	5.5	5.1	-0.4	-8
2-1	5.9	6.7	0.8	12
2-2	7.9	8.6	0.7	8
3-1	10.2	6.4	-3.8	-59
3-2	7.6	7.5	-0.1	-1
4-2	6.2	5.4	-0.8	-15
4-3	5.4	7.5	2.1	28
5-1	4.9	5.5	0.6	11
5-2	3.4	4.3	0.9	21
5-3	5.2	5.5	0.3	5
6-1	4.3	4.6	0.3	7
6-2	8.4	6.6	-1.8	-27
7-1	5.3	5.8	0.5	9
7-2	5.8	6.0	0.2	3
8-1	4.0	5.3	1.3	25
8-2	3.9	5.0	1.1	22
9-1	5.2	5.8	0.6	10
9-2	5.7	5.6	-0.1	-2
10-1	8.4	7.6	-0.8	-11
10-3	7.6	6.5	-1.1	-17
10-4	6.1	6.0	-0.1	-2
11-1	8.2	6.9	-1.3	-19
11-2	8.9	7.1	-1.8	-25
12-1	5.0	5.0	0.0	0
12-2	4.7	5.1	0.4	8
Max	10.2	8.6	2.1	28
Min	3.4	4.3	-3.8	-59
Average	6.1	6.0	-0.1	-1
Stand. Dev.	1.7	1.0	1.2	19

Table 14. Comparison of fresh air content by the gravimetric method (ASTM C138) vs hardened air content in cylinders by ASTM C457 for concrete behind paver

Site ID	Fresh air content (Gravimetric)	Hardened air content (C457)	Hardened - Fresh	(1-Fresh/Hardened)x100
	%	%	%	%
1-1	6.3	5.9	-0.4	-7
1-2	6.5	6.1	-0.4	-7
2-1	5.5	5.7	0.2	4
2-2	5.5	7.6	2.1	28
3-1	7.0	5.9	-1.1	-19
3-2	6.8	6.3	-0.5	-8
4-2	6.0	6.4	0.4	6
4-3	5.1	5.6	0.5	9
5-1	6.8	7.5	0.7	9
5-2	4.7	6.5	1.8	28
5-3	5.9	7.2	1.3	18
6-1	4.8	6.1	1.3	21
6-2	6.1	5.1	-1.0	-20
7-1	4.2	5.1	0.9	18
7-2	4.1	4.8	0.7	15
8-1	2.6	4.5	1.9	42
8-2	2.3	4.0	1.7	43
9-1	5.2	6.0	0.8	13
9-2	4.8	5.4	0.6	11
10-1	6.6	8.1	1.5	19
10-3	5.7	5.6	-0.1	-2
10-4	4.8	5.3	0.5	9
11-1	7.8	5.8	-2.0	-34
11-2	5.7	5.1	-0.6	-12
12-1	2.9	5.0	2.1	42
12-2	3.2	4.0	0.8	20
Max	7.8	8.1	2.1	43
Min	2.3	4.0	-2.0	-34
Average	5.3	5.8	0.5	9
Stand. Dev.	1.4	1.0	1.0	19

2.5.3.6 Statistical analysis of fresh air contents and hardened air contents

Paired t-tests were conducted to evaluate the significance (at 5%) of the mean differences between ASTM C457 hardened air content of the concrete cylinders and fresh air contents by different methods. The statistical results in Table 15 and the mean differences in Table 8 to Table 14 indicate that:

- Compared with ASTM C457, the pressure method overestimated the total air content for concrete in front of the paver with the mean difference of 0.6% (Table 8). For concrete behind the paver, the mean difference between the two methods was not statistically significant. Comparing the C457 measurement from the cores to the pressure method measurements suggest that pressure method compliance measurements tend to be almost 1 percent lower on average than actual air contents in the pavement.
- Compared with ASTM C457, the volumetric method overestimated the total air content for both concrete in front of and behind the paver; the mean differences were 1.1% and 0.4% respectively (Table 11 and Table 12).
- Compared with ASTM C457, the gravimetric method underestimated the total air content for concrete behind the paver with the mean difference of 0.5% (Table 14). For concrete in front of the paver, the mean difference between the two methods was not statistically significant.

Table 15. Paired t-tests for air contents of fresh concrete and hardened cylinders at significance level of 5%

Air measurement methods	Concrete in front of paver	Concrete behind paver
Pressure vs C457	Yes	No
Volumetric vs C457	Yes	Yes
Gravimetric vs C457	No	Yes

2.5.4 CHARACTERISTICS OF HARDENED AIR VOIDS IN CYLINDERS AND CORES

2.5.4.1 Total air content (ASTM C457) in cylinders and cores

The air contents (ASTM C457) in drilled cores were generally higher than in both the front and back-of-paver cylinders as shown in Figure 10. The difference between air contents in the cores and front cylinders varied from -2.1 to 4.9 percentage points with an average of 1.6 percentage points as shown in Figure 11 and listed in Table 16. The difference in the case of the cores and back cylinders varied from -0.7 to 4.4 percentage points with an average of 1.8 percentage points. On average air contents in the cores were 1.6 percentage points higher than in the front cylinders and 1.8 percentage points higher than in the back cylinders.

Air content in the back cylinder was lower than that in the front cylinder in some cases, but higher in other cases as shown in Figure 12. On average, the difference in air content between the front and back cylinders was only 0.2 percentage points.

2.5.4.2 Void frequency in cylinders vs drilled cores

Void frequencies (number of voids per inch) in drilled cores were generally higher than in both front and back cylinders as shown in Figure 13. The difference in percentage between void frequencies in the core and the front cylinder varied from -12% to 39% (Table 17). The difference in percentage between void frequencies in the core and the back cylinder varied from -33% to 43%. On average the core had 21% more air voids than the front cylinder and 19% more air voids than the back cylinder.

2.5.4.3 Spacing factor in cylinders vs drilled cores

The spacing factor of each of the tested cylinders and cores was below the recommended value of 0.008 in. Spacing factors in drilled cores were generally smaller than in both front and back-of-paver cylinders as shown in Figure 14. This agrees with the fact that there were more air bubbles and higher air content in the cores.

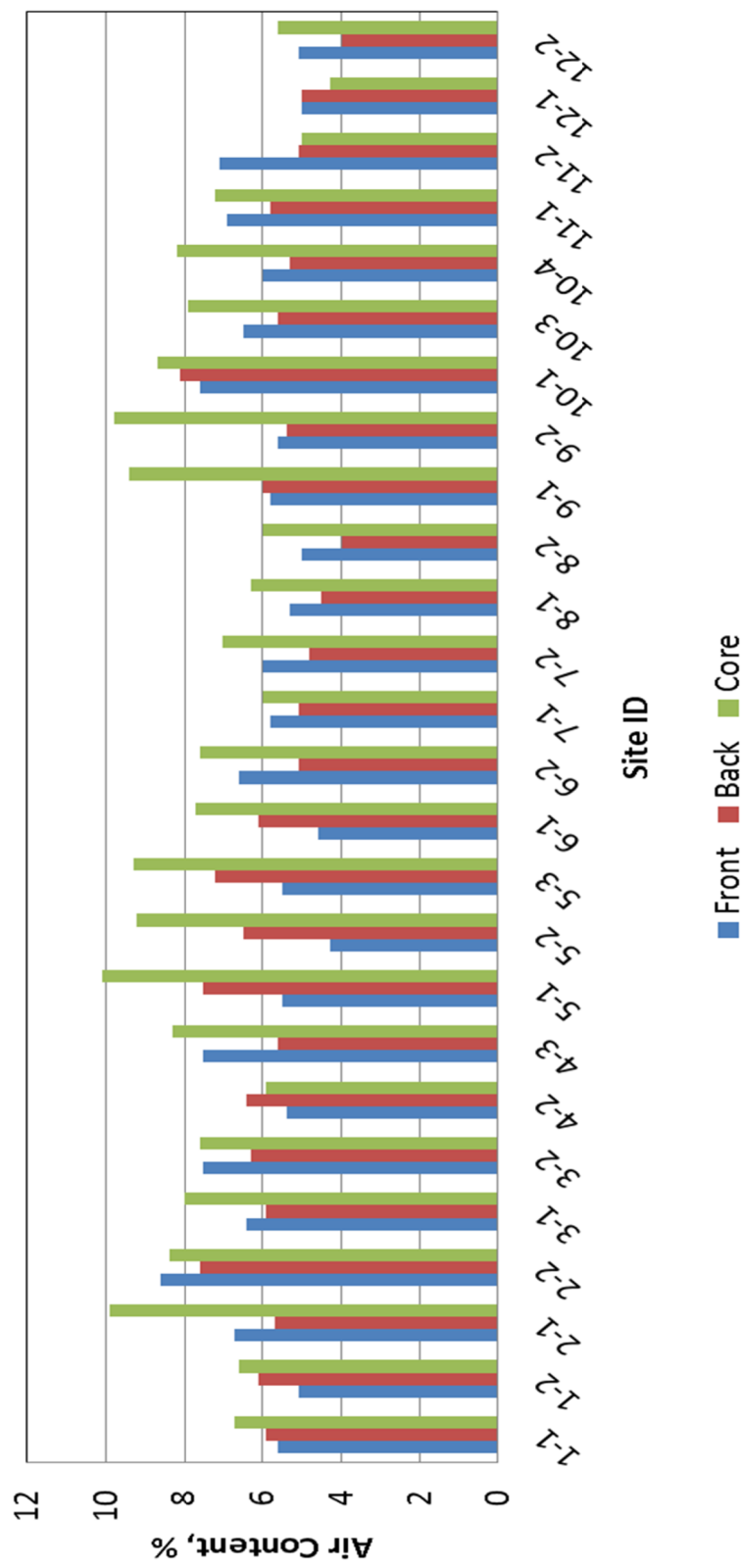


Figure 10. ASTM C457 air contents: cylinders vs drilled cores

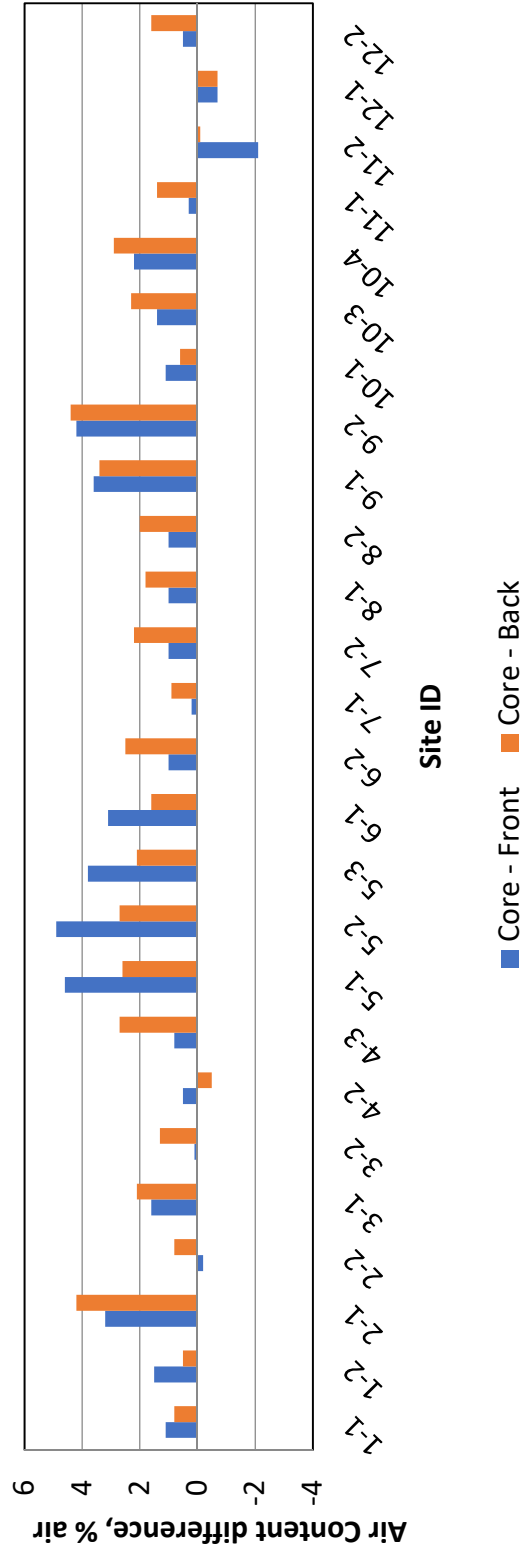


Figure 11. Difference between air contents of cores and cylinders; positive values indicate higher air content in the cores

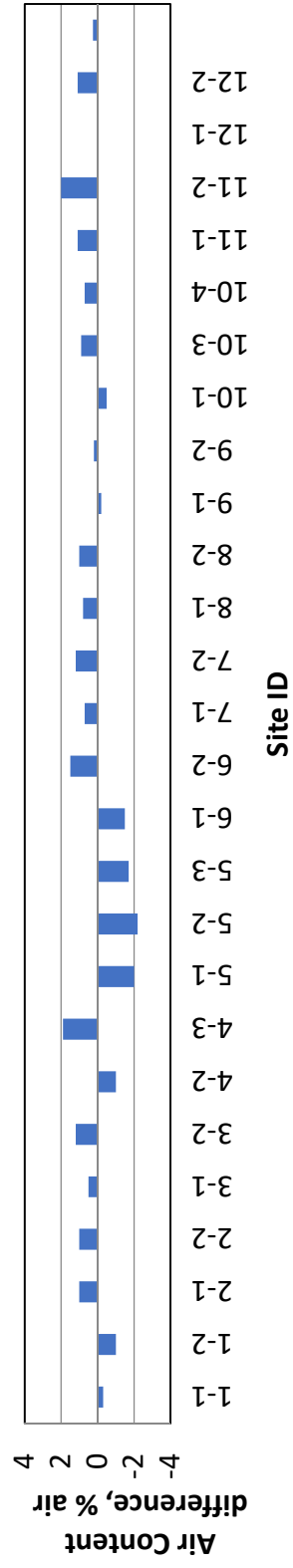


Figure 12. Difference between air contents of cylinders before and after paving; positive values indicate a decrease in air content after the paver

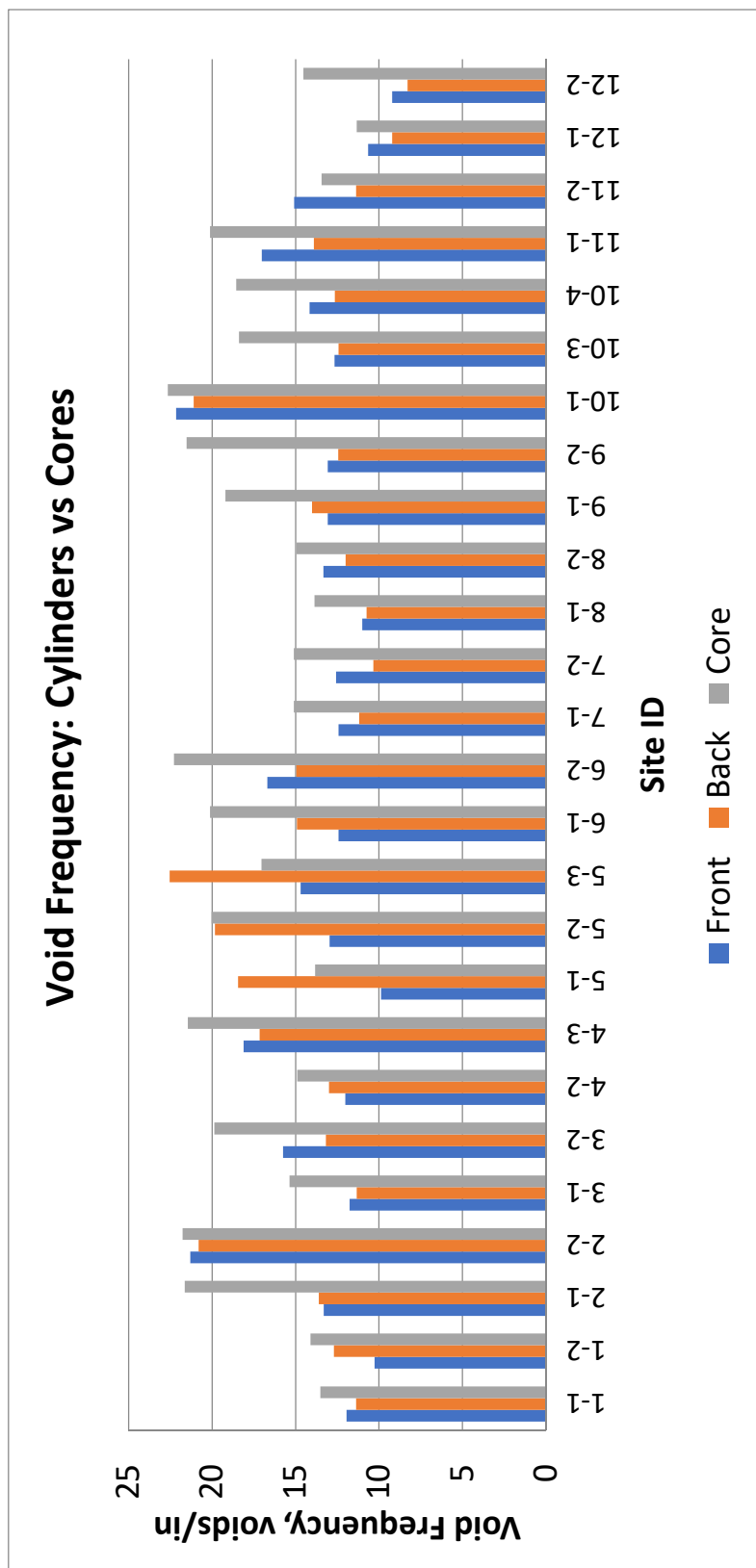


Figure 13. Void frequency: cylinders vs drilled cores

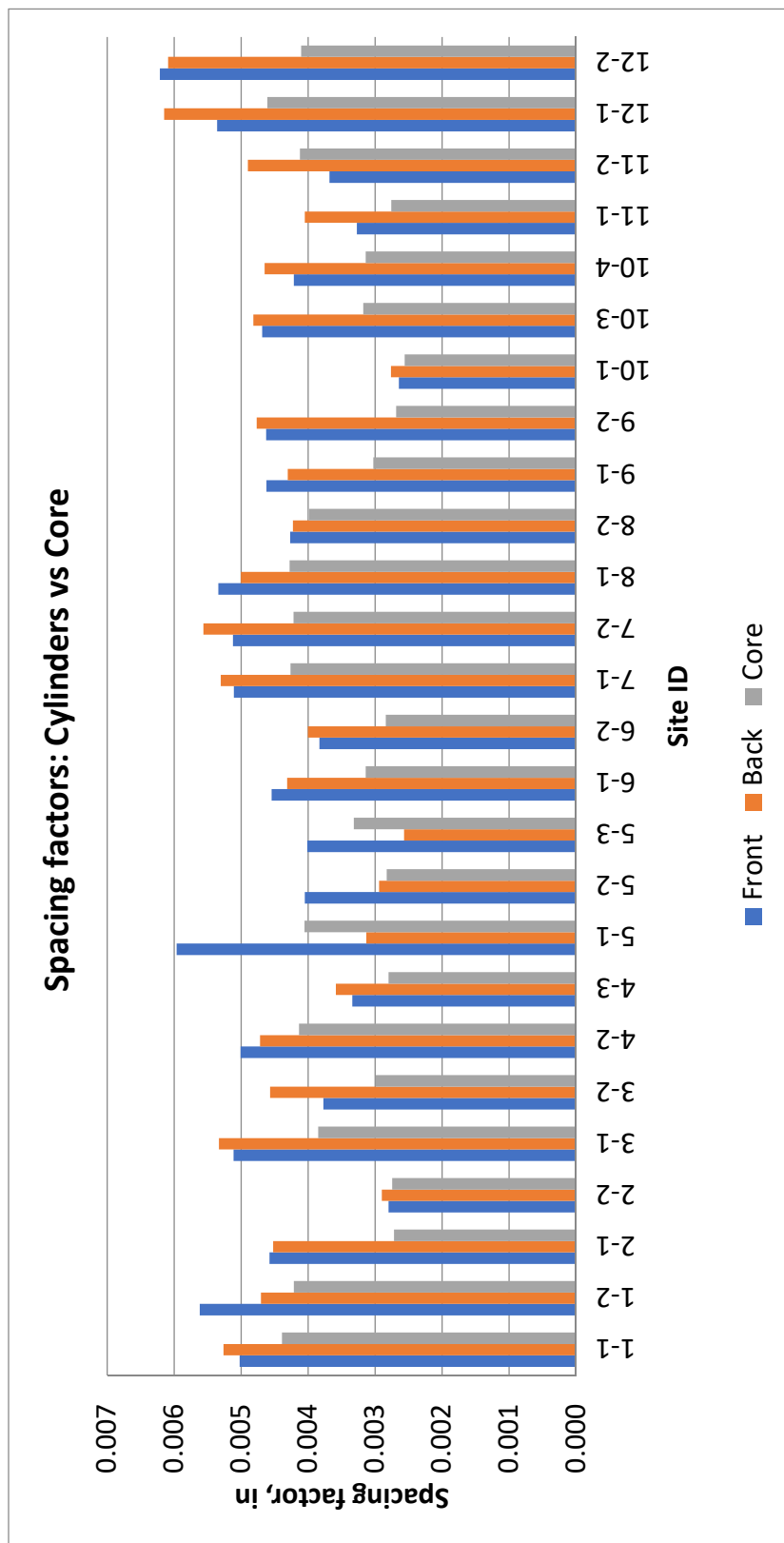


Figure 14. Spacing factor: cylinders vs drilled cores

Table 16. Comparison of hardened air contents (ASTM C457) of cylinders and drilled cores

Site ID	Front cylinder	Back cylinder	Core	Core-Front	Core-Back
	%	%	%	%	%
1-1	5.6	5.9	6.7	1.1	0.8
1-2	5.1	6.1	6.6	1.5	0.5
2-1	6.7	5.7	9.9	3.2	4.2
2-2	8.6	7.6	8.4	-0.2	0.8
3-1	6.4	5.9	8.0	1.6	2.1
3-2	7.5	6.3	7.6	0.1	1.3
4-2	5.4	6.4	5.9	0.5	-0.5
4-3	7.5	5.6	8.3	0.8	2.7
5-1	5.5	7.5	10.1	4.6	2.6
5-2	4.3	6.5	9.2	4.9	2.7
5-3	5.5	7.2	9.3	3.8	2.1
6-1	4.6	6.1	7.7	3.1	1.6
6-2	6.6	5.1	7.6	1.0	2.5
7-1	5.8	5.1	6.0	0.2	0.9
7-2	6.0	4.8	7.0	1.0	2.2
8-1	5.3	4.5	6.3	1.0	1.8
8-2	5.0	4.0	6.0	1.0	2.0
9-1	5.8	6.0	9.4	3.6	3.4
9-2	5.6	5.4	9.8	4.2	4.4
10-1	7.6	8.1	8.7	1.1	0.6
10-3	6.5	5.6	7.9	1.4	2.3
10-4	6.0	5.3	8.2	2.2	2.9
11-1	6.9	5.8	7.2	0.3	1.4
11-2	7.1	5.1	5.0	-2.1	-0.1
12-1	5.0	5.0	4.3	-0.7	-0.7
12-2	5.1	4.0	5.6	0.5	1.6
Average				1.6	1.8
Max				4.9	4.4
Min				-2.1	-0.7
S.D				1.7	1.3

Table 17. Comparison of void frequencies of cylinders and drilled cores

Site ID	Front cylinder	Back cylinder	Core	Core vs Front (*)	Core vs Back (**)
	voids/in	voids/in	voids/in	%	%
1-1	12.0	11.4	13.5	12	16
1-2	10.3	12.7	14.1	27	10
2-1	13.3	13.6	21.6	38	37
2-2	21.3	20.8	21.8	2	4
3-1	11.8	11.3	15.4	23	26
3-2	15.8	13.2	19.9	21	34
4-2	12.0	13.0	14.9	19	13
4-3	18.1	17.1	21.5	16	20
5-1	9.9	18.4	13.8	29	-33
5-2	13.0	19.8	20.0	35	1
5-3	14.7	22.5	17.0	14	-32
6-1	12.4	14.9	20.1	38	26
6-2	16.7	15.0	22.3	25	33
7-1	12.4	11.2	15.1	18	26
7-2	12.6	10.3	15.1	17	32
8-1	11.0	10.7	13.9	21	23
8-2	13.3	12.0	14.9	11	20
9-1	13.1	14.0	19.2	32	27
9-2	13.1	12.5	21.5	39	42
10-1	22.2	21.1	22.7	2	7
10-3	12.7	12.4	18.4	31	32
10-4	14.2	12.6	18.6	24	32
11-1	17.0	13.9	20.1	15	31
11-2	15.1	11.4	13.5	-12	15
12-1	10.7	9.2	11.3	6	19
12-2	9.2	8.3	14.5	37	43
Max				39	43
Min				-12	-33
Average				21	19
SD				13	18

(*) = $(\text{core} - \text{front})/\text{core} \times 100$

(**) = $(\text{core} - \text{back})/\text{core} \times 100$

2.5.4.4 Effects of Air Entraining Admixtures

Average air contents for different AEAs are shown in Figure 15. In most of the project sites where synthetic AEAs were used, there were significantly higher air contents in the drilled cores than in the cylinders both before and after the paver. In the two projects that utilized neutralized vinsol

resin or chemically similar products, however, the average air content of the front cylinder was higher than those of the back cylinder and the core.

The difference in air content between cores and cylinders varied significantly with the type of air entraining admixture as shown in Table 18. Larger differences occurred where synthetic admixtures were used. The cores' air content varied between -2.1 and +0.5 percentage points from that of the front cylinders and between -0.7 and +1.6 percentage points from the back cylinders. Because the number of projects associated with NVR was much smaller than the number of projects using synthetic AEAs, statistical analysis of the results was not conducted.

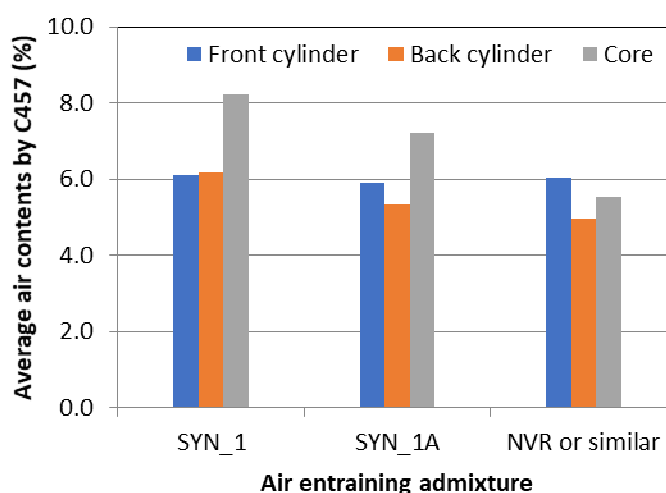


Figure 15. Average air contents for different AEAs

Table 18. Effect of AEA on the air content difference between cores and cylinders (percentage points)

No. of project	AEA	Difference between core vs cylinder <u>in front of paver</u>			Difference between core vs cylinder <u>behind paver</u>		
		Average	Max	Min	Average	Max	Min
7	Synthetic 1	2.1	4.9	-0.2	2.0	4.4	-0.5
3	Synthetic 2	1.3	3.1	0.1	1.9	2.5	1.3
2	Vinsol resin or similar	-0.5	0.5	-2.1	0.6	1.6	-0.7

2.5.4.5 Effects of Coarse Aggregates

The average differences in air content between core and cylinders were higher in mixes using gravel coarse aggregates (Table 19). It is noted, however, that these differences varied widely for both mixes using crushed stone and gravel. Due to the lower number of projects using gravel, statistical analysis on effect of coarse aggregates was not conducted. As earlier studies with Wisconsin aggregates have shown, igneous gravels often contain chemically active microfines that may interact with the synthetic AEA in unpredictable ways [19].

Table 19. Effect of coarse aggregates on the difference in air contents between cores vs cylinders (percentage points)

No. of project	Coarse Aggregate	Difference between core vs cylinder <u>in front of paver</u>			Difference between core vs cylinder <u>behind paver</u>		
		Average	Max	Min	Average	Max	Min
8	Crushed stone	0.6	3.2	-2.1	1.3	4.2	-0.7
4	Gravel	3.0	4.9	1.0	2.5	4.4	0.6

2.5.4.6 Effects of construction parameters

Most of the projects under study used the same type of mixing plant and delivery truck. Haul times were within a normal range (up to about 30 minutes). Thus, analysis on the effect of these parameters was not conducted and no obvious trends were apparent from perusing the data.

Effects of paver type and batch sequence on the differences in air content between cores and cylinders are shown in Table 20 and Table 21 respectively. There is no apparent effect of the paver type. It appears that the differences in air content were smaller for concrete batched with sequences C and D (WR and AEA added together to a water tank before mixing). However, there was only one project utilizing each of these batch sequences, preventing a more general observation.

Table 20. Effect of paver type on the difference in air contents between cores vs cylinders

Paver type ⁽¹⁾		I-A	I-B	II-A	II-B
No. of projects		1	2	8	1
Difference between core vs cylinder <u>in front of</u> paver (p.p ²)	Average	1.3	2.5	1.3	1.6
	Max	1.5	4.2	4.9	2.2
	Min	1.1	1.0	-2.1	1.1
Difference between core vs cylinder <u>behind</u> paver (p.p ²)	Average	0.7	2.9	1.6	1.9
	Max	0.8	4.4	4.2	2.9
	Min	0.5	1.8	-0.7	0.6

⁽¹⁾ I-A: Spreader plow; I-B: Spreader plow with bar inserter; II-A: Spreader auger; II-B: Spreader auger with bar inserter.

⁽²⁾ percentage point

Table 21. Effect of batch sequence on the difference in air contents between cores vs cylinders

Batch sequence ⁽¹⁾		A	B	C	D
No. of projects		6	3	1	1
Difference between core vs cylinder <u>in front of</u> paver (p.p ²)	Average	1.6	2.4	0.9	-0.9
	Max	4.9	4.2	1.6	0.3
	Min	-0.7	1.0	0.1	-2.1
Difference between core vs cylinder <u>behind</u> paver (p.p ²)	Average	1.7	2.5	1.7	0.7
	Max	4.2	4.4	2.1	1.4
	Min	-0.7	0.6	1.3	-0.1

⁽¹⁾ A: Dry materials (aggregates, cementitious materials), then AEA, WR, and water are charged into the water line at the same time; B: same as A, but AEA is sprayed directly into mixing drum; C: All admixtures are poured into the water tank, then 80% of mix water into the mixing drum, aggregates, cementitious materials, and 20% of mix water; D: same as C, but truck mixing

⁽²⁾ percentage point

2.6 Discussion

2.6.1 CONCRETE AIR CONTENT IN FRESH AND HARDENED STATES

This phase of the overall study was conducted in order to identify and characterize the air void system in concrete pavement that used synthetic air entraining agent. Two critical questions were set at the beginning of the study concerning the reliability of the ASTM C231 pressure method and the effects of concrete vibration, movement, and placement on the air void system. Analysis of the results shows that the difference between fresh air content measured by the pressure meter and the hardened air content measured by C457 is comparable to data recorded in the literature for similarly prepared specimens [8] [14]. Results of the gravimetric and volumetric method are along the same lines.

2.6.2 AIR CONTENTS OF DRILLED CORES AND CYLINDERS

The hardened air void analysis has revealed that at many of the project sites where synthetic AEAs were used, there were significantly less air voids and lower air content in the cylinders sampled from fresh concrete taken either before or after the paver than in the drilled cores. This did not occur at the sites where NVR AEA or a chemically similar product was used. The differences between the front cylinders and the cores are of interest since firstly, it reflects the disparity between the samples used for quality control tests versus the actual concrete in service and secondly, higher air in the core is generally not expected due to effects of the slip-form paver. Possible scenarios and mechanisms leading to the results at the projects where synthetic AEAs were used are as follows:

- Scenario 1: Sampling of concrete for cylinders and pressure meter tests removed air bubbles and reduced the air content significantly while paving operations did not.
- Scenario 2: Paving increased the number of air bubbles and the measured air content; but sampling of concrete behind the paver removed many air bubbles.
- Scenario 3: Measurable air bubbles formed during the finishing and setting of the concrete in the pavement but not in the cylinders.

Regarding the first scenario, it should be emphasized that the concrete sampled following standard procedures in ASTM and WisDOT specifications and that the concrete cylinders were compacted by hand-rodding. This leads to one question: does the use of synthetic AEAs result in air bubbles so unstable that many of them could be expelled from the concrete during the standard sampling procedures?

Regarding the second scenario, while it was shown that vibration could lead to higher numbers of very small air bubbles [20] [21], it is unclear how the total air content could be increased through paving operations. Furthermore, this scenario does not explain the differences between the cores and the cylinders behind the paver.

For the third scenario to be true, there must be a difference in the conditions between the concrete pavement and cylinders which may affect the dynamics of air bubbles. There has been no study where such behavior was established.

Scenarios 1 and 2 were examined through a laboratory study presented in the next chapters. Scenario 3 was not investigated in the current study.

2.7 Conclusions

The following conclusions can be drawn from the portion of the overall study presented in this chapter:

- The pressure meter (ASTM C231) and ASTM C457 measurements of air content in concrete cylinders were in reasonable agreement. The differences between air content measurements by the two methods were within ± 2 percentage points. While sampling methods may impact the air void structure, the actual measurement of air content using the standard ASTM C231 compliant pressure meter appears to be sound.
- The mean differences in air content, void frequency, and spacing factor between the cylinders made before and after the paver were negligible.
- At many project sites, the ASTM C457 air contents of cylinders sampled in front of and behind the paver were significantly lower than those of the drilled cores at approximately the same location. The pressure meter readings that would normally be used for quality control were also lower than air contents in the drilled cores. These differences on average were in the range of 1.6 to 1.8 percentage points.
- The differences between ASTM C457 air contents of the cores and cylinders appear to vary with the type of air entraining admixture (AEA). Compared to mixes using neutralized Vinsol resin (NVR), concrete using synthetic AEAs, on average, had larger differences between the cores and cylinders.

- The differences between ASTM C457 air contents of the cores and cylinders appear to vary with the type of coarse aggregate. The average differences were higher in mixes using gravel coarse aggregates. It should be noted, however, that these differences varied widely for both mixes using crushed stone and gravel.

REFERENCES FOR CHAPTER 2

- [1] F. T. Gay, "FACTOR WHICH MAY AFFECT DIFFERENCES IN THE DETERMINED AIR CONTENT OF PLASTIC AND HARDENED AIR-ENTRAINED CONCRETE.," in *Proceedings of the Fourth International Conference on Cement Microscopy.*, 1982, pp. 276–292.
- [2] Burg, "Slump Loss, Air Loss, and Field Performance of Concrete," *J. Proc.*, vol. 80, no. 4, Jul. 1983.
- [3] K. Hover, "Some Recent Problems with Air-Entrained Concrete," *Cem. Concr. Aggr Cem. Concr. Aggreg.*, vol. 11, no. 1, p. 67, 1989.
- [4] C. Ozyildirim, "Comparison of the Air Contents of Freshly Mixed and Hardened Concretes," *Cem. Concr. Aggr Cem. Concr. Aggreg.*, vol. 13, no. 1, p. 11, 1991.
- [5] K. Khayat and K. Nasser, "Comparison of Air Contents in Fresh and Hardened Concretes Using Different Airmeters," *Cem. Concr. Aggr Cem. Concr. Aggreg.*, vol. 13, no. 1, p. 18, 1991.
- [6] L. L. Sutter, *Evaluation of methods for characterizing air void systems in Wisconsin paving concrete*. [Madison, Wis.]; [Springfield, Va.]: Wisconsin Highway Research Program ; [Available through the National Technical Information Service], 2007.
- [7] J. Tanesi and R. Meininger, "Freeze-thaw resistance of concrete with marginal air content," *Transp. Res. Rec.*, no. 2020, pp. 61–66, 2007.
- [8] M. Nagi *et al.*, *Evaluating air-entraining admixtures for highway concrete*. Washington, D.C.: Transportation Research Board, 2007.
- [9] M. Nagi and D. Whiting, *Achieving and verifying air content in concrete*. Skokie, Ill.: Portland Cement Association, 1994.
- [10] P. Ram Wisconsin, Department of Transportation, Division of Business Services, I. Applied Pavement Technology, and Wisconsin Highway Research Program, *Field study of air content stability in the slipform paving process*. [Madison, Wis.]: Wisconsin Dept. of Transportation, 2012.

- [11] Eickschen, “Working mechanisms of air-entraining admixtures and their subsequent activation potential,” *Am Concr Inst ACI Spec Publ Am. Concr. Inst. ACI Spec. Publ.*, vol. 288, no. 288 SP, pp. 305–315, 2012.
- [12] D. Stark, *Effect of vibration on the air-void system and freeze-thaw durability of concrete*. Skokie, Ill.: Portland Cement Association, 1986.
- [13] R. P. Elliott, *Effect of internal vibration of Portland cement concrete during paving: final report of Research Project IHR-503*. [Springfield, Ill.]: State of Illinois, Dept. of Transportation, Bureau of Materials and Physical Research, 1974.
- [14] D. Whiting and M. Nagi, *Manual on control of air content in concrete*. Skokie, Ill.: Portland Cement Association, 1998.
- [15] S. H. Kosmatka and M. L. Wilson, *Design and control of concrete mixtures: the guide to applications, methods, and materials*. Skokie, Ill.: Portland Cement Association, 2011.
- [16] Mielenz, Vladimir E. Wolkodoff, James E. Backstrom, and, and Harry L. Flack, “Origin, Evolution, and Effects of the Air Void System in Concrete. Part 1 - Etrained Air in Unhardend Concrete,” *J. Proc.*, vol. 55, no. 7, Jul. 1958.
- [17] T. C. Powers, *The properties of fresh concrete*. New York: Wiley, 1968.
- [18] C. E. Brennen, *Cavitation and bubble dynamics*. New York: Cambridge university press, 2014.
- [19] S. Cramer, M. Anderson, M. I. Tejedor, J. F. Munoz, J. Effinger, and R. Kropp, “‘Detecting Deleterious Fine Particles in Concrete Aggregates and Defining Their Impact’, Report No. WHRP 10-13,” Wisconsin Highway Research Program, WHRP 10-13, 2010.
- [20] Backstrom, Burrows, Mielenz, and Wolkodoff, “Origin, Evolution, and Effects of the Air Void System in Concrete. Part 3 - Influence of Water-Cement Ratio and Compaction*,” *J. Proc.*, vol. 55, no. 8, Aug. 1958.
- [21] Simon, Jenkins, and K. Hover, “Influence of Immersion Vibration on the Void System of Air-Entrained Concrete,” *Spec. Publ.*, vol. 131, Mar. 1992.

CHAPTER 3

ROBUSTNESS OF CONCRETE AIR ENTRAINING ADMIXTURES AND FOAM DRAINAGE TEST

3.1 Introduction

The field study presented in chapter 2 suggests that the disparity between air content measured in quality control tests (ASTM C231) and the actual hardened air content in the pavement was larger when synthetic AEAs were used. Three scenarios possibly leading to this disparity were discussed. Given restraints in time and budget, the first two of them which appeared to be more realistic were examined in this chapter. The possible mechanisms behind these scenarios are discussed below. In addition, the potential of using the Foam Drainage Test (FDT) [1] as a tool to evaluate robustness of AEAs in concrete was investigated. This test has been proposed for evaluating AEAs, but its correlation with concrete tests has not been established.

As mentioned above, two scenarios possibly leading to the disparity in air contents at the projects using synthetic AEAs are examined in this chapter:

Scenario 1: Sampling of concrete for cylinders and pressure meter tests removed air bubbles and reduced the air content significantly while paving operations did not. It should be emphasized that sampling of concrete in front of paver followed standard procedures in ASTM and WisDOT specifications and that the concrete cylinders were compacted by hand-rodging. This leads to one question: does the use of some synthetic AEAs result in air bubbles so unstable that many of them could be expelled from the concrete during the standard sampling procedures? To the author's knowledge there has been no study in the literature that examined this hypothesis.

Scenario 2: Paving increased the number of air bubbles and the measured air content; but sampling of concrete behind the paver removed many air bubbles. While it was shown that vibration could lead to higher numbers of very small air bubbles [2] [3], it is unclear how the total air content could be increased through paving operations. Discussion on possible mechanisms is provided below.

- i) **AEA reactivation.** Eickschen (2012) [4] proposed one mechanism to explain the issue of high air contents in pavement cores. It was shown in laboratory experiments that certain synthetic active agents, when overdosed, exhibited the potential to be reactivated and so to stabilize new air bubbles created during extended mixing while wood-resin AEAs did not show this potential. This behavior was believed to be associated with the higher solubility of the synthetic AEAs in calcium hydroxide solution. Although this mechanism was shown to occur in the laboratory experiments, there is still a question how it might happen in the field: how is air introduced into concrete during paving? Slip-form pavers have two main actions: spreading and vibrating. The vibrators are generally immersed in the concrete and do not have the opportunity to introduce air from the environment into the concrete. Spreading action of the auger or plow may entrap some additional air into the concrete but this action is noticeably much less extensive than mixing.
- ii) **Steady diffusion.** Air of higher pressure tends to move to a space of lower pressure. Diffusion of air from small, higher pressure bubbles into surrounding fluid and into larger, lower pressure ones tends to reduce the number of air bubbles and increase the total measured air content. Although this mechanism has been suggested to justify the discrepancy between fresh and hardened air contents, it does not explain the differences between the cores and cylinders reported in the current study unless the conditions in the pavement were more favorable for this to happen. A review of literature regarding this mechanism does not suggest any connection with the more common use of synthetic AEAs.
- iii) **Rectified diffusion.** As mentioned in the previous paragraph, steady diffusion results in dissolution of small air bubbles into surrounding fluid. When the fluid is under oscillating pressure, however, the bubbles can be preserved and even grow due to a phenomenon called “rectified diffusion” [5]. Air bubbles expand and contract in each cycle of pressure oscillation. When the bubble contracts, its internal pressure increases, and air migrates out of the bubble into the fluid. When the bubble expands, air migrates from the fluid into the bubble. Because the bubble’s surface area and its boundary layer’s thickness are different between expanding and contracting half cycles, there is

a net inflow of air into the bubble after each cycle. Mathematical models and experiments of this phenomenon can be found in textbooks of bubble dynamics [6]. The study by Crum (1980) [5], which measured the growth of a single air bubble in a liquid by the action of an acoustic field, showed that when the liquid-vapor surface tension was reduced by use of surfactants, the growth rate was abnormally higher than predicted by theory as shown in Figure 16. More recent studies [7] [8] with air bubbles under the effect of an acoustic field also showed higher growth rate of bubbles with higher concentration of surfactants. In concrete, vibration produces an oscillating pressure field on air bubbles and reduces cohesive strength of the fresh concrete, providing favorable conditions for the growth of air bubbles due to rectified diffusion. The studies on bubble dynamics mentioned above suggest that AEAs may play an important role in the growth of air bubbles in concrete. It is suggested that synthetic AEAs stabilize air bubbles in concrete by reducing the liquid-vapor surface tension while NVR does not change the surface tension considerably [9] [10]. Recent studies [11] [12] observed that the shell of air bubbles entrained by “synthetic” AEA was relatively strong in tension and did not crack when the external pressure decreased. On the other hand, the shell of bubbles entrained by NVR seemed to be very weak in tension and cracked when the external pressure is reduced. From the above discussion, a new hypothesis is proposed that air bubbles in concrete may grow during vibration due to rectified diffusion and that air bubbles entrained by synthetic AEAs would have higher potential to grow than those entrained by NVR. This hypothesis may explain the recently reported problem of high air content in concrete pavement cores that is believed to have connection with the more common use of synthetic AEAs. That said, it should be noted that the growth rate of bubbles even in a surfactant solution is still relatively low. Figure 16 indicates that a 50- μm bubble in a surfactant solution with a surface tension of 40 dyn/cm or mN/m could grow at approximately 6 $\mu\text{m}/100$ sec, meaning that the concrete needs to be vibrated for 100 seconds, which is five to seven times longer than typical vibration time in slip-form paving, for such a bubble to increase its diameter by 12% or its volume by 40%.

To summarize, two hypotheses explaining the disparity in air contents found in the field study in Chapter 2 were subsequently evaluated. One suggests a significant loss of air bubbles during specimen preparation while the other suggests an increase of air content due to vibration. A preliminary evaluation of each hypothesis was first carried out. Based on the preliminary results, additional tests were proposed and conducted to verify the significance of the results.

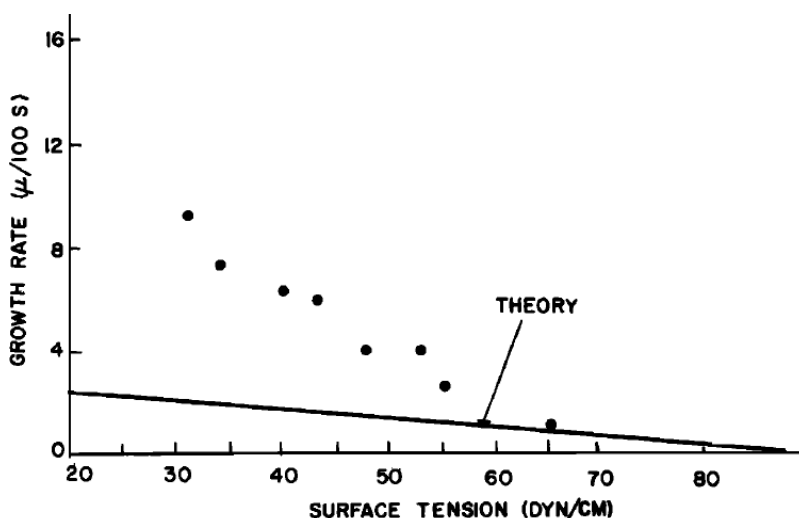


Figure 16. Variation in the growth rate of air bubble by rectified diffusion with surface tension for a bubble of radius 50 μm , a gas saturated liquid, and an acoustic pressure amplitude of 0.22 bar, frequency of 22.1 KHz [5]

3.2 Samples and Materials

3.2.1 PRELIMINARY CONCRETE TESTS

Preliminary tests were carried out to evaluate each of the two hypotheses discussed previously. Two concrete mixes were made, one using a sodium olefin sulfonate synthetic AEA (SYN_1) and one using an NVR AEA. The mix proportions are given in Table 22. This mixture met WisDOT specifications and had a water-cementitious-materials (w/cm) ratio of 0.40. The target slump was 1 to 3 inches, and target air content was 4.5% to 7.5%. An ASTM C294 Type A water reducer was used as necessary to achieve the specified slump. All the aggregates met WisDOT specifications and their properties are given in Table 23.

Table 22. Concrete mixture proportions in preliminary tests (lb)

Concrete volume	Type I cement	Class C fly ash	3/4-in coarse agg. OD (*)	Fine agg. OD	Mix water (**)
1 yd ³	395	170	1884	1256	259.38
1.5 ft ³	21.94	9.44	104.67	69.78	14.41

(*) OD = oven dry; (**) Total mix water includes water that would be absorbed into aggregates

Table 23. Properties of aggregates

Properties	Coarse Aggregate	Fine Aggregate
Specific gravity (oven dry)	2.707	2.656
Absorption (%)	1.153	0.928

There were three types of specimens: uncompact concrete cast into a 3x4x16-in prism form with minimal manipulation, hand-rodded 6x12-in. cylinder, and vibrated small slab of 6x8x12-in. as shown in Figure 17.a. The vibrator was inserted at one point approximately 4 in. from the form walls and remained in place for 10 or 30 sec. The size of specimen was selected based on an assumed 4-in radius of action (for the vibrator to be used, ACI 309R suggests a radius of action of 3-6 in). After the concrete hardens, two slices of concrete were cut from the slab for air void analysis following ASTM C457 Procedure A - Linear traverse. Traverse lines were perpendicular to the top plane of the slab so that variation of the air void system with distance from the vibrator could be observed (Figure 17.b). Since the uncompact sample would likely contain many large air voids which are not stabilized by AEAs, intercept chords greater than 1 mm were considered entrapped air voids and excluded from the ASTM C457 analysis to achieve a meaningful comparison between compacted and uncompact samples.

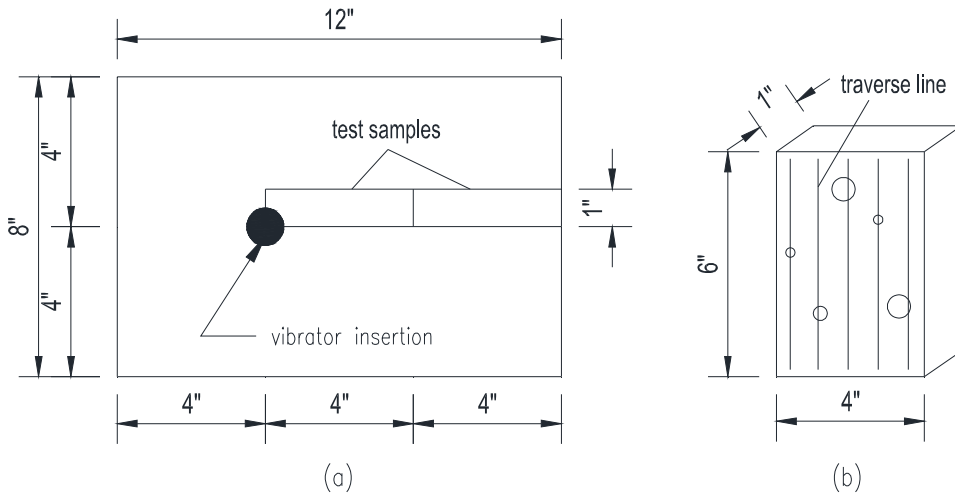


Figure 17. Vibrated specimen: (a) plan view; (b) C457 sliced sample

3.2.2 PRIMARY CONCRETE TESTS

Based on the preliminary results which will be discussed later, additional concrete tests were conducted to verify the significance of the hypothesis that air bubbles entrained with synthetic AEAs are less stable, leading to more air loss during the standard sample preparation procedure than concrete using NVR AEA (Scenario 1 described in Section 3.1). To achieve this objective, the difference between hardened air contents (using the ASTM C457 linear traverse procedure) of uncompacted and compacted concretes was determined for three AEAs: neutralized vinsol resin (NVR), sodium (C14-16) olefin sulfonate synthetic (SYN_1), or sodium (C10-16) benzene sulfonate synthetic (SYN_2).

The uncompacted concrete was cast into a 3x4x16-in prism form with minimal manipulation. The compacted concrete was cast into a 6x12-in cylinder form and hand-rodded in accordance with ASTM C192. For each AEA, three replicate batches of concrete were made. One 4x5-in sample was cut from each prism/cylinder and lapped sequentially with diamond grinding discs of 260, 70, 30, 15, and 6 μm grit sizes. As mentioned earlier, intercept chords greater than 1 mm were excluded from the ASTM C457 analysis to achieve a meaningful comparison between compacted and uncompacted samples.

All the concrete mixes had the same proportions as shown in Table 24. The mixture met WisDOT specifications and had a water-cementitious-materials (w/cm) ratio of 0.36. The target slump was 1 to 3 in. and target fresh air content (ASTM C231) was 4.5% to 7.5%. The same aggregates were used in the preliminary and additional tests.

Table 24. Concrete mixture proportions (lb)

Concrete volume	Type I cement	Class C fly ash	3/4-in coarse agg. OD (*)	Fine agg. OD	Mix water (**)
1 yd ³	395	170	1920	1280	237.42
1.5 ft ³	21.94	9.44	106.67	71.11	13.19

(*) OD = oven dry; (**) Total mix water includes water that would be absorbed into aggregates

3.2.3 MODIFIED FOAM DRAINAGE TEST

Foam in the context of this research is a mixture of liquid and bubbles in which the volume of bubbles is several times larger than that of liquid. Foam drainage is the downward flow of liquid due to gravity while air bubbles rise to the surface. As the liquid and bubbles are separated during drainage, the bubbles get closer to each other, leading to coalescence and collapse. Thus, slower drainage indicates a more stable foam. Foam drainage rate is affected by many factors including properties of the air bubbles, presence of surfactants, and solid particles. Surfactant molecules attached to the air bubbles can provide some resistance against the drainage. Certain solid particles can also attach to the bubbles and provide a physical barrier against coalescence and reduce drainage. An illustration of particle stabilization is given in Figure 18.

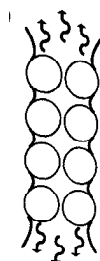


Figure 18. Particles attached to air bubbles can reduce flow of the liquid film between the bubbles [13]

The Foam Drainage Test (FDT) was proposed by Taylor et al (2015) [1] for evaluating AEAs used in concrete. According to this protocol, 300 ml of water and 10 ml of AEA regardless of the type of AEA are mixed in a kitchen blender for 10 seconds; the foam mixture was then poured into a 1-liter graduated cylinder. The volume of liquid drained to the bottom of the foam is recorded at different times for one hour to achieve a drainage curve. An example of foam drainage in a graduated cylinder is provided in Figure 19. Two indicators for foam stability, V_0 and $1/k$, are then obtained from a linear equation of V_d vs $1/t$ as follows:

$$V_d = V_0 - (1/k) \times (1/t)$$

where V_d is the volume of liquid drained to the bottom of the cylinder, t is time, V_0 is the drainage volume at $t = \infty$, and $1/k$ is an indicator of drainage rate. Smaller V_0 and larger $1/k$ indicate a more stable foam. This protocol has several drawbacks. First, using the same amount of AEA regardless of the AEA type does not align with common concrete practices where AEA dosages should be adjusted to achieve the same target air content. Second, the use of two indicators typically leads to inconclusive results because one may be favorable to an AEA while the other unfavorable, and neither of the indicators alone is appropriate for evaluating foam stability. Physically the drainage volume at $t = \infty$, V_0 , should equal the total liquid volume before foaming, and thus, is the same regardless of AEA type. In addition, the V_d vs $1/t$ equation above is invalid for small times since it predicts negative values of V_d .

A modified protocol was created in this study with two changes from the original. First, the amounts of AEA and water for each mixture were adjusted such that the total volume of liquid (water + AEA) before mixing was 300 ml and the foam volume immediately after mixing was 900 ± 50 ml. Second, only one indicator was used to evaluate foam stability. The selection of this indicator is discussed later. A 1-liter glass graduated cylinder with an outer diameter of 70 mm was used in this study.

Drainage behaviors for the three AEAs in three different solutions, deionized (DI) water, lime water, and DI water plus cement, were compared. The lime water was saturated and filtered through 2.5- μm filter paper. The amount of cement in the water-plus-cement mixture was varied

from 2 g to 15 g. For mixtures using 2 g or 15 g cement, two replicate samples were tested. For all other mixtures, 3 replicate samples were tested.

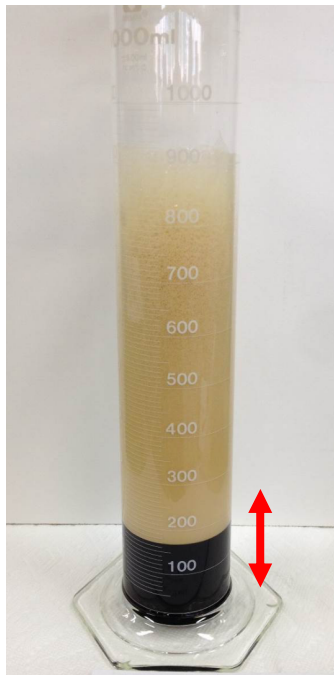


Figure 19. An example of foam drainage in a graduated cylinder; the arrow indicates the drained liquid volume

3.3 Results and Discussion

3.3.1 PRELIMINARY CONCRETE TESTS

The air contents excluding intercept chords equal or larger than 1 mm for different samples are shown for comparison in Figure 20. Hardened air void characteristics of all mixtures are shown in Table 25. Compared with the uncompact sample, hand-rodding resulted in an air loss of 23% and a reduction of 19% in void frequency in the synthetic AEA mix; in the NVR mix, hand-rodding led to an air loss of 4% and no reduction in void frequency. Vibration appeared to be less detrimental to the air voids than hand rodding in the mix using synthetic AEA. Vibration for 10 seconds and 30 seconds led to 4% and 7% reduction in the total air content respectively. Vibration for 30 seconds resulted in 4% reduction in the void frequency and vibration for 10 seconds did not reduce the void frequency. In the NVR mix, vibration for 10s decreased the air content by 7% and

increased the void frequency. Vibration for 30s decreased the total air content by 17% and slightly increased the void frequency. Regardless of the AEA type, compaction either by hand-rod or vibration did not exhibit any considerable impact on the spacing factor (Table 25).

In summary, the preliminary concrete test results showed that vibration did not increase air content in any mix as predicted by the rectified diffusion theory and that air loss due to hand-rod was higher in the synthetic than in the NVR AEA mix. This appears to support the hypothesis that air bubbles entrained with a synthetic AEA are less stable than those entrained by an NVR AEA under physical impacts such as hand-rod. The additional tests presented in the next section were conducted to verify this result.

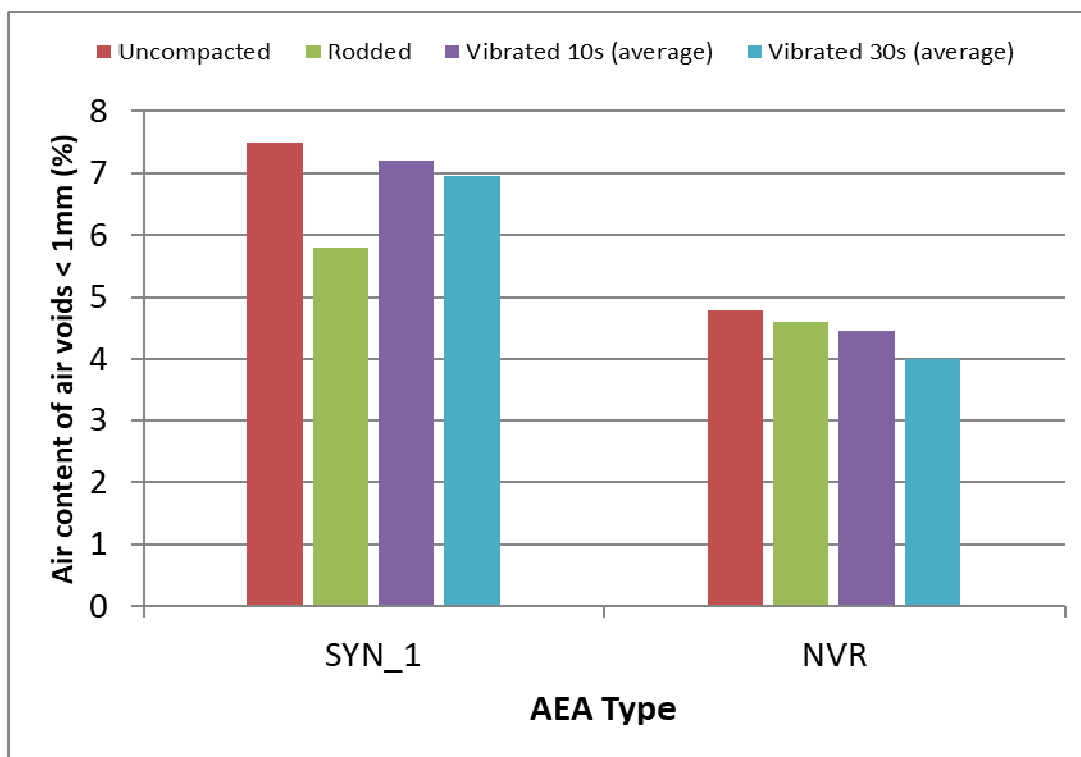


Figure 20. Comparison of hardened air contents in preliminary tests

Table 25. Characteristics of hardened air voids in preliminary tests

Sample	SYN_1			NVR		
	Air content	Void frequency	Spacing factor	Air content	Void frequency	Spacing factor
	%	void/inch	inch	%	void/inch	inch
Uncompacted	7.5	25.7	0.0024	4.8	17.0	0.0033
Rodded	5.8	20.9	0.0030	4.6	18.2	0.0030
Vibrated 10s (average)	7.2	26.4	0.0024	4.5	20.0	0.0028
Vibrated 10s (0-4")	7.4	28.0	0.0022	4.6	22.7	0.0024
Vibrated 10s (4-18")	7.0	24.7	0.0025	4.3	17.2	0.0031
Vibrated 30s (average)	7.0	25.1	0.0025	4.0	17.9	0.0029
Vibrated 30s (0-4")	6.8	27.4	0.0022	4.1	19.2	0.0027
Vibrated 30s (4-8")	7.1	22.7	0.0027	3.9	16.6	0.0031

3.3.2 PRIMARY CONCRETE TESTS

Slumps, air contents, and admixture dosages for all concrete batches are given in Table 26. Air loss due to standard compaction techniques was evaluated using two parameters: total air content and void frequency which is an indicator of void density in the concrete.

Average reduction of air content and void frequency due to hand compaction are given in Figure 21. Detailed results are provided in Table 27 and Table 28. It can be seen from Figure 21 that reductions of air content and void frequency were larger with the synthetic than NVR AEA, supporting the hypothesis from the field study. This result suggests the following consequences of using synthetic AEAs to replace NVR:

- Higher air loss during hauling, placing, and sampling of concrete,
- Larger disparity between QC tests and actual air contents of the pavement, and
- More difficulties in controlling air contents.

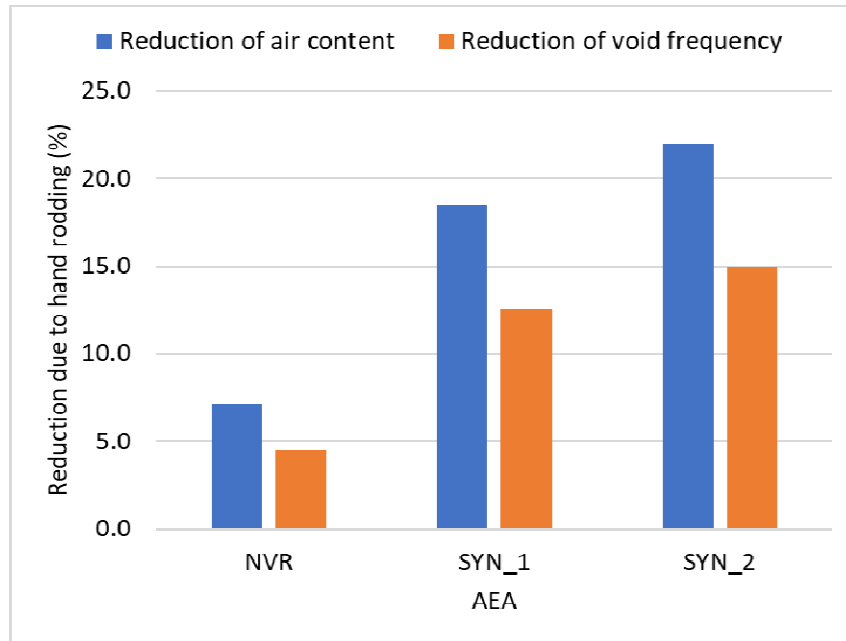


Figure 21. Reductions of air content and void frequency due to hand rodding for different AEAs (each data point is an average of three sets of samples)

Table 26. Properties of fresh concrete mixtures

Batch #	AEA type	Slump (in)	Fresh air content (ASTM C231) (%)	Admixture dosages for 1.5 ft ³ concrete (ml)	
				AEA	WR
A-1	NVR	1.50	4.5	6.5	30.0
A-2	NVR	2.25	6.4	12.0	30.0
A-3	NVR	3.00	7.6	12.0	30.0
B-1	SYN_1	2.00	5.2	8.0	25.0
B-2	SYN_1	2.00	6.5	12.0	25.0
B-3	SYN_1	2.25	5.8	8.0	25.0
C-1	SYN_2	1.75	4.6	12.0	25.0
C-2	SYN_2	2.00	5.0	21.0	25.0
C-3	SYN_2	2.00	5.8	30.0	25.0

Table 27. Reduction of air content due to hand-rodding for different AEAs

AEA	Batch #	Air contents (%)		Relative air loss (%)		
		Rodded	Uncompacted	Per batch	Mean	S.D
NVR	1	3.5	3.9	10.3	7.1	3.0
NVR	2	6.4	6.6	3.0		
NVR	3	8.0	8.7	8.0		
SYN_1	1	4.9	5.9	16.9	18.4	1.2
SYN_1	2	4.9	6.0	18.3		
SYN_1	3	4.8	6.0	20.0		
SYN_2	1	3.6	4.8	25.0	22.0	5.5
SYN_2	2	4.2	4.9	14.3		
SYN_2	3	4.4	6.0	26.7		

Table 28. Reduction of void frequency due to hand-rodding for different AEAs

AEA	Batch #	Void frequency (voids/in)		Reduction of void frequency (%)		
		Rodded	Uncompacted	Per batch	Mean	S.D
NVR	1	14.5	16.3	11.0	4.5	6.0
NVR	2	29.2	28.2	-3.5		
NVR	3	33.5	35.6	5.9		
SYN_1	1	22.7	27.8	18.3	12.6	4.2
SYN_1	2	28.7	31.3	8.3		
SYN_1	3	25	28.1	11.0		
SYN_2	1	15.9	19.8	19.7	15.0	6.9
SYN_2	2	20.1	21.2	5.2		
SYN_2	3	22.8	28.5	20.0		

3.3.3 MODIFIED FDT

Drainage curves for different AEAs in DI water, lime water, and DI water with 5 g cement are given in Figure 22, Figure 23, and Figure 24 respectively. The amount of drainage at a given time is presented in terms of V_d/V_0 , a ratio of the drained liquid volume to the initial liquid volume. In DI water (Figure 22) foams for different AEAs had almost the same drainage behavior in which over 90% of the liquid drained within 20 minutes. In lime water (Figure 23), drainage in the synthetic AEA foams after 20 minutes slightly decreased to 90% while drainage in the NVR foam

dropped to 76%. Previous studies [9] [10] [14] proposed that absorption of calcium salts created from a reaction of NVR and calcium hydroxide onto air bubbles are the main bubble stabilization mechanism for NVR in concrete; but for the first time, contribution of such a reaction to bubble stability was measured in a quantitative manner in the current study.

In DI water with 5 g of cement (Figure 24), the differences among the three AEA foams were more remarkable. For the benzene sulfonate synthetic AEA (SYN_2) cement had little effect on foam drainage with 93% of liquid drained after 20 minutes. For the olefin sulfonate AEA (SYN_1) presence of cement increased foam stability and reduced drainage after 20 minutes to 61%. For the NVR foam with 5g cement drainage stopped after 2 minutes and only 9% of the liquid drained out of the foam after 1 hour. This result shows that cement particles play a major role in stability of the foam of NVR AEA.

At this point it is important to consider the optimal indicator for evaluating performance of AEAs through foam drainage. Three options for the indicator are as follows:

- i. Drainage rate determined from a drainage equation
- ii. Time corresponding to a certain drainage
- iii. Drainage corresponding to a certain time

For option (i) Bikerman [15] presented a nonlinear equation as follows:

$$V_d = V_0^2 kt / (1 + V_0 kt)$$

Where V_d is the volume of liquid drained to the bottom of the foam at time t , V_0 is the initial volume of liquid and k is an empirical constant. Differentiation of V_d gives the drainage rate: $dV_d/dt = k(V_0 - V_d)^2$ in which $(V_0 - V_d)$ is the volume of undrained liquid remaining in the foam. Since the initial volume of liquid in the foam is the same for all mixtures, k could be used as an indicator to compare drainage rates of different mixtures. To determine k , a nonlinear regression of the drainage equation is needed, which could be challenging for a routine engineering test.

Options (ii) and (iii) are simpler to apply than (i). The disadvantage of option (ii) is that the time corresponding to a certain drainage percentage is often unknown before testing, leading to uncertainty on the required time for testing, an inconvenience from a practical point of view. For the reasons discussed above, option (iii) was chosen in this study. The time chosen should be long enough to allow considerable drainage to occur but not too long because at infinite time all of the liquid is expected to be drained for any foam mixture. Given the data for different AEAs presented above, 20 minutes was selected as the option (iii) parameter. The drainage after 20 minutes is denoted as D_{20} and ranges from 0 to 1. Lower D_{20} indicates a more stable foam. D_{20} values for all mixtures including those with varied amounts of cement given in Table 29 confirm observations discussed previously that in presence cement NVR foams were remarkably more stable than synthetic AEA foams. D_{20} values for different AEAs with different cement contents are also compared in Figure 25. It can be seen from this figure that drainage of NVR foam was the most sensitive to cement addition and was significantly slower than that of synthetic AEA foams. Since foam drainage is dependent on properties of the air bubbles, the FDT results suggest that in a cement mixture air bubbles entrained with NVR are more stable than those entrained with synthetic AEAs. The results also indicate that the more robust performance of NVR in a cement mixture can be attributed mostly to the presence of the cement particles and to a lesser extent, the interaction of calcium hydroxide in the solution and NVR.

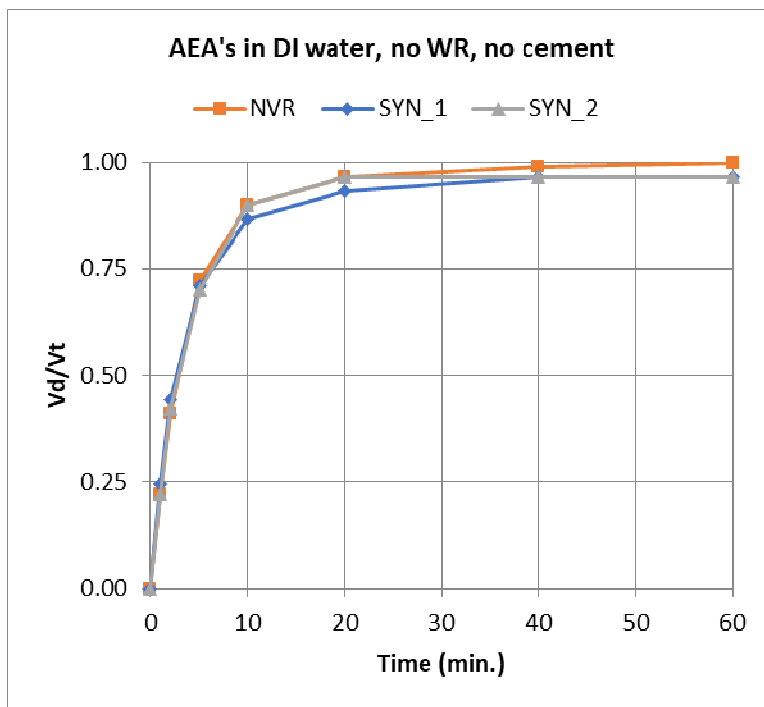


Figure 22. Drainage curves for different AEAs in DI water

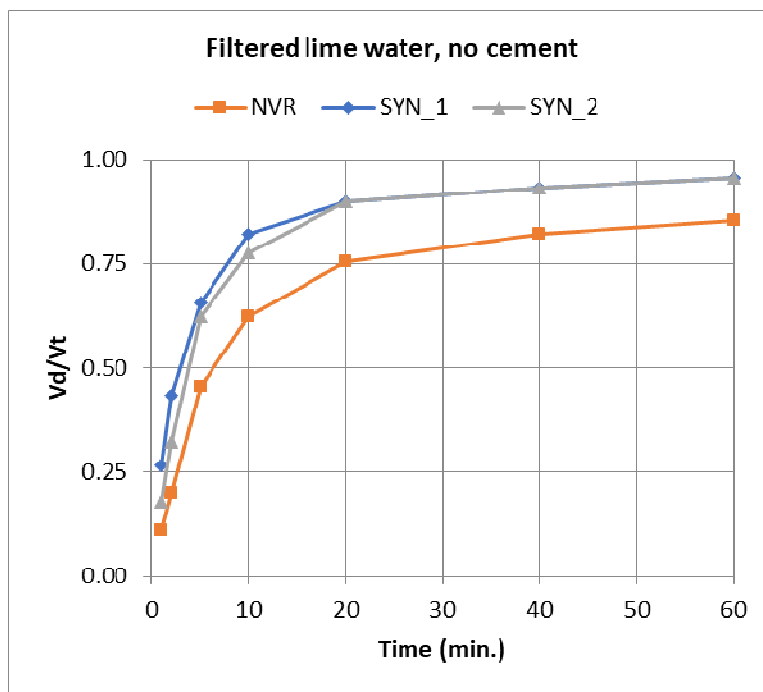


Figure 23. Drainage curves for different AEAs in lime water

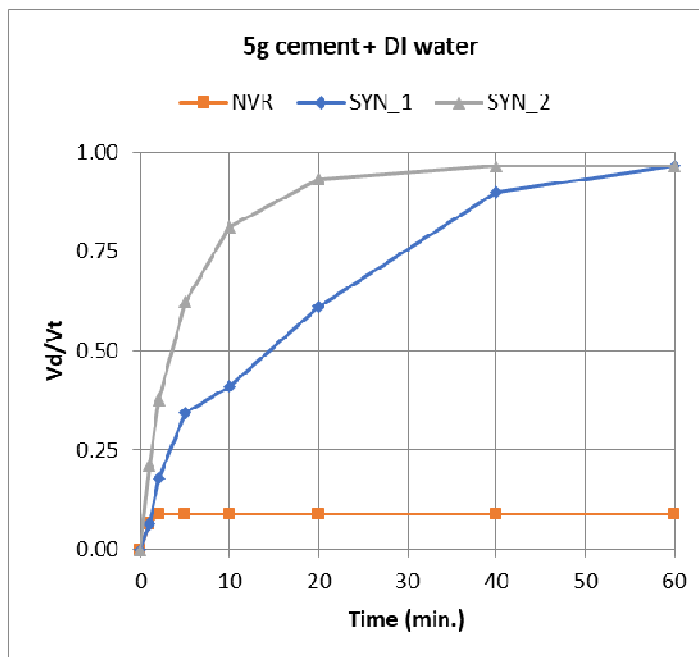


Figure 24. Drainage curves for different AEAs in DI water with 5g cement

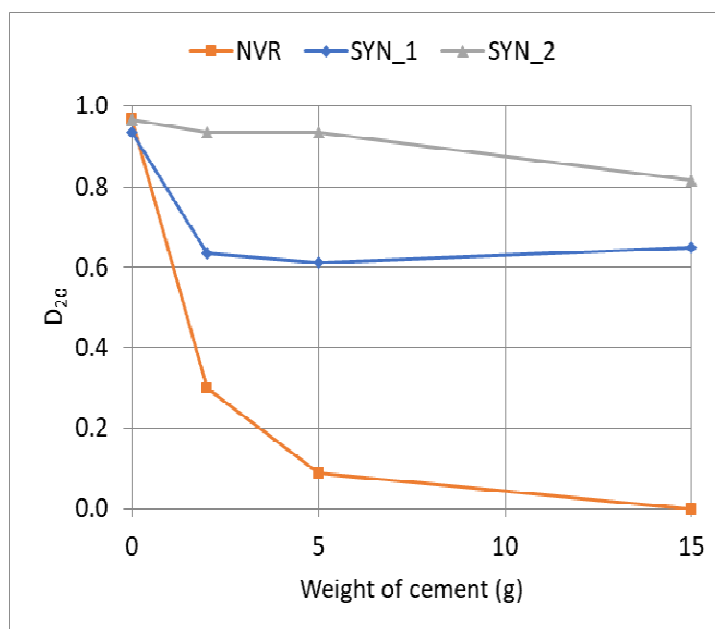


Figure 25. Effect of cement on drainage for different AEAs

Table 29. Drainage after 20 minutes, D_{20} , for different mixtures

AEA	Weight of cement (g)				Lime water
	0	2	5	15	
NVR	0.97	0.30	0.09	0.00	0.76
SYN_1	0.93	0.63	0.61	0.65	0.90
SYN_2	0.97	0.93	0.93	0.82	0.90

3.4 Conclusions

The concrete laboratory tests reported in this chapter show that in concrete using synthetic AEAs, air loss due to the standard hand-rodding compaction was higher than in mixtures using the NVR AEA. This supports the hypothesis that air bubbles in concrete entrained with synthetic AEAs are less stable than those entrained with an NVR AEA and explains the disparity between the air content measured in QC tests or cylinders and the actual air content in concrete pavement using synthetic AEAs, which was reported in Chapter 2.

A modified protocol of the foam drainage test was created and evaluated in this study, showing correlation between foam drainage characteristics and results of the concrete tests. Foams of the synthetic AEAs in DI water with cement were significantly less stable than those of the NVR AEA, supporting the hypothesis mentioned in the previous paragraph. In addition, the FDT results suggest that the difference in performance of the AEAs could be attributed mostly to the interaction of the AEAs and cement particles and to a much lesser extent, the reaction of AEAs and calcium hydroxide in the solution. These results disagree with a hypothesis proposed in previous studies [9] [10] [14] that the NVR-calcium hydroxide reaction is the main bubble stabilization for NVR in concrete.

REFERENCES FOR CHAPTER 3

- [1] P. Taylor, X. Wang, and X. Wang, *Concrete pavement mixture design and analysis (MDA) : evaluation of foam drainage test to measure air void stability in concrete*. 2015.
- [2] Backstrom, Burrows, Mielenz, and Wolkodoff, “Origin, Evolution, and Effects of the Air Void System in Concrete. Part 3 - Influence of Water-Cement Ratio and Compaction*,” *J. Proc.*, vol. 55, no. 8, Aug. 1958.
- [3] Simon, Jenkins, and K. Hover, “Influence of Immersion Vibration on the Void System of Air-Entrained Concrete,” *Spec. Publ.*, vol. 131, Mar. 1992.
- [4] Eickschen, “Working mechanisms of air-entraining admixtures and their subsequent activation potential,” *Am Concr Inst ACI Spec Publ Am. Concr. Inst. ACI Spec. Publ.*, vol. 288, no. 288 SP, pp. 305–315, 2012.
- [5] L. A. Crum, “Measurements of the growth of air bubbles by rectified diffusion,” *J Acoust Soc Am J. Acoust. Soc. Am.*, vol. 68, no. 1, p. 203, 1980.
- [6] C. E. Brennen, *Cavitation and bubble dynamics*. New York: Cambridge university press, 2014.
- [7] T. Leong, S. Wu, S. Kentish, and M. Ashokkumar, “Growth of Bubbles by Rectified Diffusion in Aqueous Surfactant Solutions,” *J. Phys. Chem. C*, vol. 114, no. 47, pp. 20141–20145, Dec. 2010.
- [8] Lee, Kentish S, and Ashokkumar M, “Effect of surfactants on the rate of growth of an air bubble by rectified diffusion.,” *J. Phys. Chem. B*, vol. 109, no. 30, pp. 14595–8, 2005.
- [9] S. Chatterji, “Freezing of air-entrained cement-based materials and specific actions of air-entraining agents,” *CECO Cem. Concr. Compos.*, vol. 25, no. 7, pp. 759–765, 2003.
- [10] T. C. Powers, *The properties of fresh concrete*. New York: Wiley, 1968.
- [11] M. T. Ley, K. J. Folliard, and K. C. Hover, “Observations of air-bubbles escaped from fresh cement paste,” *CEMCON Cem. Concr. Res.*, vol. 39, no. 5, pp. 409–416, 2009.
- [12] M. . Ley, R. Chancey, M. C. . Juenger, and K. . Folliard, “The physical and chemical characteristics of the shell of air-entrained bubbles in cement paste,” *Cem. Concr. Res.*, vol. 39, no. 5, pp. 417–425, 2009.
- [13] B. P. Binks and T. S. Horozov, *Colloidal particles at liquid interfaces*. Cambridge; New

York: Cambridge University Press, 2008.

[14] Mielenz, Vladimir E. Wolkodoff, James E. Backstrom, and, and Harry L. Flack, "Origin, Evolution, and Effects of the Air Void System in Concrete. Part 1 - Entrained Air in Unhardend Concrete," *J. Proc.*, vol. 55, no. 7, Jul. 1958.

[15] J. J. Bikerman, *Foams*. Springer Berlin Heidelberg, 1973.

CHAPTER 4

MECHANICAL PROPERTIES AND MICROSTRUCTURE OF AIR BUBBLE SHELLS IN CEMENT PASTE

4.1 Introduction

Previous chapters provided evidence that air bubbles in concrete entrained with synthetic air entraining admixtures (AEA) were less robust than those entrained with neutralized vinsol resin (NVR), leading to higher air loss during sampling and compaction, and larger disparity between QC test results and the actual air contents in pavement. Foams of synthetic AEAs were shown to be less stable than those of NVR in the presence of cement in the foam mixture. In this chapter micro-properties of individual air bubbles were examined to identify links between them and the bulk properties of the entire air bubble system in concrete samples and foam tests discussed in previous chapters.

Difficulties in controlling air content and air void system in concrete pavement associated with synthetic AEA's have been reported in several studies [1] [2]. It has been proposed that synthetic and NVR AEAs stabilize air bubbles in concrete by different mechanisms [3] [4]. Synthetic AEAs stabilize air bubbles by lowering surface tension of water and the total free surface energy of the system while NVR stabilizes air bubbles by interacting with the cementitious solution and creating insoluble calcium salts that attach to the bubble. But disagreement exists, a recent study on tensiometry by Tunstall et al. (2017) [5] indicated that a synthetic AEA based on olefin sulfonate actually interacted with Ca^{2+} ions stronger than the NVR.

Air bubbles in concrete have been shown to have shells of solid particles [6]. Properties of the individual shell are critical to stability of each air bubble in fresh concrete [7], [8] and could affect freeze-thaw resistance of hardened concrete [5]. Ley et al. (2009) [8] observed air bubbles that escaped from cement pastes and suspended in the bleed water under different external pressure and concluded that the shells of bubbles entrained with a synthetic AEA were relatively strong in tension while the shells of bubbles entrained with NVR seemed very weak in tension and cracked as the pressure decreased. The different behaviors of the AEAs were attributed to the difference in

the chemical compositions of the shell. That study also investigated changes of mineral phases in the bubble shell with hydration time and provided an estimate of thickness of the bubble shell for an air void in hardened cement paste. Corr et al (2002) [6] and Rashed and Williamson (1991) [9] utilized low temperature scanning electron microscope (LTSEM) technique to examine morphology of air bubbles extracted from cement paste and air voids in cement paste as early as five minutes after hydration started. Studies by Mielenz et al. [10] in the 1950s suggested that a film of insoluble precipitate around air bubbles entrained with NVR may be critical to their stability in concrete. Key findings and techniques used in the previous studies are summarized in Table 30.

While the previous studies mentioned above revealed interesting characteristics of bubble shells, they were mostly qualitative, and no correlation between fundamental properties of the bubbles and performance of the air void system in concrete has been established. In the current study, different techniques including Atomic Force Microscopy (AFM), nanoindentation, and quantitative Scanning Electron Microscopy (SEM) were used to evaluate physical and mechanical properties including stiffness and thickness of air bubbles and the bubble shells extracted from cement paste. The objective was to quantify micro-scale properties of air bubbles and identify link between those properties and behaviors of the air void systems in concrete. Surface tensions of AEA solutions in different conditions were also tested and the effect of surface tension on formation and stability of the bubble shell is discussed.

Table 30. Previous research on bubble shells in cementitious systems

Characteristics of bubble shells and techniques used	Sources
<p>Thickness of an air void shell was about 1 μm. Technique: SEM of 60-day old cement paste.</p> <p>C_3S, C_2S, C_3A, C_4AF, ettringite, and gypsum were identified in shell materials. Phase concentrations varied with AEAs and time. Non-crystalline phases were not studied. Technique: Powder XRD</p> <p>Materials on an air void wall in hardened paste had morphology similar to C-S-H and an average Ca/Si ratio of 1.1. Technique: SEM-EDXA.</p> <p>Shells of NVR and synthetic bubbles behaved differently when compressed and decompressed. Technique: light microscope.</p>	Ley et al. (2009) [8]
<p>Bubble shells were composed of heterogeneous fine particles having sizes of 1-5 μm, part of them may be cement particles. Technique: LTSEM of minutes-old paste and bubbles extracted from paste</p>	Corr et al (2002) [6]
<p>At early ages (5-min of hydration) air voids had thin shells made of very fine particles (0.2 μm); materials having morphology similar to C-S-H were observed. Technique: LTSEM of minutes-old paste</p>	Rashed and Williamson (1991) [9]
<p>A film around air bubbles in cement slurry was observed and believed to be calcium salt from reaction of NVR and calcium hydroxide; no properties of this film were available. Technique: light microscope</p>	Mielenz et al. (1958) [10]

4.2 Experimental Methods

4.2.1 MATERIALS AND BUBBLE EXTRACTION

Three distinct AEAs were used in this study: NVR, synthetic olefin sulfonate (SYN_1) and synthetic benzene sulfonate (SYN_2). The cement paste used in this study was composed of 500g Type I cement, 225g deionized (DI) water, and 0.45 ml AEA. Paste mixing followed procedures of the ASTM C192 *Standard Practice for Making and Curing Concrete Test Specimens in the Laboratory*.

4.2.2 AFM TESTS OF AIR BUBBLES IN LIQUID

Atomic Force Microscopy (AFM) is a technique that allows application of nanoscale loads on samples under liquid. Key components of the AFM include a piezo-controlled probe in the form of a flexible micrometer sized cantilever, a laser source, and a position-sensitive photo-detector (Figure 26). A laser beam strikes the back of the cantilever and the reflected beam is received by the photo-detector, allowing determination of the deflection of the cantilever. With the stiffness of the cantilever, commonly called spring constant, known, the applied force on the sample can be determined. In a scanning mode, the cantilever is moved over the sample surface while a constant contact force is maintained, giving images of the sample surface. In a force mode which was used in the current study, the cantilever is moved vertically onto the sample, giving force-deflection curves of the sample. The AFM force mode has been used to test bubbles before where the bubbles function as ultrasound contrast agents, drug delivery agents, and in the food industry applications [11] [12] [13] [14].

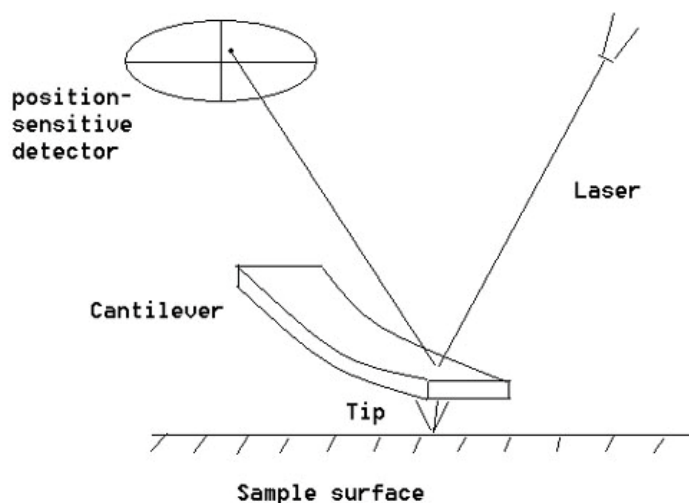


Figure 26. A diagram showing key components of an AFM [15]

In the current study, a Bruker Catalyst Bioscope AFM (Bruker Nano Inc., USA) was used in two separate ways, i) to measure stiffness of individual bubble shells (Figure 27a) and ii) coalescence resistance of a pair of bubbles (Figure 27b). Coalescence resistance is important because it

indicates the bubbles' resistance against breakage when they are exposed to the air. Coalescence also causes the loss of small air bubbles, resulting in coarser air void systems.

For stiffness testing, the air bubbles were extracted, after 30 minutes of hydration, from cement paste into lime water using a magnetic stirrer in the cement paste and then captured under a petri dish in a similar manner to the operation of the Air Void Analyzer [16]. The bubbles were cured under the petri dish in lime water for 24 hours. After curing, most of the air bubbles remained attached to the dish and under liquid when the petri dish was inverted due to the binding of hydrated products onto the dish. The lime water was used to mimic the ability to supply Ca^{2+} ions of the pore solution in cement paste. In the stiffness testing, a vertical force was applied on an air bubble lying on a petri dish (Figure 27a). A tipless cantilever (TL-NCL probe from Nanosensors, Switzerland) with a nominal spring constant of 41 N/m was used. The loading rate was 10 $\mu\text{m/s}$. Force-displacement curves were recorded, and the bubble shell stiffness was deducted.

For coalescence testing, air bubbles were extracted from cement paste in a similar manner described above except that lime water was replaced with deionized (DI) water for a reason discussed at the end of this section. The dish was then inverted and placed onto the AFM stage. The bubbles were tested at approximately one to four hours after mixing using a tipless cantilever (CLFC silicon probe from Bruker Nano Inc., USA) with a nominal spring constant of 1.3 N/m. To conduct a coalescence test, the cantilever was first pressed down on an air bubble lying on a petri dish and then slowly lifted. Due to buoyancy and differences in hydrophobicity between the silicon cantilever and the glass substrate, the bubble was attached to the cantilever underside and lifted off the substrate. The cantilever with the attached bubble was then moved over another bubble on the petri dish and carefully positioned so that the centers of the two bubbles were aligned (Figure 27b). To examine the effect of both force and time on coalescence, two loading schemes were conducted as described below. In both cases, the loading and unloading rate was 0.5 $\mu\text{m/s}$.

- a) Loading and unloading: after loading, the cantilever was withdrawn immediately
- b) Loading, holding, and unloading: after loading, the cantilever was held in place for a specified time before being withdrawn

It should be noted that attempts to conduct coalescence testing of bubbles in lime water failed as few bubbles remained attached to the dish after it was inverted. In addition, a solid shell visible on those bubbles prevented them from being picked up with the cantilever. This observation suggested that the containing solution into which air bubbles were released influenced the properties of the shell. This topic deserves further study.

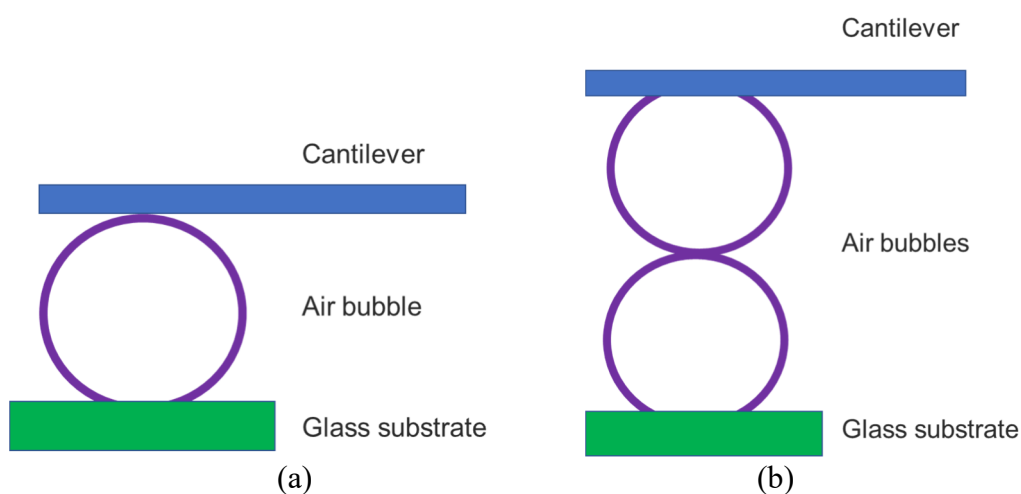


Figure 27. AFM Testing of air bubbles in liquid: (a) Individual bubble; (b) Pair of bubbles

4.2.3 NANOINDENTATION TEST OF DRIED BUBBLE SHELLS

While the AFM described in the previous section allowed testing of air bubbles in liquid, its load capacity did not permit determination of the breaking force or strength of the bubble shell. Another technique that provides nano-scale loading is nanoindentation. In this study, a Hysitron TI 950 Tribo-Indenter with a cono-spherical probe having a cone angle of 60° and radius of $5\ \mu\text{m}$ was used to determine strength of the bubble shell. This probe, however, can only be used for samples in dry condition. It was observed in this study that after several hours of hydration the shell of an air bubble extracted from cement paste maintained its shape after being dried. Air bubbles were extracted from cement paste into water in a similar manner described in section 4.2.2. The bubbles were kept under water for 24 hours, then air dried for 3 days before testing. The loading rate was $1\ \mu\text{m/s}$. The maximum displacement was approximately half of the diameter of the dried bubble shell. A diagram of the nanoindentation testing of dried bubble shell is shown in Figure 28.

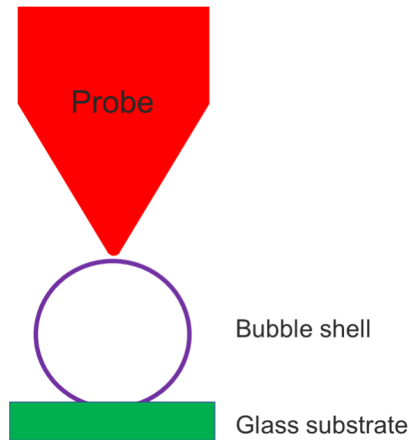


Figure 28. Nanoindentation testing of a dried bubble shell

4.2.4 MICROSTRUCTURE OF BUBBLE SHELLS USING SEM

For SEM testing, the air bubbles were extracted from cement paste into saturated lime water in the same manner as for the AFM stiffness testing described in section 4.2.2. The bubbles were cured in lime water for 4 hours or 24 hours, then submersed in isopropyl alcohol (IPA) for several hours and then dried in a vacuum chamber. IPA has been recommended for stopping hydration and for ion exchange of cement samples before drying [17].

Microstructure of the bubble shells was examined using a field emission SEM Leo 1530 equipped with energy dispersive X-ray spectroscopy (EDS). After curing and drying, the bubble shells were gently placed on a conductive carbon tape which adhered on a thin square copper plate of approximately 7/8 x 7/8 inch. The shells were gold coated for conductivity.

4.2.5 SHELL THICKNESS MEASUREMENTS USING SEM

For thickness testing, the bubble shells were obtained in the same manner described in section 4.2.4 and were cured in lime water for 24 hours. To prepare a flat polished section of the bubble shell for thickness measurements, the dried bubble shells were gently placed on a piece of double-sided Kapton tape adhered to a glass slide, and then embedded in Epofix epoxy (Struers Inc., USA). After the epoxy was cured, the sample was lapped using diamond discs with grit sizes of 6 – 15 μm to expose the shells, then cleaned and dried before being coated with a thin layer of low-

viscosity M-Bond 610 adhesive (Micro-Measurements, USA). The function of the adhesive was to fill the voids inside the shell and minimize pull-out of shell materials during polishing. The coated sample was lapped using a 6- μm diamond disc to expose the shells again and then polished using 6- μm , 3- μm , and 1- μm diamond suspension pastes to obtain a flat test surface (Figure 29). A 15-nm thick carbon coating was applied for conductivity. Images of the shells for thickness measurements were taken using a Hitachi 3400 SEM.

As shown in Figure 29, the observed thickness (λ_t) is larger than the actual thickness (t) of the shell and varies with the distance (c) from the center of the sphere to the test surface. The method used in this study does not allow determination of this distance or the actual thickness of an arbitrary shell. If a number of shells are tested, however, it is possible to estimate a representative actual shell thickness (t) in terms of the average observed thickness (λ_{to}) and diameter (λ_{do}) using statistical analysis. If one assumes that all bubble shells for each AEA have uniform diameter and thickness, the actual outer diameter (D) and thickness (t) can be statistically estimated from the average observed diameter and thickness as follows [18] [19]:

$$D = 1.5\lambda_{do}$$

$$\lambda_{to} = \frac{4t(t^2 - 1.5tD + 0.75D^2)}{3(t^2 - tD + 0.5D^2)}$$

For $t \ll D$, which is true as shown in section 4.3.3, the second equation gives $t = 0.5 \lambda_{to}$.

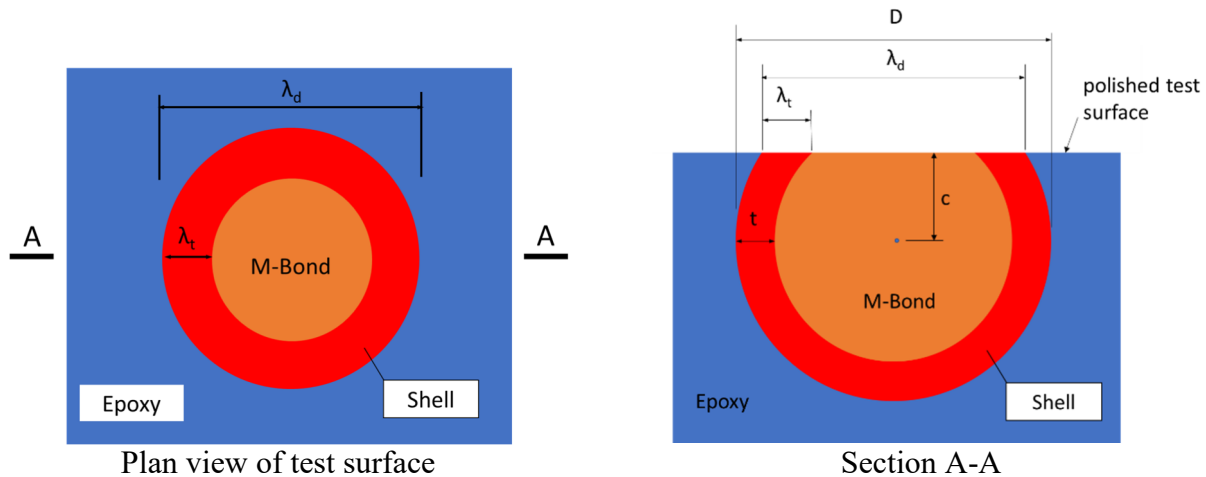


Figure 29. An epoxy-embedded bubble shell for thickness measurements (not to scale)

4.2.6 SURFACE TENSION OF AEA SOLUTIONS

It is well known in surface chemistry that surfactants stabilize air bubbles by reducing surface tension of the air-water interface. The solution in concrete or cement paste contains many ions including Ca^{2+} , Na^+ , K^+ , OH^- , and SO_4^{2-} , which can affect the surface tension. A previous study [5] showed that calcium hydroxide and ions in the pore solution of cement paste had significant effect on surface tension of AEA solutions; but a link between surface tension and behaviors of air bubbles in fresh concrete was not investigated.

In the current study, surface tensions of AEA solutions in deionized (DI) water and lime water were conducted to identify link between surface tension of AEA solutions and performance of air bubbles in concrete. Surface tension testing were conducted using the Wilhelmy plate method (ASTM D1331). AEA concentrations ranged from 0.01% to 10% for DI water and from 0.01% to 1% for lime water. The manufacturer's recommended dosage for the three AEAs is within 0.125 – 3 fl oz per 100 lbs of cement. For a concrete mixture with $w/c = 0.4$, the recommended AEA concentration is approximately 0.02% - 0.5% which is well within the tested range. It should be noted that the AEA solutions in lime water were not filtered as done by Tunstall et al. [5] and in this way possible contribution of the solid phase created from the interaction of AEA and Ca^{2+} ions to surface tension was included.

4.3 Results and Discussion

4.3.1 AFM TEST RESULTS

4.3.1.1 AFM Tests of Individual Bubbles in Lime Water

An example of force-displacement curve of the bubble shell using the AFM is given in Figure 30. The curve starts with a linear part (dotted red line), then exhibits multiple break points (green arrows) and lines with reduced slopes. The non-linear behavior suggests that the shell was damaged and lost its stiffness and strength. It was observed that although the shell experienced damage, the bubble did not collapse after multiple loading-unloading cycles.

The slope of the curve is the total stiffness (K_t) of the system which was composed of the bubble shell and the cantilever (Figure 31). Assuming that the bubble and cantilever work as linear elastic springs, the total stiffness and the stiffnesses of the bubble shell (K_b) and cantilever (K_c) have the following relationship:

$$1/K_t = 1/K_b + 1/K_c$$

Knowing the total stiffness and the stiffness of the cantilever, the bubble shell stiffness can be determined from this equation. The average bubble shell stiffnesses for the three AEAs are shown in Figure 32. On average, the stiffnesses of bubble shells entrained with SYN_1 and SYN_2 were smaller than that of NVR bubble shells by 75% and 70% respectively. The difference in stiffness between the NVR and each of the synthetic AEAs is statistically significant at 5% while the difference between the two synthetic AEAs is not. This suggests that there are differences in the shell thickness or materials between NVR and the synthetic AEAs. No relationship between stiffness and diameter was observed within the data range tested (Figure 33).

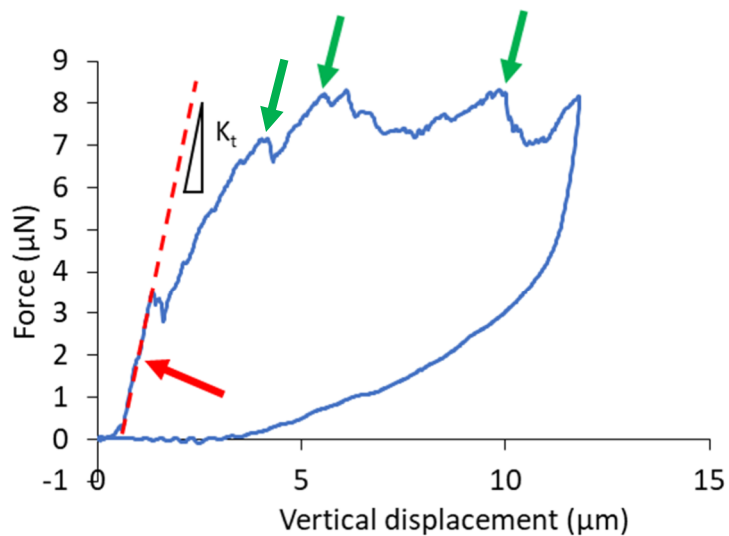


Figure 30. An example of force – displacement curve of bubble shell; red arrow indicates the linear part where the shell stiffness was determined; green arrows indicate damages in the shell

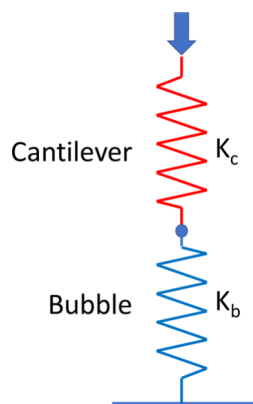


Figure 31. Diagram of bubble-cantilever system; K_b and K_c are stiffness values of the bubble and cantilever respectively

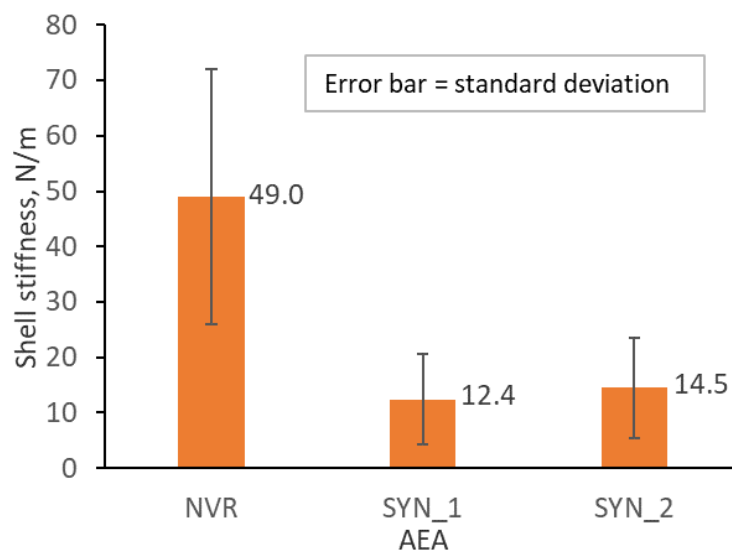


Figure 32. Comparison of average shell stiffnesses for different AEAs (10 samples per AEA)

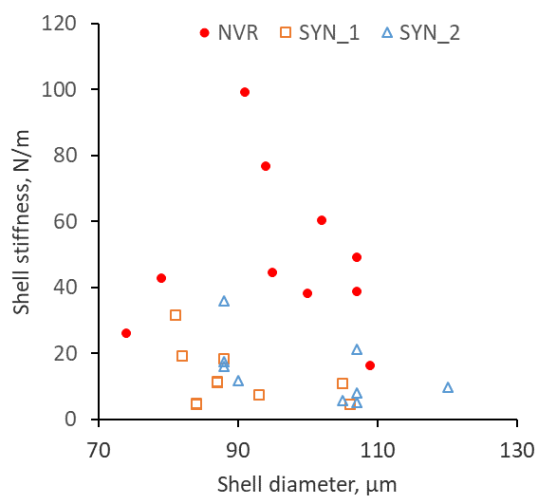


Figure 33. Shell stiffness and diameter of individual bubble shells

4.3.1.2 AFM Tests of Two Bubbles in Water

While the AFM tests of individual bubbles suggested that an individual bubble does not break under liquid, the AFM tests of two air bubbles showed that they can coalesce, and the coalescence resistance depended on both contact force and time. The results also showed that coalescence can happen during loading, holding, or unloading. As mentioned before, two loading schemes were used: a) loading-unloading and b) loading-holding-unloading. An example of coalescence occurring during loading using scheme a) is shown in Figure 34. Tests results for NVR and SYN_1 in water using scheme a) are shown in Table 31. On average, the coalescence resistance of bubbles entrained with NVR was higher than that of bubbles with SYN_1; but the difference was not statistically different and repeatability of the test was low. Given the small sample sizes, it is unclear if the results of this test indicate a true difference in coalescence resistance between bubbles entrained with NVR and those with SYN_1 AEA.

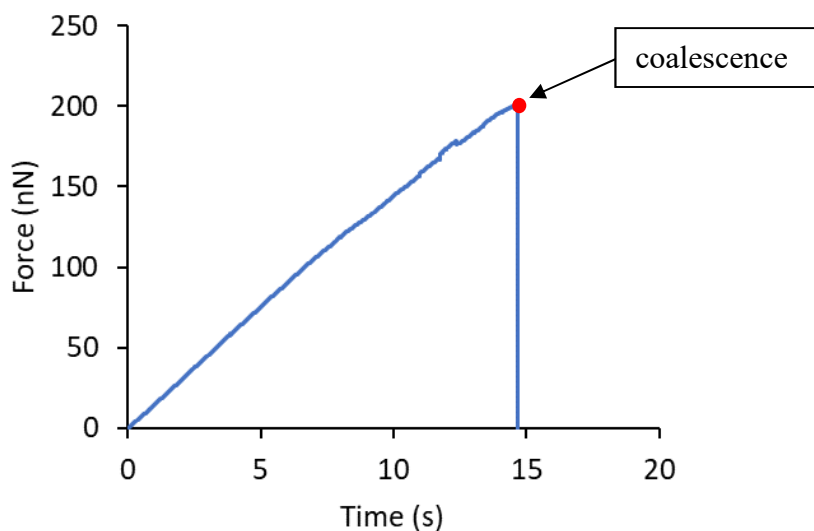


Figure 34. Example of coalescence occurring during loading

Table 31. Coalescence resistance of air bubbles extracted from cement paste

AEA	Mean (μN)	Standard deviation	C.O.V	# of samples
NVR	372	133.5	36%	4
SYN_1	239	88.5	37%	5

Examples of coalescence occurring during holding and unloading using scheme b) are given in Figure 35 and Figure 36 respectively. Coalescence during holding suggests that air bubbles in

concrete can change their sizes when at rest (as opposed to when being agitated during placement or compaction). Since the equipment did not allow control of the holding force, no comparison of coalescence resistance in terms of time among the types of AEAs using loading scheme b) was available.

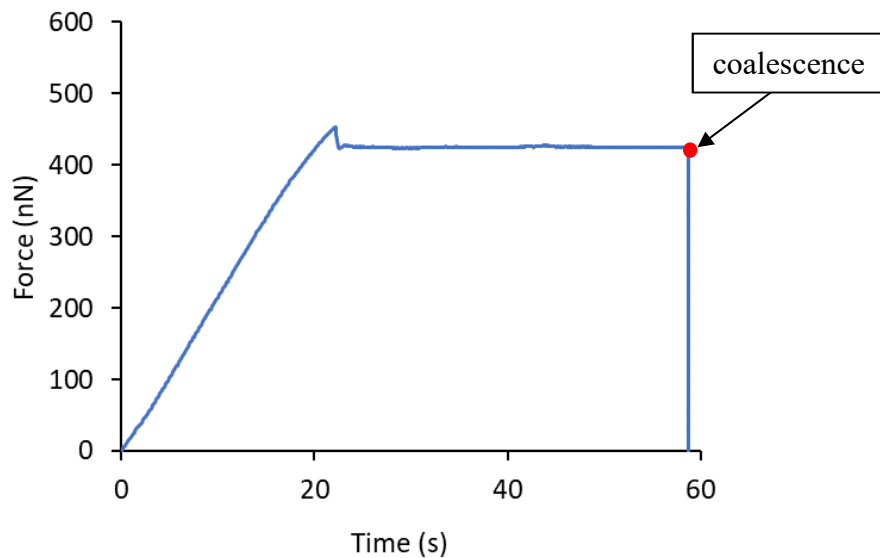


Figure 35. Example of coalescence occurring during holding using loading scheme b)

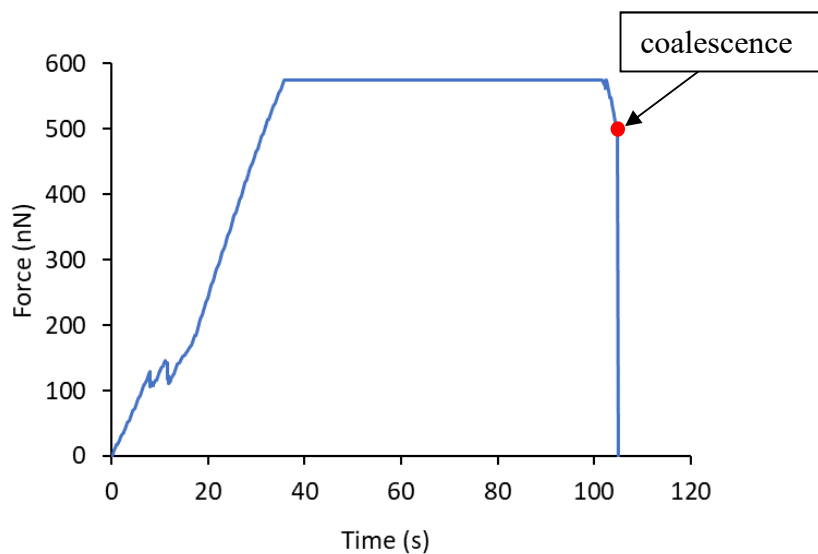


Figure 36. Example of coalescence occurring during unloading using loading scheme b)

4.3.2 NANOINDENTATION

Nanoindentation test results for NVR and SYN_1 are summarized in Table 32. On average the strength of bubble shells entrained with NVR was higher than those entrained with SYN_1. The variation expressed in terms of coefficient of variation, however, was large (71% and 85% for NVR and SYN_1 respectively). Possible reasons for these variations include possible local damages of the bubble shell caused by the drying process and the small size of the probe. Results for individual bubble shells are shown in Figure 37. Two main failure modes were observed:

- Punch-through failure (Figure 38): failure started with the probe punching a hole on the shell; as the probe continued to move down, the hole became bigger until total collapse of the shell.
- Fracture failure (Figure 39): the shell cracked and broke into several pieces.

Due to the large variation observed, nanoindentation tests for bubble shells were not pursued further.

Table 32. Nanoindentation test results

AEA and curing condition	Strength (μN)		Coefficient of Variation (%)	Number of samples
	Mean	Standard Deviation		
NVR in water	279	199	71	14
SYN_1 in water	179	153	85	14

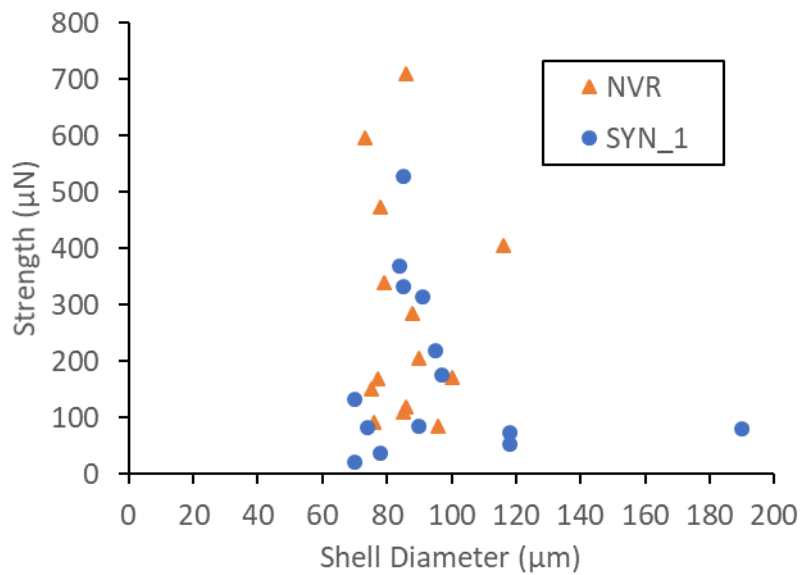


Figure 37. Strengths of dried bubble shells measured using nanoindenter

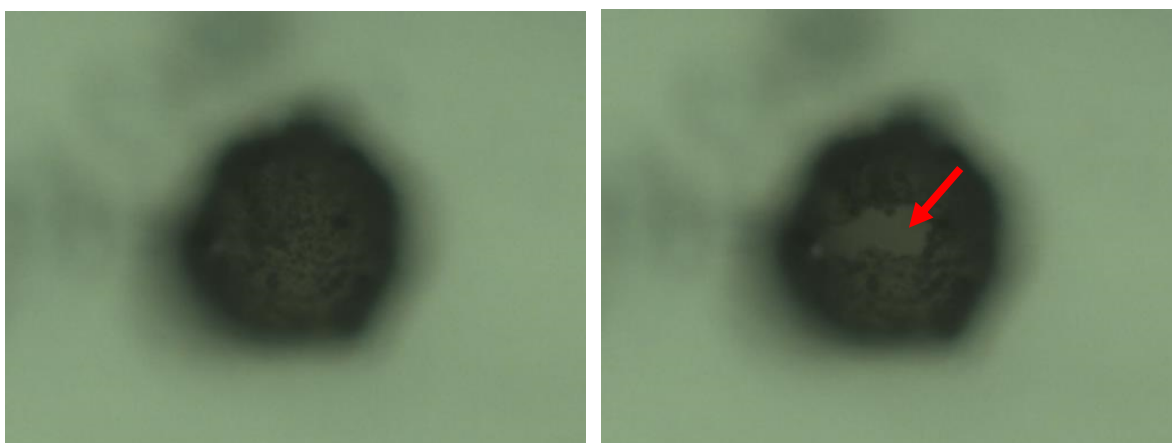


Figure 38. Punch-through failure of dried bubble shell; left: before testing; right: after failure, arrow indicates the hole punched by the nanoindenter

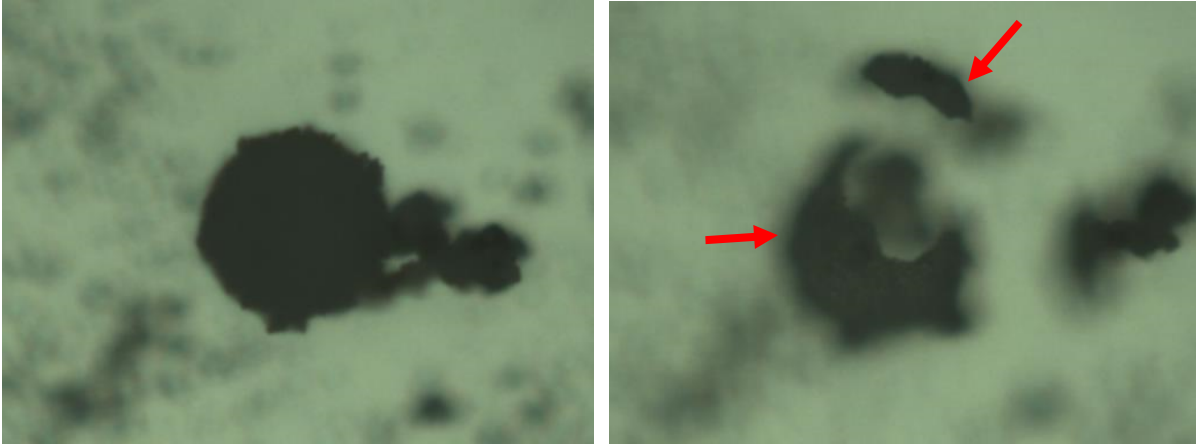


Figure 39. Fracture failure of dried bubble shell; left: before testing; right: after failure, arrows indicate shell fragments after failure

4.3.3 SEM-EDS

4.3.3.1 Microstructure bubble shells

4.3.3.1.1 *The outer surface of bubble shells*

SEM images of the outer surfaces of NVR bubble shells are presented in Figure 40. For four-hour hydration (4-h) samples, the shell was shown to be composed of cement particles covered with C-S-H having reticular network or spongy morphology (marked with a blue ellipse). This type of C-S-H morphology has been observed by other researchers [21]. Short ettringite rods (marked with a red cross) can be seen between the cement particles. For 24-hour hydration (24-h) samples, the shell became denser with more sponge-like C-S-H filling the space between the cement particles. Thinner ettringite rods can be seen protruding out of the C-S-H. SEM images of the outer surfaces of bubble shells for the two synthetic AEAs are presented Figure 41 and Figure 42. In general, they look similar to the shell for NVR.

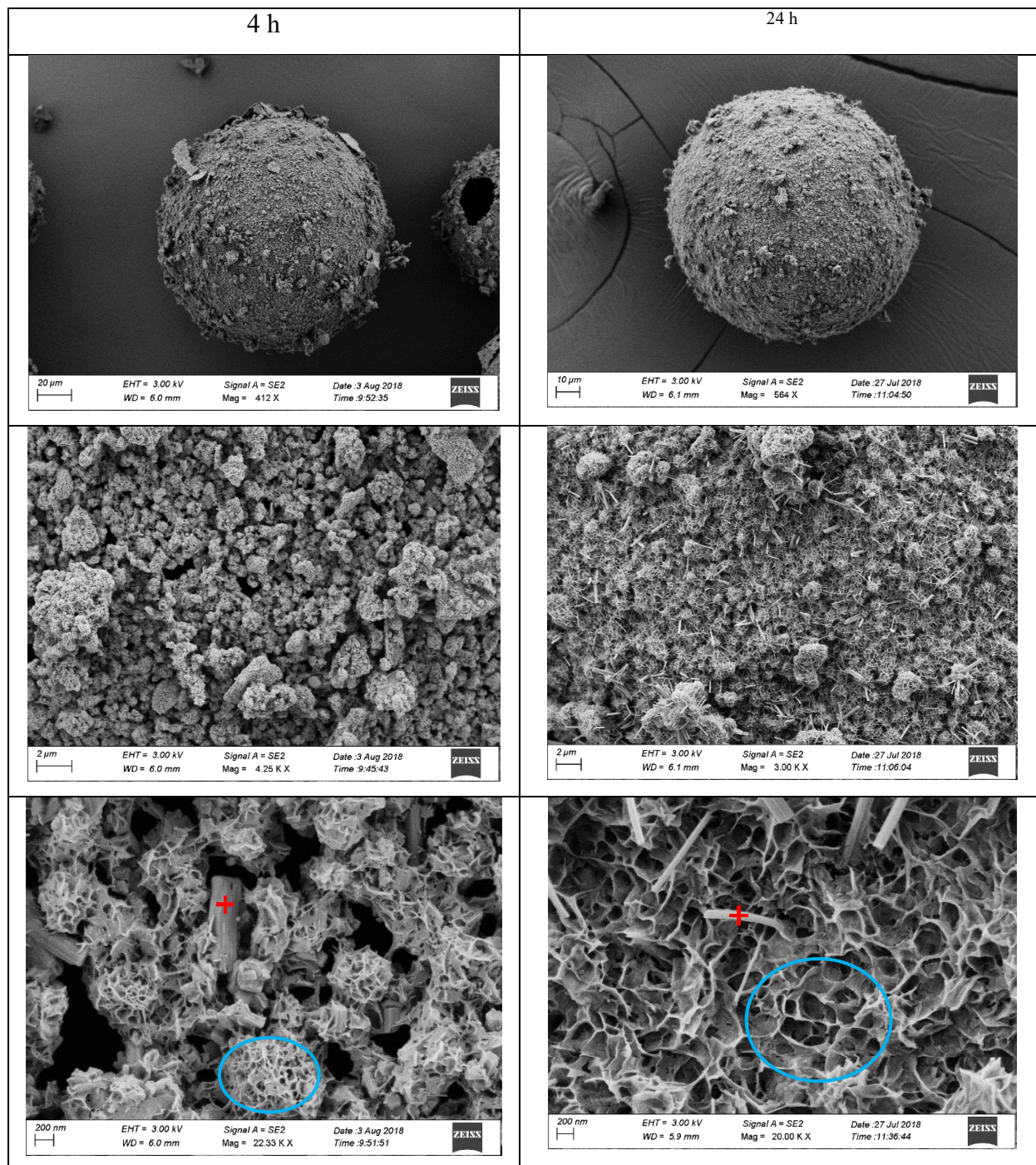


Figure 40. The outer surface of NVR bubble shells hydrated for 4 h and 24 h at different magnifications; blue ellipse indicates a C-S-H area; red cross indicates ettringite

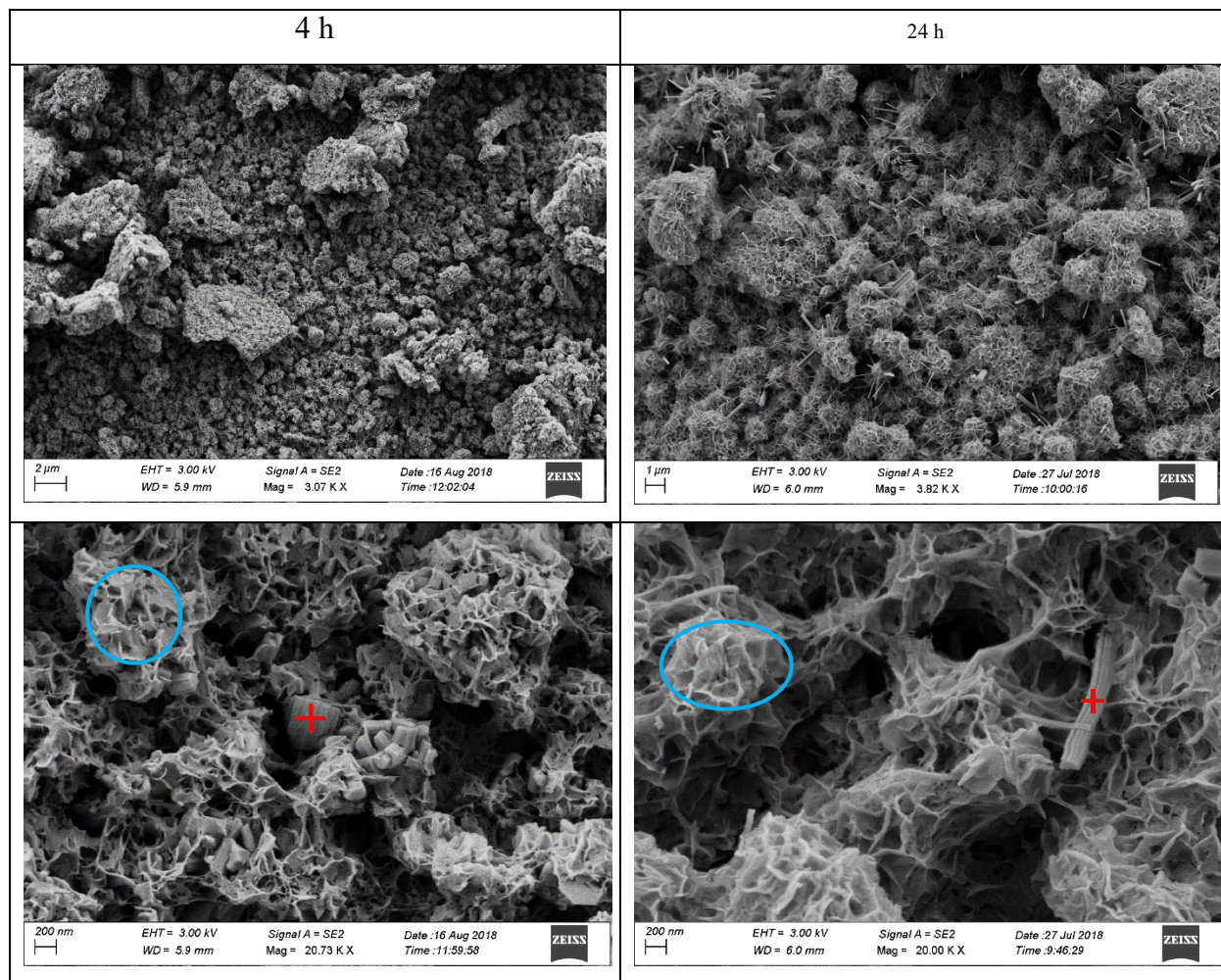


Figure 41. The outer surface of SYN_1 bubble shells hydrated for 4 h and 24 h at different magnifications; blue ellipse indicates a C-S-H area; red cross indicates ettringite

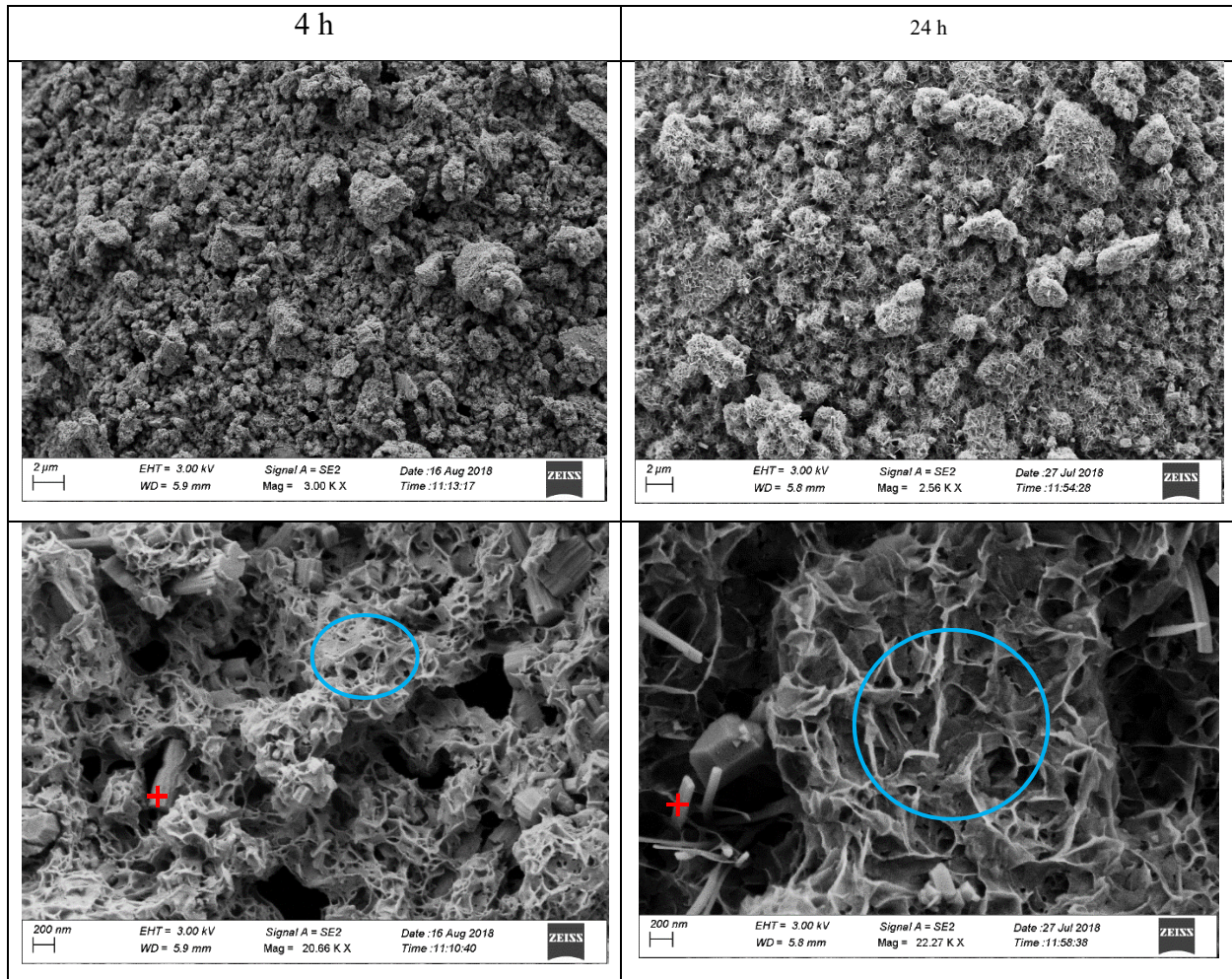


Figure 42. The outer surface of SYN_2 bubble shells hydrated for 4 h and 24 h at different magnifications; blue ellipse indicates a C-S-H area; red cross indicates ettringite

4.3.3.1.2 The inner surface of bubble shells

SEM images of the inner surfaces of the bubble shells for all three AEAs are presented in Figure 43. Some C-S-H is present in the forms of honey comb, but the amount of C-S-H is much less than on the outer surfaces likely because the inner surfaces had less contact with water and thus a lower level of hydration. The particles forming the inner portion of the shells are very small ranging from about 100 nm to several μm. Short rods of ettringite can be seen intermixed among cement particles. No difference is observed between the NVR images and SYN_1 images. In the

shell for SYN_2, there appears to be a thin membrane covering the surface of the particles. The nature of this membrane could not be established.

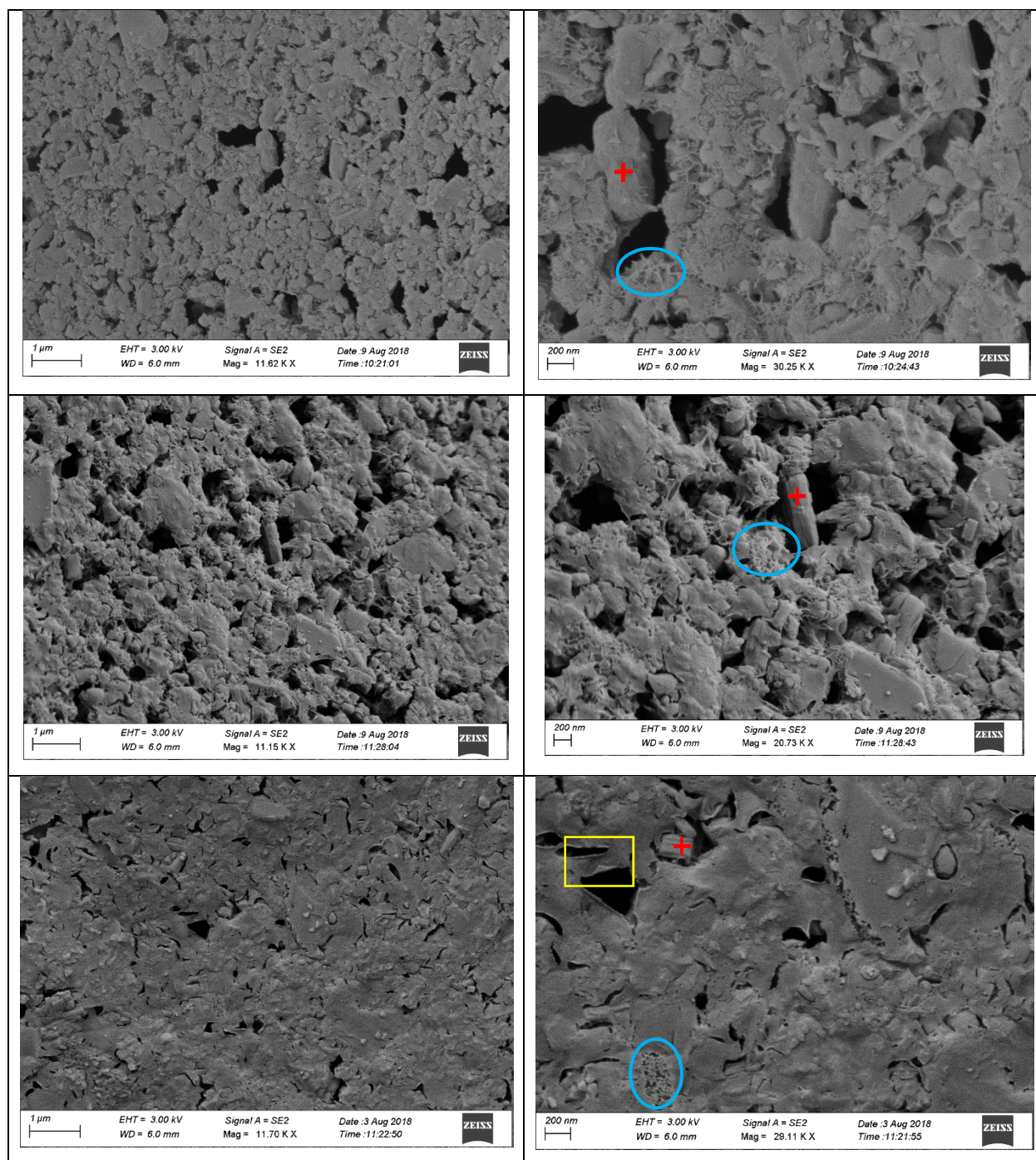


Figure 43. Inner surfaces of 4-h bubble shells for NVR (top row), SYN_1 (second row) and SYN_2 (third row); blue ellipse indicates a C-S-H area; red cross indicates ettringite; yellow rectangle indicates a membrane of unknown nature

4.3.3.1.3 Cross-section of the shell

The cross-section image of a broken NVR bubble shell hydrated for 4 hours is shown in Figure 44. Sponge-like C-S-H is observed through the cross-section. Thickness varies along perimeter of the shell. Although images of the broken shell like this allows an estimation of the shell thickness, this measurement is subjected to considerable variation due to topography of the shell wall. To reduce variation, a flat cross-section of the shell needs to be obtained, which was done by embedding the shell in epoxy as described earlier and the results are presented in a later section.

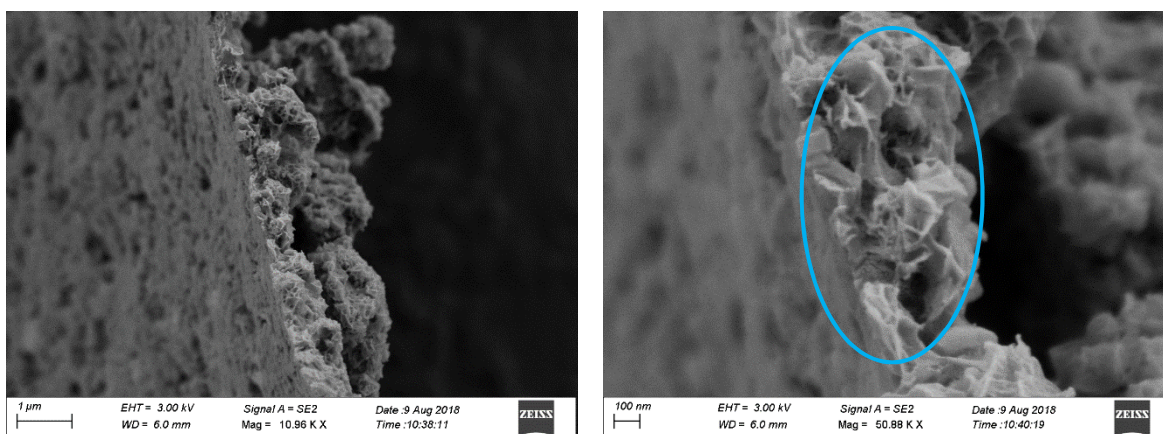


Figure 44. Cross section of a 4-h NVR bubble shell; blue ellipse indicates a C-S-H area

4.3.3.1.4 Ca/Si ratios

It has been suggested that the calcium salt of AEA may be part of the shell and the amount of calcium in the shell could vary from one AEA to another [5]. In the current study, Ca/Si was determined for the three AEAs for 4-h and 24-h shells. The average Ca/Si atomic ratios obtained by EDS for each AEA are provided in Table 33. Six samples were tested for each condition. After 4 hours of hydration, the ratios were 3.6 regardless of the AEA. After 24 hours, the ratios for all the AEAs decreased to 2.6, 2.7, and 2.8 for NVR, SYN_1, and SYN_2 respectively. The decrease of Ca/Si ratio was likely due to dissolution of calcium hydroxide into the solution during the hydration of the shell. If this is true, hydration of the NVR shell appears to be slightly faster than the synthetic AEAs between 4 and 24 hours.

Table 33. Ca/Si ratios of the bubble shells (standard deviations in parentheses)

Hydration time	AEA		
	NVR	SYN_1	SYN_2
4 h	3.6 (0.07)	3.6 (0.13)	3.6 (0.05)
24 h	2.6 (0.19)	2.7 (0.12)	2.8 (0.12)

4.3.3.2 Shell thickness

An example of polished cross-section of epoxy embedded bubble shell used to measure the shell thickness is shown in the SEM image in Figure 45. The bright circular ring is the cross-section of the shell. The dark background is epoxy and the slightly brighter circular area inside the shell is the M-Bond adhesive. For each shell, the thickness was measured at 10 to 15 locations along its perimeter to obtain an average. The average shell thicknesses and outer diameters for individual samples are presented in Figure 46. No thickness-diameter relationship is observed for any of the AEAs. Since the shell thickness was much smaller than diameter (the average D/t ratio was larger than 210 for all the AEAs), the equation $t = 0.5\lambda_{do}$ applies, where t is the actual shell thickness and λ_{do} is the average observed thickness. The average observed thickness and diameters and corresponding actual values are provided in Table 34. On average, the bubble shells for SYN_1 and SYN_2 were respectively 37% and 56% thinner than that for NVR.

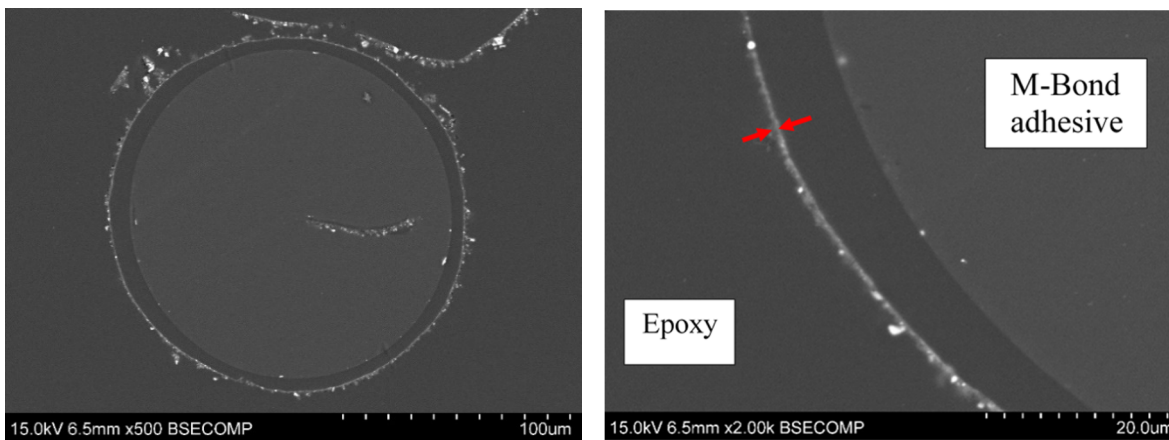


Figure 45. SEM images of an epoxy-embedded bubble shell; red arrows indicate the observed thickness

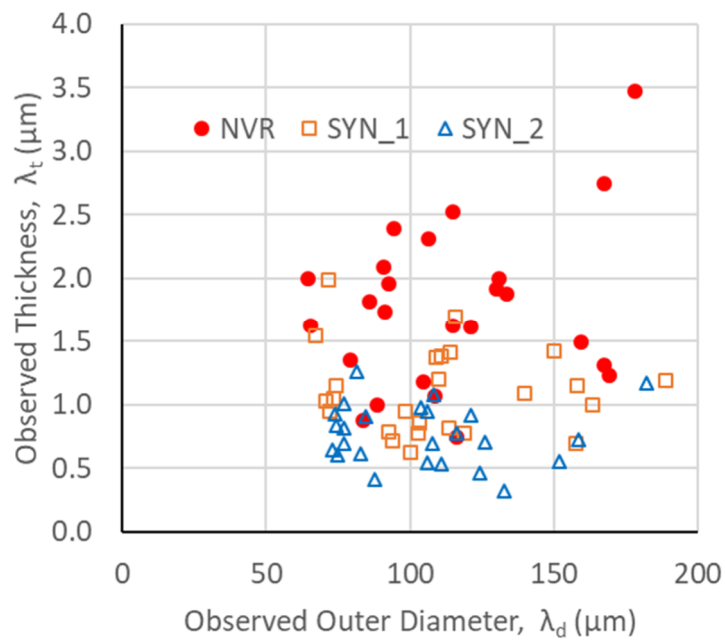


Figure 46. Observed thicknesses vs diameters of bubble shells

Table 34. Observed and actual thicknesses and diameters of bubble shells (standard deviations in parentheses)

AEA Type	NVR	SYN_1	SYN_2
Average observed thickness, λ_{to} (μm)	1.76 (0.62)	1.10 (0.33)	0.77 (0.23)
Actual thickness, t (μm)	0.88	0.55	0.38
Average observed outer diameter, λ_{do} (μm)	123	103	105
Actual outer diameter, D (μm)	185	155	157

4.3.4 SURFACE TENSION TEST RESULTS

Surface tensions of NVR solutions in DI water and lime water are shown in Figure 47. Within the AEA concentration range tested, surface tension decreased when concentration increased and no critical micelle concentration (CMC) was observed. CMC is the concentration above which surface tension remains constant or changes slowly with increasing concentration due to formation of aggregates or micelles of surfactant molecules.

Surface tensions of SYN_1 and SYN_2 solutions are shown in Figure 48 and Figure 49 respectively. For both synthetic AEAs, presence of calcium hydroxide in the lime water significantly reduced the CMC. For SYN_1, the CMC was approximately 0.5% in DI water and 0.05% in lime water. For SYN_2, the CMC was approximately 1% in DI water and 0.05% in lime water. As a result, surface tensions of the synthetic AEA solutions in lime water at concentrations up to the CMC were significantly smaller than those in DI water. During surface tension testing, precipitates were observed in solutions of AEAs and lime water. It is possible that these precipitates were insoluble calcium salts of the AEAs that can absorb onto the air-liquid interface, leading to reduction of its surface tension. Reduction of surface tension due to absorption of hydrophobic solid particles onto the air-liquid interface has been reported in colloid and interface science [22] [23]. Contrary to the results above, a recent study by Tunstall et al. (2017) [5] reported that lime water increased surface tension of a synthetic AEA of the same type with the SYN_1 in the current study. In that study, however, the AEA solutions in lime water were filtered to remove insoluble precipitates before surface tension testing, and thus, possible effects of these precipitates on surface tension were excluded.

Surface tensions of different AEA solutions in lime water were compared in Figure 50. Within the tested concentration range which well covers the manufacturer's recommended range, the surface tension of NVR in lime water was lower than that of synthetic AEA's by 15% – 32%. Possible effect of this result on stabilization of air bubbles in concrete is discussed in the next section.

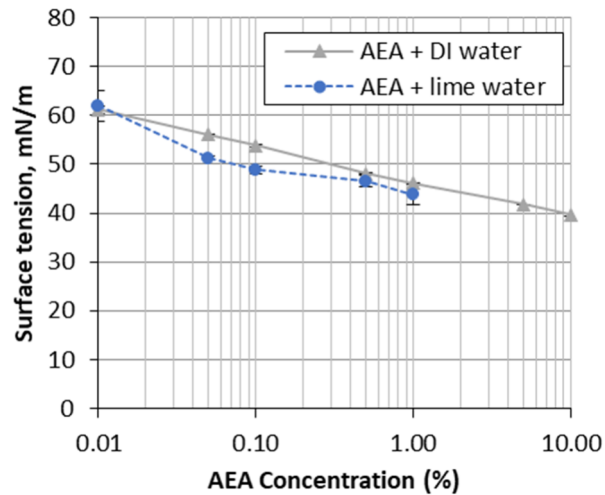


Figure 47. Surface tensions of NVR solutions in DI and lime waters

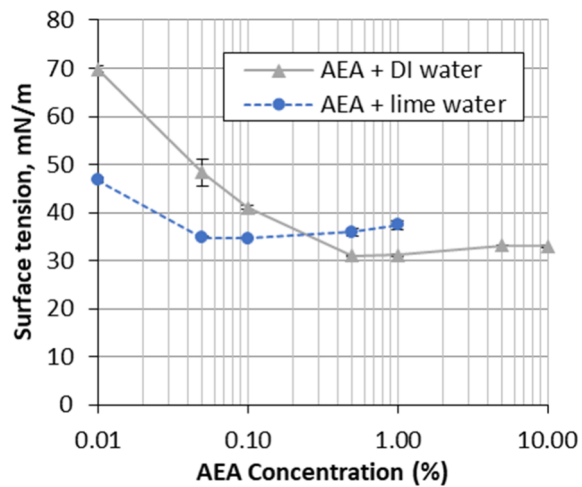


Figure 48. Surface tensions of SYN_1 solutions in DI and lime waters

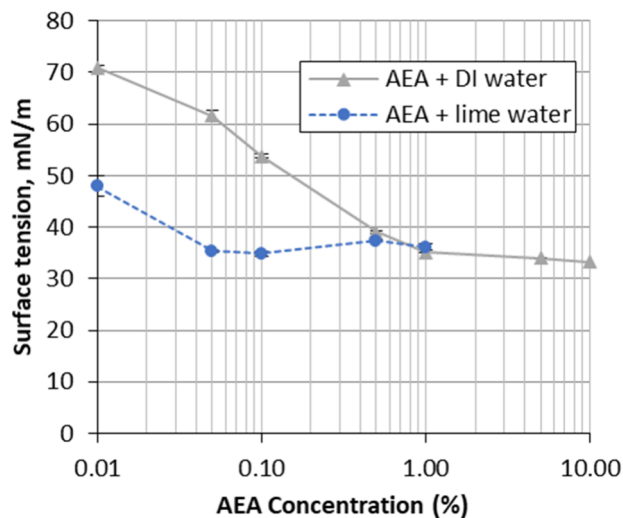


Figure 49. Surface tensions of SYN_2 solutions in DI and lime water

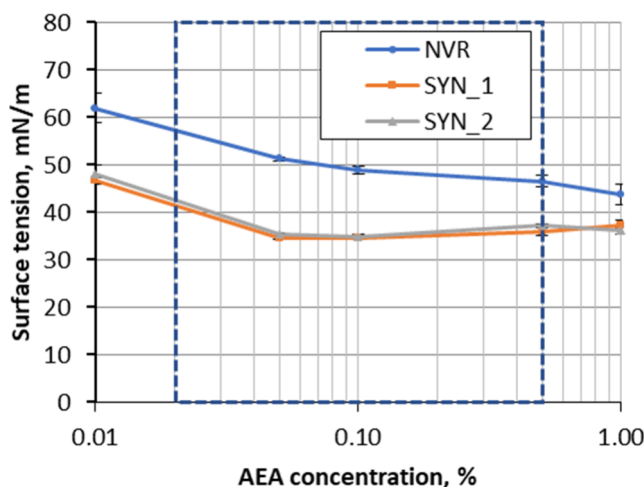


Figure 50. Surface tensions of solutions of different AEAs in lime water; the dotted frame indicates manufacturer's recommended dosages for $w/c = 0.4$

4.3.5 MECHANISM FOR FORMATION AND STABILITY OF THE AIR BUBBLE SHELL

The AEAs used in this study are composed of anionic surfactants whose molecules consist of a negatively-charged head and a non-polar hydrophobic tail. In water, the surfactant stabilizes air bubbles by lowering surface tension. In a cement mixture, bubble stabilization is more complicated due to presence of cement. It has been suggested that the surfactant's polar head adsorbs on cement particles by electrical attraction, increasing hydrophobicity and attachment of cement onto air

bubbles, providing a mechanical barrier against bubble coalescence and breakage [24]. A diagram illustrating the attachment of cement particles is provided in Figure 51. It should be noted that there has been no study suggesting a link between properties of this cement shell and the type of AEA.

Results of the current study agree with previous studies suggesting that the air bubbles had a shell made of cement particles. In addition, it now has been shown that the shell for of air bubbles entrained with synthetic AEAs were thinner than those associated with an NVR AEA. A possible explanation based on the particle-stabilized bubble theory is discussed below.

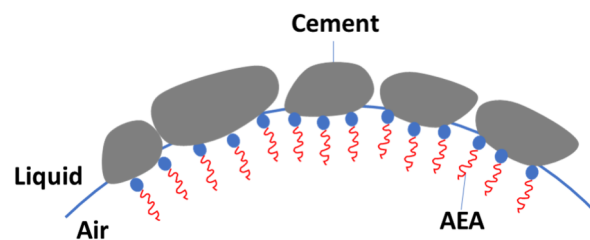


Figure 51. Formation of a cement shell on an air bubble

The effectiveness of solid particles in stabilizing air bubbles depends on wetting energy of the particle, the energy needed to expel a particle away from the air-liquid interface. Thermodynamic analysis gives an equation of this wetting energy for a spherical particle as follows [25]:

$$\Delta E = \pi r^2 \gamma_{\text{air/liquid}} (1 \pm \cos\theta)^2$$

where r is radius of the particle, $\gamma_{\text{air/liquid}}$ is the surface tension of the air-liquid interface, and θ is the contact angle at the interface of the three phases (air, liquid, and solid). Contrary to an AEA solution without solid phase particles, in a cement mixture lowering surface tension results in smaller wetting energy and thus is unfavorable to stability of the bubble shell if the contact angle is unchanged. If one assumes that the contact angle is the same for different AEAs, this theory suggests the synthetic AEAs would be less effective than NVR in stabilizing cement particles on air bubbles, which supports the results reported in this study. In reality, contact angle and surface tension are interdependent [25] and thus both need to be measured to prove/disprove the hypothesis

discussed here. A reliable method to measure contact angle of a partially hydrated cement particle in an AEA solution is not known to the authors. Such a method deserves more study.

4.4 Conclusions

The following conclusions can be drawn from this investigation of the micro-properties of air bubbles and bubble shells:

- On average, the stiffness values of bubble shells entrained with synthetic AEAs were smaller than that of NVR bubble shells by 70-75% as measured in lime water after 24 h of hydration.
- Coalescence resistance of two air bubbles extracted from cement paste and stored under water was measured for the synthetic AEA SYN_1 and NVR, showing no statistically significant difference between the two AEAs. An attempt to conduct the coalescence test for bubbles kept in lime water failed as a solid shell visible on those bubbles prevented them from being picked up with the cantilever. This observation suggested that the containing solution into which air bubbles were released influenced properties of the shell. This topic deserves further study.
- On average, the bubble shells entrained with synthetic AEAs, SYN_1 and SYN_2, were thinner than that for NVR by 37% and 56% respectively, consistent with the results of stiffness testing.
- The bubble shells were composed of small particles of different sizes from 100 nm to several μm , many of them are cement particles. Ettringite rods were also observed.
- There appears to be a thin layer of materials on the inner surface of the shell for synthetic benzene sulfonate AEA (SYN_2) which was not observed in the shells for NVR and SYN_1. Neither the nature of this layer could not be established.
- No considerable difference in elemental compositions of the shells hydrated for 4 or 24 hours was observed among the three AEAs.
- Surface tensions of synthetic AEA solutions in lime water were lower than that of NVR within the concentration range tested. Particle-stabilized bubble theory suggests that the lower surface tension could be unfavorable to stability of the cement bubble shell.

The accumulated evidence consistently shows the shells surrounding air bubbles prompted by the use of synthetic air entraining agents are less robust compared to shells associated with the use of NVR air entraining agents.

REFERENCES FOR CHAPTER 4

- [1] P. Ram, T. Van Dam, L. Sutter, G. Anzalone, and K. Smith, “Field Study of Air Content Stability in the Slipform Paving Process,” *Transp. Res. Rec. J. Transp. Res. Board*, vol. 2408, pp. 55–65, Aug. 2014.
- [2] Eickschen, “Working mechanisms of air-entraining admixtures and their subsequent activation potential,” *Am Concr Inst ACI Spec Publ Am. Concr. Inst. ACI Spec. Publ.*, vol. 288, no. 288 SP, pp. 305–315, 2012.
- [3] L. Du and K. J. Folliard, “Mechanisms of air entrainment in concrete,” *Cem. Concr. Res.*, vol. 35, no. 8, p. 1463, 2005.
- [4] T. C. Powers, *The properties of fresh concrete*. New York: Wiley, 1968.
- [5] L. E. Tunstall, G. W. Scherer, and R. K. Prud’homme, “Studying AEA interaction in cement systems using tensiometry,” *Cem. Concr. Res.*, vol. 92, pp. 29–36, Feb. 2017.
- [6] D. J. Corr, J. Lebourgeois, P. J. M. Monteiro, S. J. Bastacky, and E. M. Gartner, “Air void morphology in fresh cement pastes,” *Cem. Concr. Res.*, vol. 32, no. 7, pp. 1025–1031, Jul. 2002.
- [7] M. T. Ley, K. J. Folliard, and K. C. Hover, “Observations of air-bubbles escaped from fresh cement paste,” *CEMCON Cem. Concr. Res.*, vol. 39, no. 5, pp. 409–416, 2009.
- [8] M. . Ley, R. Chancey, M. C. . Juenger, and K. . Folliard, “The physical and chemical characteristics of the shell of air-entrained bubbles in cement paste,” *Cem. Concr. Res.*, vol. 39, no. 5, pp. 417–425, 2009.
- [9] A. I. Rashed and R. B. Williamson, “Microstructure of entrained air voids in concrete, Part I,” *J Mater Res J. Mater. Res.*, vol. 6, no. 09, pp. 2004–2012, 1991.
- [10] Mielenz, Vladimir E. Wolkodoff, James E. Backstrom, and, and Harry L. Flack, “Orgin, Evolution, and Effects of the Air Void System in Concrete. Part 1 - Etrained Air in Unhardend Concrete,” *J. Proc.*, vol. 55, no. 7, Jul. 1958.
- [11] C. Chen, “An experimental study on the stiffness of size-isolated microbubbles using atomic force microscopy,” *IEEE Trans. Ultrason. Ferroelectr. Freq. Control*, vol. 60, no. 3, pp. 524–34, 2013.

- [12] S. Mahalingam, “Formation, stability, and mechanical properties of bovine serum albumin stabilized air bubbles produced using coaxial electrohydrodynamic atomization,” *Langmuir*, vol. 30, no. 23, pp. 6694–6703, 2014.
- [13] F. Cavalieri, “Mechanical Characterization of Ultrasonically Synthesized Microbubble Shells by Flow Cytometry and AFM,” *ACS Appl. Mater. Interfaces*, vol. 5, no. 21, pp. 10920–10925, 2013.
- [14] V. Sboros, “Nanomechanical probing of microbubbles using the atomic force microscope.,” *Ultrasonics*, vol. 46, no. 4, pp. 349–54, 2007.
- [15] Wenjie Mai, “Fundamental Theory of Atomic Force Microscopy.” [Online]. Available: <http://www.nanoscience.gatech.edu/zlwang/research/afm.html>. [Accessed: 27-Oct-2018].
- [16] Federal Highway Administration, “Air Void Analyzer,” 2017. [Online]. Available: <https://www.fhwa.dot.gov/pavement/concrete/airvoid.cfm>. [Accessed: 13-Oct-2018].
- [17] Z. Zhang, G. W. Scherer, and A. Bauer, “Morphology of cementitious material during early hydration,” *Cem. Concr. Res.*, vol. 107, pp. 85–100, May 2018.
- [18] K. B. Carlisle, M. Koopman, K. K. Chawla, R. Kulkarni, G. M. Gladysz, and M. Lewis, “Microstructure and compressive properties of carbon microballoons,” *J. Mater. Sci.*, vol. 41, no. 13, pp. 3987–3997, Jul. 2006.
- [19] R. L. Fullman, “Measurement of Particle Sizes in Opaque Bodies,” *J. Met.*, vol. 5, no. 3, pp. 447–452, Mar. 1953.
- [20] A. K. Chesters and G. Hofman, “Bubble coalescence in pure liquids,” *Appl. Sci. Res.*, vol. 38, no. 1, pp. 353–361, Jan. 1982.
- [21] Z. Zhang, G. W. Scherer, and A. Bauer, “Morphology of cementitious material during early hydration,” *Cem. Concr. Res.*, vol. 107, pp. 85–100, May 2018.
- [22] T. Okubo, “Surface Tension of Structured Colloidal Suspensions of Polystyrene and Silica Spheres at the Air-Water Interface,” *J. Colloid Interface Sci.*, vol. 171, no. 1, pp. 55–62, Apr. 1995.
- [23] P. R. Waghmare and S. K. Mitra, “Contact Angle Hysteresis of Microbead Suspensions,” *Langmuir*, vol. 26, no. 22, pp. 17082–17089, Nov. 2010.
- [24] V. S. Ramachandran, *Concrete Admixtures Handbook: Properties, Science and Technology*. Elsevier Science, 1997.

[25] R. Pugh, *Bubble and foam chemistry*. 2016.

CHAPTER 5

CONCLUSIONS AND RECOMMENDATIONS

5.1 Conclusions

This study was conducted to find the root cause of the increasing difficulties in controlling the air contents in portland cement concrete associated with synthetic AEAs. Main challenges included the lack of existing techniques to evaluate AEAs and air bubbles in concrete, and lack of data to help identify causes. Given these challenges, a multi-scale experimental research project that included testing of field and laboratory concrete, and testing of foam and individual air bubbles was undertaken. Detailed findings discussed in previous chapters are summarized as follows.

5.1.1 FINDINGS FROM EXPERIMENTAL STUDY ON THE AIR VOID SYSTEM IN WISCONSIN CONCRETE PAVEMENTS (CHAPTER 2):

- The pressure meter (ASTM C231) and microscopic measurements (ASTM C457) of air content in concrete cylinders were in reasonable agreement. The differences between air content measurements by the two methods were within ± 2 percentage points. While sampling methods may impact the air void structure, the actual measurement of air content using the standard ASTM C231 compliant pressure meter appears to be sound.
- The mean differences in air content, void frequency, and spacing factor between the cylinders made before and after the paver were negligible.
- At many project sites, the ASTM C457 air contents of cylinders sampled in front of and behind the paver were significantly lower than those of the drilled cores at approximately the same location. The pressure meter readings that would normally be used for quality control were also lower than air contents in the drilled cores. These differences on average were consistently in the range of 1.6 to 1.8 percentage points.
- The differences between ASTM C457 air contents of the cores and cylinders appear to vary with the type of air entraining admixture (AEA). Compared to mixes using an NVR AEA,

concrete using synthetic AEAs, on average, had larger differences between the cores and cylinders.

- The differences between ASTM C457 air contents of the cores and cylinders appear to vary with the type of coarse aggregate. The average differences were higher in mixes using gravel coarse aggregates. It should be noted, however, that these differences varied widely for both mixes using crushed stone and gravel.

5.1.2 FINDINGS FROM ROBUSTNESS OF AEAS AND THE FOAM DRAINAGE TEST (CHAPTER 3)

- In concrete using synthetic AEAs air loss due to the standard hand-rodding compaction was higher than in mixtures using the NVR AEA.
- A modified protocol of the foam drainage test was created and evaluated in this study, showing correlation between foam drainage characteristics and results of the concrete tests. Foams of the synthetic AEAs in DI water with cement were significantly less stable than those of the NVR AEA.
- The difference in foam stability associated with different AEAs could be attributed mostly to the interaction of the AEAs and cement particles and to a lesser extent, the reaction of AEAs and calcium hydroxide in the solution.

5.1.3 FINDINGS FROM MICRO-PROPERTIES OF THE SHELLS OF AIR BUBBLES (CHAPTER 4)

- On average, the stiffnesses of bubble shells entrained with synthetic AEAs were smaller than that of NVR bubble shells by 70-75% as measured in lime water after 24 h of hydration.
- Coalescence resistance of two air bubbles extracted from cement paste and stored under water was measured for the synthetic AEA SYN_1 and NVR, showing no statistically significant difference between the two AEAs. An attempt to conduct the coalescence test for bubbles kept in lime water failed as a solid shell visible on those bubbles prevented them from being picked up with the cantilever. This observation suggested that the containing solution into which air bubbles were released influenced properties of the shell. This topic deserves further study.

- On average, the bubble shells entrained with synthetic AEAs, SYN_1 and SYN_2, were thinner than that for NVR by 37% and 56% respectively, consistent with the results of stiffness testing.
- The bubble shells were composed of small particles of different sizes from 100 nm to several μm , many of them are cement particles. Ettringite rods were also observed.
- There appears to be a thin layer of materials on the inner surface of the shell for synthetic benzene sulfonate AEA (SYN_2) which was not observed in the shells for NVR and SYN_1. Nature of this layer is unknown.
- No considerable difference in elemental compositions of the shells hydrated for 4-24 hours was observed among the three AEAs.
- Surface tension of synthetic AEA solutions in lime water was lower than that of NVR within the concentration range tested. Particle-stabilized bubble theory suggests that the lower surface tension could be unfavorable to stability of the cement bubble shell.

5.1.4 OVERALL CONCLUSIONS

The results indicate that the disparity between QC test results and the actual air contents observed in concrete pavements associated with the use of synthetic AEAs can be attributed to air bubbles that are less robust than their counterparts induced through the use of the NVR AEA. The lack of robustness or survivability during concrete manipulation of the air bubbles entrained with synthetic AEA's has been demonstrated through a series of tests at multiple scales that provide a consistent body of evidence. Ultimately the lack of robustness can be traced to observable differences in the shells surrounding air bubbles in concrete. Through this research new test protocols were developed to measure stiffness and thickness of the shell of air bubbles extracted from cement paste and to quantify stability of foams of AEAs in a cementitious environment. These tests could be used by researchers and practitioners who are interested in developing new admixtures and/or evaluating performance of AEAs used in concrete.

5.2 Recommendations for Future Research

Results of the modified foam drainage test were consistent with concrete air void tests and micro-properties of bubble shells, showing the less robustness of bubbles produced using synthetic AEAs compared to those associated with the NVR AEA. The FDT protocol developed in this study can be used as a practical, field-office or plant-site screening tool to identify AEAs that will lead to unacceptable discrepancies between existing field quality control tests and microscopically verified actual air contents. To this end, further research to establish acceptance criteria for AEAs is needed.

Although not a focus of this study, further research may suggest modifications to the field quality control test to reduce measured air content discrepancies. Preliminary laboratory data suggested consolidation by vibration may be less destructive to the synthetic-AEA-driven air void system than hand rodding. However, in any circumstance, this research has shown the air bubbles induced with the synthetic air entraining agents are less robust and this may have repercussions throughout the construction process.

The difficulties in controlling the air content in concrete associated with synthetic AEAs were ultimately traced to properties of the bubble shells. The shells of air bubbles in concrete entrained with synthetic AEAs were thinner and less stiff than those associated with an NVR AEA. Theory on particle-stabilized bubbles suggested that the lower surface tensions of synthetic AEA solutions in lime water could be unfavorable to stabilization of the bubble shell and lead to the thinner shells. Contact angle, which is interdependent with surface tension, is also critical to bubble stabilization. Further research on measurement of the contact angle for cement particles in AEA solutions is recommended to verify the mechanism for bubble stabilization discussed in the current study. Such research would be valuable to design of more robust AEAs for use in concrete.

APPENDIX - LITERATURE SURVEY FOR CHAPTER 2

A 1. Accuracy of the ASTM C231 Pressure Method

The accuracy of the ASTM C231 pressure meter has long been debated. This method measures the total air volume in fresh concrete through its relationship to pressure (Boyle's law). Several authors reported significantly higher air contents in hardened concrete than was obtained using the pressure meter [1], [2], [3], [4]. Other authors have not shown such an increase [5], [6], [7], [8]. Some authors suspect that the accuracy of the pressure method is in question; some others indicated that the difficulties associated with the ASTM C457 test may be the main reason leading to the reported discrepancy between measurements by the two methods [9], [10].

There are concerns that the pressure meter is less effective when the air bubbles are very small. A theoretical analysis by Hover [11] showed that the smaller the bubble size, the less accurate the pressure method. For this bubble-size effect to be significant, however, the accumulative volume of bubbles less than 10 μm in diameter must be significant, which is not the case observed in concrete. Data of an actual concrete specimen was introduced in the paper, showing that although the number of air voids less than 50 μm was large, the volumetric contribution of these bubbles was insignificant. The author further commented that air voids with a diameter of less than 10 μm are difficult to detect and measured in ASTM C457 test; thus, not only would the air meter "miss" these small bubbles, but the petrographer would likewise. The study concluded that the bubble-size effects are of little practical significance.

Nagi and Whiting [12] conducted research to resolve the discrepancies in measurement of concrete air content in fresh and hardened states. This study concluded that discrepancies between the air content measurements in fresh concrete (by pressure meter ASTM C231-Type B and volumetric method ASTM C173) and hardened concrete (by ASTM C457) existed but were inconsistent and not significant (below 2 percentage points) in most cases. Effects of four AEA types used in this study (solution of fatty acid, solution of acid salts, neutralized Vinsol resin, and solution of resinous acid) were not very significant. The interaction effect of AEA type and cement alkali level

on air content discrepancy were significant in a two-factor ANOVA test at 5% level of significance.

A 2. Changes of Air Voids in Fresh Concrete at Rest and in Movement

A source of the discrepancy between air contents of fresh and hardened is from the changes in air bubble system that may occur when the concrete is at rest or in movement. When fresh concrete is at rest, air in the smaller, higher pressure air voids could migrate into surrounding solution and into lower pressure, larger voids, leading to a net increase in air volume [1]. Ley et al. [13] observed that air bubbles that had escaped from cement pastes and suspended in the bleed water changed their sizes in the case of non-air-entrained mix. For all the four AEAs investigated including Vinsol resin and synthetic AEA, however, there was no measurable change in the diameters of the bubbles. Bruere [14] attempted to verify the results by Mielenz et al. [1]. However, the experiments with air-entrained cement pastes that have different setting periods ranging from 3 minutes to 4 hours did not show any considerable change in the air void system during concrete setting. Discussing the discrepancy between the studies by Bruere and by Mielenz et al., Powers [15] stated that it is doubtful that the cohesive strength of fresh concrete (at rest) would allow the enlargement of large bubbles.

Studies have shown that consolidation by vibration tends to reduce air content in air-entrained concrete. In recognition of the air loss due to vibration, several state DOTs require the fresh air content to be measured with concrete sampled from behind the paver. Some other agencies raise the required air content measured in front of a slip-form paver [16]. In Wisconsin, the required air content measured by the pressure meter for slip-formed pavement is 1% higher than when concrete is hand-placed (Section 501.3.2.4.2 in WisDOT 2015 Standard Specifications).

An early study on influence of water to cementitious materials ratio (w/cm ratio) and compaction on the air void system in concrete was conducted by Backstrom et al. (1958). Results showed that compaction whether accomplished by hand rodding or vibration resulted in decreased air content and decreased average size of air voids; however, the spacing factor remained relatively constant and this was true regardless whether the concrete contained an AEA. Increasing periods of

vibration from 2 seconds to 50 seconds also resulted in lower air content and void frequency and higher specific surface, but relatively unchanged spacing factor. Air entraining admixture made of sodium soaps of wood resins, which are also known as Vinsol resin, was used.

A field study by Elliot [18] investigated the effects of paving using internal vibration on the properties of Portland cement concrete pavement. Nominal vibrator frequencies of 7200 revolutions per minute (rpm), 8600 rpm and 10,000 rpm were used. Three vibrator eccentrics of 1 5/8-in, 1 3/4-in, and 1 7/8-in nominal size were employed. Paver speeds varied from 6-ft/minute to 12-ft/minute. Cores were taken in and between the vibrator paths which were 2-ft 10-in apart. This study showed that larger vibrator and higher frequency increased air loss of concrete in the vibrator path. Air content of concrete between vibrators appeared unchanged through the paving process. Information on admixtures used was not available in the report of this study.

A laboratory study by Stark [19] demonstrated effect of vibration on the air void system and freeze-thaw durability of concrete. In this study, concretes made with different water-cement (w/c) ratios were subjected to internal vibration at frequencies of 8000, 11,000 and 14,000 vibrations per minute (vpm) for 20 seconds. The vibrator head was 1-3/8-in in diameter and neutralized Vinsol resin was used as the air entraining admixture. After being vibrated in a 0.25-ft³ bucket, concrete was remixed for 30 seconds and then placed in prism molds. Test data showed that for all w/c ratios, internal vibration generally adversely affected the quality of the entrained air void systems, compared with those in unvibrated concretes. Vibrations led to reduced air content and void frequency and increased average void sizes and spacing factor. Effect of vibration varies with w/cm ratio and vibration frequency. Changes in air-void parameters were reflected in the overall trends in freeze-thaw durability of the tested specimens.

A laboratory study by Simon et al. [21] investigated variation of air-void parameters with distance from vibrator insertion point. A vibrator with a head diameter of 1-3/8 inches and a frequency in air of 10,500 vpm (175 Hz) was used. The vibrator was immersed in concrete for 7 seconds in one experiment and 10 seconds in another. In experiment A, AEA was organic acid salts without WR. In Experiment B, AEA was Vinsol resin and WR was ligno-sulfonate. For the vibrator used, vibration had little or no effect on air-void systems at distances of 5, 8, or 10 in. (125, 200, or 250

mm) from the point of insertion. In both experiments, concrete directly at the point of insertion had a reduced air content, a lower spacing factor, higher void frequency, and higher specific surface than concrete away from the point. It is remarkable that the number of chord intercepts across the air voids with a length of about 40 micrometers or less is higher at the vibrator insertion point. This study hypothesized that some of the air released in the collapse of the larger bubbles is re-introduced into much smaller ones.

In a field study on pavement in Iowa State [21], vibrator trails, which exhibited low air content, occurred at high vibration frequencies or with prolonged vibration time.

Under WHRP 0092-11-06, Applied Pavement Technologies with others attempted to quantify the loss of air content as paving concrete passes through the slip-form paver [16]. This research utilized both the ASTM C231 and ASTM C457 test methods. Cores were also taken from the pavement for comparison with the field cast cylinders. Although it is well known that vibration influences the air content of concrete, the concrete samples obtained for fresh air content (ASTM C231) tests and for preparation of 4-in by 8-in cylinders were consolidated with an internal vibrator and thus the research results were confounded. Post-paver concrete was consolidated by vibration twice, once by the paver and once by the technician, while pre-paver concrete was consolidated once. As a result, the most reliable data would have been obtained from ASTM C457 analysis of cores taken from these projects but results from these cores were inconclusive and did not corroborate the field cylinder data. A loss of 1% to 2% of air was observed in the pressure meter ASTM C231 between the front and the back of the paver using concrete that was consolidated by vibration. However, in 8 out of 14 cases, hardened air contents in the cores were higher (up to 3%) than those in cylinders made with concrete in front of paver. This raised the question whether the cylinders were “overvibrated” or not. In 11 out of 14 cases, air contents in the cores were higher (up to 4.7%) than those measured by pressure meter in front of the paver.

Studies by Eickschen in Germany [22] investigated the air void formation as a function of the type and quantity of air entraining admixture and of mixing time. The results showed that when the admixture was overdosed, certain synthetic active agents exhibited higher potential to be reactivated with extended mixing and so to produce more air bubbles while wood-resin AEA did

not show or showed lower reactivation potential. This behavior was believed to be related to the higher solubility of the synthetic AEAs in CaOH solution. Effect of vibration in the case of admixture over-dosage was not investigated.

A 3. Effects of Type of AEA on Concrete Air Voids

Commercially available AEAs are usually blends of chemically complex materials; thus, it is difficult to define them chemically except by broad classification. Such a classification [23] will be used in this document in which an AEA may be categorized into one of four groups: wood-derived products, synthetic detergents, vegetable acids, and others. AEAs based on Vinsol resin are by-products of a process for recovering solvents and rosins from pine wood which are later neutralized with sodium hydroxide to form soluble sodium soap. AEAs based on Vinsol resin, wood rosin, and tall oils belong to the group of wood-derived products. Synthetic detergents used as AEAs are manufactured from by-products of the production of lubricating oils and kerosene. In recent years, these so-called “synthetic” AEAs have been commonly used in concrete pavement in replace of neutralized Vinsol resin (NVR). These and other non-VR AEAs must conform to the requirements of ASTM C260 test method in which their performance is compared with that of Vinsol resin. In spite of meeting these requirements, many highway structures where these admixtures were used have exhibited poor performance or unacceptable properties [24].

The South Dakota DOT conducted a comprehensive investigation to define the causes of compressive strength reduction observed during the construction season of 1997 [25]. The investigation concluded that an interaction between synthetic AEA and low-alkali cements led to the clustering of air voids and non-uniform cement paste around the aggregate particles. High summertime temperatures exacerbated the problem. The tested synthetic AEAs were more hydrophobic, formed thinner-walled bubbles than Vinsol resin AEAs and thus likely promoted flocculation of air voids at the aggregate interface.

A lab study by [26] found that when the concrete was retempered, non-VR AEAs including tall oil, fatty acid and resin/rosin tended to cause more severe clustering of air voids around aggregate particles, than with Vinsol resin. The so-called “synthetic” AEA was not investigated in this study.

A study by Ansari [27] showed that concrete with synthetic AEAs had lower strength than concrete made with Vinsol resin and concluded the reason was that synthetic AEAs caused larger air voids.

Taylor et al. [28] attempted to identify incompatible combinations of concrete materials related to air void systems using the foam drainage test. Study found that mixtures with different AEAs exhibited largely different performances varying from the lowest to the higher value in the performance scale. It should be noted that, however, there was little correlation between the foam drainage test and other parameters of the air void system measured by ASTM C457 in this study.

Research by Sutter [7] showed that mixtures prepared with synthetic AEAs performed better than the Vinsol based AEA when the admixtures were used in low dosages. It also showed good correlations between fresh and hardened air contents in concrete mixed in laboratory using synthetic AEAs although the possibility of improper addition of AEA dosage was warned.

In a comprehensive NCHRP study by Nagi et al. [24], 6 AEAs were divided into 4 groups based on their chemical compositions including Vinsol group, resin/rosin group, benzene group, and alpha olefin sulfonate group. Spacing factor varied from 0.0039 in to 0.0055 in. The Vinsol group had slightly higher spacing factors and relatively higher strength than the other groups.

A study by Tanesi and Meininger [29] investigated durability of concrete with marginal designed air content (2.5% - 4.5%) made with Vinsol resin and a synthetic AEA. The synthetic admixture used in this study did not show the same acceptable performance as the Vinsol resin admixture even though air voids with made synthetic AEAs seemed finer (having higher specific surface and lower spacing factor) than those with Vinsol resin. It was noted that the air voids made with synthetic AEA were well distributed with no clustering.

A study in Germany showed that synthetic AEAs are more soluble and have higher reactivation potential than Vinsol resin AEA [22].

Ley et al. [30] observed air bubbles that escaped from cement pastes and suspended in the bleed water under different external pressure. It was found from observation that the shells of bubbles

entrained with a synthetic AEA appeared relatively strong in tension while the bubbles entrained with Vinsol resin seemed very weak in tension and cracked as the pressure decreased.

Dubovoy et al. [31] studied the effects of cement-alkali level on concrete when different types of AEAs were used. The four AEAs were based on neutralized vinsol resin, salts of fatty acids, sulfonated hydrocarbon and alkyl-benzyl-sulfonate. According to the classification in [23], the last two AEAs appeared to belong to the group of synthetic detergents. It is not clear whether the AEA based on salts of fatty acids was in the group of wood-derived products or vegetable acids. After initial mixing, the concrete was agitated using nine cycles of 9 minutes rest and 1 minute mixing for a total of 90 minutes. Samples were taken right after the initial mixing and at 30-minute intervals and tested for fresh and hardened air contents, slump, and unit weight. The results showed that for all samples at any level of alkaline and with any AEA, more agitation led to a decrease in the total air content and an increase in the spacing factor. It appeared that as the cement-alkali level increased, concretes using sulfonated hydrocarbon-based and alkyl-benzyl-sulfonate-based AEAs had relatively less stable air-void systems, which means higher air loss and larger increase in spacing factor, under the impact of agitation than those using air-entraining admixtures based on neutralized Vinsol resin or salts of fatty acids.

Eickschen and Muller [32] investigated effects of different combinations of AEA, plasticizer and cement types on the air void system. It showed that when polycarboxylate ethers (PCE) plasticizers were added to the concrete mix and followed by additional mixing, concrete using synthetic surfactants had significant increase in air content.

Paleti et al. [33] utilized the foam index test, foam drainage test, and AASHTO T137 (Standard Method of Test for Air Content of Hydraulic Cement Mortar) in an attempt to identify potential problems related to generation and stability of air void system due to interaction of low-alkaline cement, Class F fly ash, water reducers and AEAs. This study found that mixtures with synthetic AEA exhibited more stable foam system than those prepared with Vinsol resin and that lignin-based water reducer seemed more favorable to generation of air bubbles than polycarboxylate superplasticizer.

A 4. Instability of Air Bubbles in Concrete

In air entrained concrete, AEAs help stabilize the air bubbles formed during mixing. Thermodynamically, however, these bubbles in fresh concrete are intrinsically unstable [15]. From the point of foam instability, Du and Folliard [34] summarized three fundamental physical mechanisms that may lead to the collapse of air bubbles as follows:

- i) Diffusion of air from smaller bubbles into the surrounding solution and/or to larger bubbles,
- ii) Bubble coalescence,
- iii) Rapid hydrodynamic drainage of liquid between bubbles leading to rapid collapse.

The first mechanism can occur when the concrete is at rest and it was investigated by many researchers [1], [14], [30]. This would result in increased total air content and decreased number of small air bubbles. As noted in section A 2, however, the cohesiveness of fresh concrete at rest would likely not allow an abrupt change in the air bubble system.

The second mechanism can occur when the concrete is in movement. For example, vibration may force air bubbles to come into contact and coalesce into larger ones. On the other hand, vibration can also force large bubbles out of the concrete or break them into smaller ones.

The third mechanism listed above is not likely in fresh concrete because the air bubbles are immersed in mix water.

It is known in the field of bubble dynamics that gas bubbles can grow in a fluid under an oscillating pressure field such as an acoustic field, a phenomenon called “rectified diffusion” [35]. Consolidation of concrete by vibration imposes an oscillating pressure on the air bubbles and theoretically, can make the bubbles grow. There has been no study on possible impacts of this phenomenon on concrete air void systems.

REFERENCES FOR APPENDIX

- [1] Mielenz, Vladimir E. Wolkodoff, James E. Backstrom, and, and Harry L. Flack, "Origin, Evolution, and Effects of the Air Void System in Concrete. Part 1 - Entrained Air in Unhardend Concrete," *J. Proc.*, vol. 55, no. 7, Jul. 1958.
- [2] F. T. Gay, "FACTOR WHICH MAY AFFECT DIFFERENCES IN THE DETERMINED AIR CONTENT OF PLASTIC AND HARDENED AIR-ENTRAINED CONCRETE.," in *Proceedings of the Fourth International Conference on Cement Microscopy.*, 1982, pp. 276–292.
- [3] Burg, "Slump Loss, Air Loss, and Field Performance of Concrete," *J. Proc.*, vol. 80, no. 4, Jul. 1983.
- [4] K. Hover, "Some Recent Problems with Air-Entrained Concrete," *Cem. Concr. Aggr Cem. Concr. Aggreg.*, vol. 11, no. 1, p. 67, 1989.
- [5] C. Ozyildirim, "Comparison of the Air Contents of Freshly Mixed and Hardened Concretes," *Cem. Concr. Aggr Cem. Concr. Aggreg.*, vol. 13, no. 1, p. 11, 1991.
- [6] K. Khayat and K. Nasser, "Comparison of Air Contents in Fresh and Hardened Concretes Using Different Airmeters," *Cem. Concr. Aggr Cem. Concr. Aggreg.*, vol. 13, no. 1, p. 18, 1991.
- [7] L. L. Sutter, *Evaluation of methods for characterizing air void systems in Wisconsin paving concrete*. [Madison, Wis.]; [Springfield, Va.]: Wisconsin Highway Research Program ; [Available through the National Technical Information Service], 2007.
- [8] J. Tanesi and R. Meininger, "Freeze-thaw resistance of concrete with marginal air content," *Transp. Res. Rec.*, no. 2020, pp. 61–66, 2007.
- [9] H. C. Ozyildirim Virginia Transportation Research Council, *Comparison of air void content measurements in fresh versus hardened concretes*. Charlottesville, Va.; Springfield, Va.: Virginia Transportation Research Council; Available through the National Technical Information Service, 1990.
- [10] K. C. Hover, *Chapter 26, Significance of tests and properties of concrete and concrete-making materials: STP 169D*. West Conshohocken: ASTM International, 2006.

- [11] K. Hover, "Analytical Investigation of the Influence of Air Bubble Size on the Determination of the Air Content of Freshly Mixed Concrete," *Cem. Concr. Aggr Cem. Concr. Aggreg.*, vol. 10, no. 1, p. 29, 1988.
- [12] M. Nagi and D. Whiting, *Achieving and verifying air content in concrete*. Skokie, Ill.: Portland Cement Association, 1994.
- [13] M. T. Ley, K. J. Folliard, and K. C. Hover, "Observations of air-bubbles escaped from fresh cement paste," *CEMCON Cem. Concr. Res.*, vol. 39, no. 5, pp. 409–416, 2009.
- [14] G. M. Bruere, "Rearrangement of Bubble Sizes in Air-Entrained Cement Pastes During Setting," *Aust. J. Appl. Sci.*, vol. 13, no. 3, pp. 222–227, 1962.
- [15] T. C. Powers, *The properties of fresh concrete*. New York: Wiley, 1968.
- [16] P. Ram Wisconsin, Department of Transportation, Division of Business Services, I. Applied Pavement Technology, and Wisconsin Highway Research Program, *Field study of air content stability in the slipform paving process*. [Madison, Wis.]: Wisconsin Dept. of Transportation, 2012.
- [17] Backstrom, Burrows, Mielenz, and Wolkodoff, "Origin, Evolution, and Effects of the Air Void System in Concrete. Part 3 - Influence of Water-Cement Ratio and Compaction*," *J. Proc.*, vol. 55, no. 8, Aug. 1958.
- [18] R. P. Elliott, *Effect of internal vibration of Portland cement concrete during paving: final report of Research Project IHR-503*. [Springfield, Ill.]: State of Illinois, Dept. of Transportation, Bureau of Materials and Physical Research, 1974.
- [19] D. Stark, *Effect of vibration on the air-void system and freeze-thaw durability of concrete*. Skokie, Ill.: Portland Cement Association, 1986.
- [20] Simon, Jenkins, and K. Hover, "Influence of Immersion Vibration on the Void System of Air-Entrained Concrete," *Spec. Publ.*, vol. 131, Mar. 1992.
- [21] S. Tymkowicz and R. F. Steffes, "Vibration study for consolidation of portland cement concrete," *Transp. Res. Rec.*, vol. 1996, no. 1574, 1996.
- [22] Eickschen, "Working mechanisms of air-entraining admixtures and their subsequent activation potential," *Am Concr Inst ACI Spec Publ Am. Concr. Inst. ACI Spec. Publ.*, vol. 288, no. 288 SP, pp. 305–315, 2012.

- [23] D. Whiting and M. Nagi, *Manual on control of air content in concrete*. Skokie, Ill.: Portland Cement Association, 1998.
- [24] M. Nagi *et al.*, *Evaluating air-entraining admixtures for highway concrete*. Washington, D.C.: Transportation Research Board, 2007.
- [25] W. Cross, E. Duke, J. Kellar, and D. Johnston, *Investigation of low compressive strengths of concrete paving, precast and structural concrete*. Pierre, SD: South Dakota Dept. of Transportation, 2000.
- [26] R. L. Kozikowski, R. L. Kozikowski, and Portland Cement Association, *Factors affecting the origin of air-void clustering*. Skokie, Ill.: Portland Cement Association, 2005.
- [27] F. Ansari, Rutgers University, Center for Advanced Infrastructure & Transportation, New Jersey, Department of Transportation, and Division of Research and Technology, *Effects of synthetic air entraining agents on compressive strength of portland cement concrete: mechanism of interaction and remediation strategy : final report*. Trenton, NJ: New Jersey Dept. of Transportation, 2001.
- [28] P. C. Taylor, L. A. Graf, J. Z. Zemajtis, V. Johansen, R. L. Kozikowski, and C. F. Ferraris, *Identifying incompatible combinations of concrete materials Volume I, Volume I*. McLean, Va.: Turner-Fairbank Highway Research Center, 2006.
- [29] J. Tanesi, R. C. Meininger, and Turner-Fairbank Highway Research Center, *Freeze-thaw resistance of concrete with marginal air content*. McLean, VA: US Dept. of Transportation, Federal Highway Administration, Research Development and Technology, Turner-Fairbank Research Center, 2006.
- [30] M. . Ley, R. Chancey, M. C. . Juenger, and K. . Folliard, “The physical and chemical characteristics of the shell of air-entrained bubbles in cement paste,” *Cem. Concr. Res.*, vol. 39, no. 5, pp. 417–425, 2009.
- [31] V. S. Dubovoy, S. H. Gebler, and P. Klieger, *Cement-alkali level as it affects air-void stability [sic], freeze-thaw resistance, and deicer scaling resistance of concrete*. Skokie, Ill.: Portland Cement Association, 2002.
- [32] Eickschen E and Muller C, “Interactions of air-entraining agents and plasticizers in concrete,” *Cem Int Cem. Int.*, vol. 11, no. 2, pp. 88–101, 2013.

- [33] C. Paleti, J. Olek, and T. E. Nantung, "Potential Issues with Generation and Stability of Air-Void System due to Incompatibility of Components in Plain and Fly Ash Cementitious Mixtures," presented at the Transportation Research Board 92nd Annual Meeting, 2013.
- [34] L. Du and K. J. Folliard, "Mechanisms of air entrainment in concrete," *Cem. Concr. Res.*, vol. 35, no. 8, p. 1463, 2005.
- [35] C. E. Brennen, *Cavitation and bubble dynamics*. New York: Cambridge university press, 2014.